Elemental Mercury Removal from Flue Gas by Metal/Metal Oxide Decorated Graphene Oxide Composites

by

Yuxi Liu

A thesis submitted in partial fulfillment of the requirements for the degree of

Master of Science

in

Chemical Engneering

Department of Chemical and Materials Engineering
University of Alberta

ABSTRACT

The toxic elemental mercury (Hg^0) released from coal-fired flue gases is a huge threat to the environment and health of human beings. In this work, silver nanoparticles (NPs), nano ferrite, manganese dioxide, zinc oxide and copper oxide were successfully deposited on graphene oxide (GO) and applied as novel adsorbents for Hg^0 removal. GO, magnetic ferrite nanoparticle-GO (MGO), Ag nanoparticle–GO (GO-Ag), MGO-Ag, GO-MnO_2, GO-ZnO and GO-CuO were successfully synthesized and characterized. All the composite materials were tested for the mercury breakthrough by using a Cold Vapour Atomic Fluorescence Spectrophotometer at various temperatures. The presence of Ag NPs on GO greatly enhances the Hg^0 removal capability of GO-Ag and MGO-Ag as compared to that of pure GO, which is mainly attributed to the amalgamation of Hg^0 on Ag NPs. MGO-Ag shows the best Hg^0 removal performance and thermal tolerance among all the adsorbents developed, with Hg^0 removal efficiency of ~100% from 50 ℃ to 200 °C and even ~40% at 250 ℃. The MGO-Ag composite can be fully regenerated for reuse through a thermal treatment process. The results indicate that MGO-Ag and GO-MnO_2 can be effective candidates and have great potential applications in Hg^0 removal from practical flue gas.

PREFACE

Chapter 2 of this thesis has been submitted for publication as Liu, Y.; Tian, C.; Yan, B.; Lu, Q.; Xie, Y.; Gupta, R.; Xu, Z.; Kuzinicki, S M.; Liu, Q.; Zeng, H., "Ag Nanoparticle-modified Graphene Oxide and Magnetic Graphene Oxide for Elemental Mercury (Hg^0) Adsorption." *ACS Appl. Mater. Interfaces.*

Chapter 3 of this thesis will be submitted for publication as Liu, Y.; Tian, C.; Xie, Y.; Liu, Q.; Gupta, R.; Zeng, H., "Enhanced Mercury Adsorption Capacity by Metal Oxide Nanoparticles-Modified Graphene Oxide."

For the work of these two chapters, I was responsible for the experimental design and conduction, data analysis and integration, and the manuscripts composition. Dr. B. Yan, Dr. C. Tian and Dr. Q. Lu assisted with the revision of the manuscripts. Y. Xie assisted for the mercury capture test. Dr. R. Gupta, Dr. Z. Xu and Dr. S M. Kuzinicki provided some suggestions for the revision of the paper manuscript. Dr. Q. Liu and H. Zeng involved with relevant concept formation as the supervisory authors. Dr. H. Zeng was the corresponding author and involved with the experiments and manuscripts.

ACKNOWLEDGEMENT

I would like to express my most sincere gratitude to my supervisor Dr. Hongbo Zeng and co-supervisor Dr. Qingxia Liu for their instruction and support during the last two years of my graduate study. With the valuable inspirations and suggestions from Dr. Zeng and Dr. Liu, I could then solve all the difficulties and setbacks that I encountered in my study and research.

Dr. Zeng was always sagacious, patient and supportive in every meeting I had with him, not to mention he himself is a hard-working role model for me. Dr. Liu was full of industrial experience and was so knowledgeable that I could always find insightful ideas and new research perspectives in the discussions with him.

I am grateful for Dr. Rajender Gupta for his allowance to work in his lab and use the Cold Vapour Atomic Fluorescence Spectrophotometry. And thanks for the financial support from the Helmholtz-Alberta Initiative-Energy & Environment (HAI-E&E) program and the Natural Sciences and Engineering Research Council of Canada (NSERC) that I can work on this interesting project.

In addition, I would also like to use this opportunity to thank all my group fellows. Dr. Qingye Lu, Dr. Chong Tian and Dr. Teresa Bisson trained me for using many instruments and helped me a lot in my research. Dr. Bin Yan always knew the answers of my questions. Yijun Xie who worked on the same project with me offered help to me whenever I needed. And I want to thank other group members including Ling Zhang, Lin Li, Jingyi Wang, Jun Huang, Qiuyi Lu, Lei Xie, Jiawen Zhang, Chen Shi, Shanshan Wang for their support and cooperation.

Finally, I would like to thank my family and my best friends Huicong Chen and Yahui Xiang, without whose understanding and support I could not live in this new country alone.

TABLE OF CONTENTS

LIST OF TABLES

LIST OF FIGURES

LIST OF ACRONYMS

TEs	Trace Elements
EPA	Environmental Protection Agency
SCR	Selective Catalytic Reduction
ESP	Electrostatic Precipitator
FGD	Flue Gas Desulfurization
SNCR	Selective Noncatalytic Reduction
APCD	Air Pollution Control Device
FE-SEM	Field Emission-SEM
TEM	Transmission Electron Microscopy
XRD	X-ray Diffraction
XPS	X-ray Photoelectron Spectroscopy
CVAFS	Cold Vapour Atomic Fluorescence Spectrophotometry
AC	Activated Carbon
XANES	X-ray Absorption Near Edge Structure
XAFS	X-ray Absorption Fine Structure

CHAPTER 1 INTRODUCTION

1.1 Global Coal Consumption and Coal Combustion Emissions

1.1.1 Worldwide Coal Consumption and the Hazard Effect

Contemporary energy resources include conventional resources (fossil fuels) and non-conventional resources (e.g., solar, wind, biomass), of which conventional energy (e.g., petroleum, coal, natural gas) dominates the energy supply for human.[1, 2] As the world is rapidly developing, the consumption of energy is increasingly expanded. As renewable energy improvement is still continuously underway, the conventional energy resources demand will keep rising slowly in the next 30 years.[3, 4] Figure 1.1[5] provides global energy consumption forecast until 2050 in three scenarios (reference, basic and advanced), showing the large demand for coal.

Coal will be sent to different plants after mining. The major coal utilizations technologies are coal-fired power generation technology, iron making technology, coal gasification and coal liquefaction technology.[6] Due to the large scale of the coal-fired power plants and the project goals, this thesis will focus on coal-fired power plant emission purification.

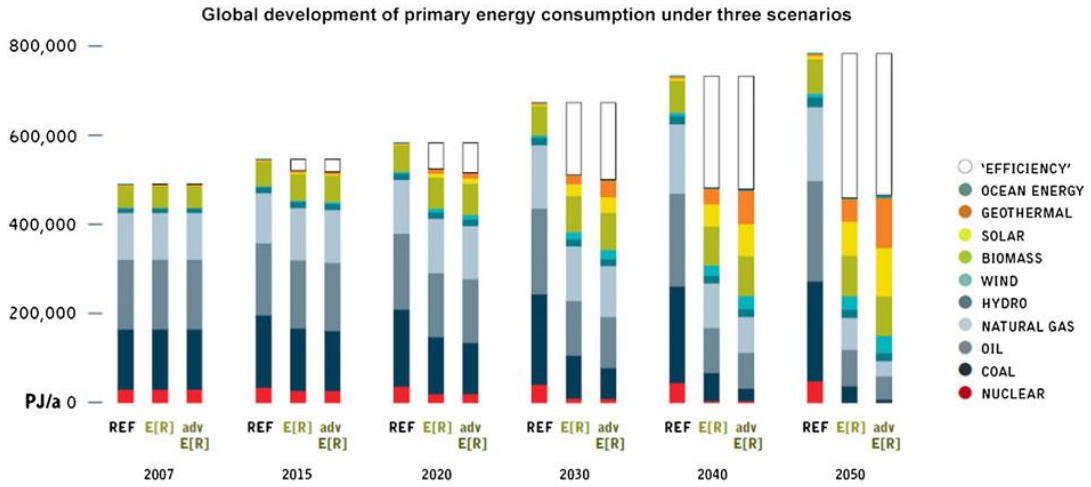

Figure 1.1. Global development of primary energy consumption.[5]

Coal-fired power plants release large amount of waste gases mainly like CO_2, NO_x, SO_2 and waste ashes like fly ash and other particulates.[7, 8] The emissions are affected by the compositions of coals, which differ from region to region as coal formation highly relates to the local geology.[9] The major elements of coal are C, H, O. Nearly, N, S, minor minerals, halogens and trace elements (TEs) account for less than 10 %.[9-11] With large coal consumption, many environmental challenges can be raised, including global warming, particulate matter, water and soil pollution and impacts on local biodiversity.[12, 13]

Lots of efforts have been made to reduce CO_2 to meet the requirements imposed by various worldwide policies. One way is to improve the energy conversion efficiencies of coal and the other way is to capture and store the CO_2 subsequently. Correspondingly, technologies like oxy-combustion and pre/post-combustion are developed and improved, all followed by CO_2 separation through adsorption, cryogenic and membrane processes.[14] Excluding CO_2, all other gases will cause serious damages to the environment and human beings' lives.[15] SO_2/NO_x attached acidic particulates harm human lungs. And once SO_2 and NO_x lead to the acid rain, the

crops, forests, soil and buildings will become the victims of the destructive acid rain. NO_x can even provoke chronic respiratory diseases.[12]

More recently, pollutions brought by residues (ashes produced in different apparatus), including particulate matters and trace elements pollution, have become pressing environmental concerns. The residues are generally deposited in settling ponds and landfills or are emitted to the atmosphere. As a result, the trace elements and toxic compounds will pollute the soil and enter into the bio-system by giving birth to plants, gradually moving up to higher trophic level. Aquatic creatures can be also contaminated directly through precipitation, ash basin effluent and surface runoff, and indirectly as well, via permeation of residue ponds and landfills.[13]

Lots of diseases have been found to relate to the released trace elements (e.g., As, Be, Cd, Co, Cr, F, Hg, Se) bio-accumulation. For example, arsenic can cause the hearing loss, skin basalioma cancer and arsenic poisoning. Other trace elements also cause serious health issues, especially mercury which will be further discussed later.[15, 16]

Some proper utilization technologies of the residues have been proposed and implemented. One of the most common usages is to amend poor soils and thereby improve the soil fertility, texture and water-holding capacity. However, potential problems may occur, such as reduction in available N and P, element excessiveness or imbalance. Also, the fly ash in residues is widely used as construction material, the environmental impact of which is under investigated.[13]

To protect the environment and human health, global and national policies or laws are proposed. United States Environmental Protection Agency (EPA) updated the new guidelines for carbon pollution cutdown in 2014: by 2030, reduce 30 % carbon emission, 25 % particle pollution, nitrogen oxides and sulfur dioxide below 2005 levels; shrink 8 % electricity bills through reducing demand and improving energy efficiency.[17] Local administration department

like Alberta Energy also published their own acts or policies to control the emissions from coal plants.[18]

1.1.2 Air Pollution Control Devices (APCDs) for Flue Gas

Post-treatment technologies, also called as air pollution control devices like electrostatic precipitator (ESP), help to dispose and control the coal-fired power plant residues. After combustion, one part of the residues comes out as the bottom ash consist of both fine and coarse-grained materials, the other part-flue gas-will go through first the ESP and then the desulfurization scrubber combined with selective catalytic reduction (SCR) for NO_x removal before releasing.[13]

Just as the name implies, ESPs are used for capture particulates and bulk particles range from 20 nm to 200 μm. The modern ESP technologies are thoroughly reviewed by Jaworek et al.[19] Two general types of ESP-dry and wet-can capture most of the particles, leaving two size groups difficult to be removed: the finer particles around 0.07 μm; and the larger particles around 0.04 μm. Due to the low charging of fine particles in the range 0.1-1 μm, other technologies such as gas conditioning, wide-plate-spacing, ultrasonic agglomeration are applied as supplement.

The coal-fired power plants use wet/dry flue gas desulfurization (FGD) which can be classified as once-through or regenerable techniques to remove the generated SO_2. The used sorbents will be discarded in one-through FGD, while in the regenerable FGD they will be regenerated and reused after SO_2 releasing. In addition, the released SO_2 can be further sent to produce H_2SO_4, elemental sulphur and liquid SO_2. However, the higher costs of the regenerable FGD become the essential concern of the generalization of the technique. Either limestone or lime is added in the reaction tank to form slurries and promote the sulphite/sulphate

crystallization in one-through wet FGD. FGD system can perform 90% or above SO_2 removal on the premiss of stable electricity supply.[20]

The conventional means used to reduce nitrogen oxides includes combustion modification (to limit the NO_x formation), reburning, SCR and selective noncatalytic reduction (SNCR). The difference is these reactions occur at high temperature in SNCR while SCR catalyst makes them effective even at low temperatures. All these primary and secondary systems can achieve 35-63% and 15-66% NO_x reduction, respectively. SCR can make it higher to 80-90%. The relative insufficiency of NO_x reduction and expensive cost stimulate the development of new technologies and system, such as nonthermal plasma, pressure swing adsorption and biological removal.[21, 22] Barman and Philip (2006)[22] developed an integrated system consist of photocatalytic oxidation achieved by TiO_2 or ozone oxidation of NO_x and scrubbing/biological denitrification which improved the NO_x removal efficiency to 72% or 100% with 10% ozone.

A trend of developing multipurpose pollution control technologies is popular recently.[21] For example, the electron beam process can remove both NO_x as high as 90% and SO_2 as high as 95%. Other technologies like SNOX and SO_x-NO_x-Rox-Box also achieve very high simultaneous removal of NO_x and SO_2. Besides, processes as activated coke process and electrocatalytic oxidation process can remove some mercury additionally.

1.2 Mercury Released from Coal Combustion

1.2.1 The Fate of Trace Elements in Coal

As it is mentioned before, coal contains various metal elements. The air pollution control devices for particles, SO_2 and NO_x can simultaneously concentrate and retain most trace elements.[12, 24] Most TEs will attach to solid residues and collected by ESP or resolve in the

slurries and enter into the aquatic system, the small remaining of which will exist as vaporized elements (e.g., Hg^0) in the flue gas. Consequently, TEs finally distribute in bottom ash or slag, fly ash, desulfurization wastes, sub-micron ash (resulted from homogenous condensation of themselves) and flue gas.[11, 23]

Table 1.1 is extracted from Vejahati et al.'s report (2010)[11] which listed the elements affinity with different compositions of coal. Figure 1.2 from Xu's review[23] further displayed the volatility levels of the elements contained in coals which can instruct the existing phases of the elements in the coal-fired power plant residues. As shown in this Figure, Hg, B and Se are partially released in vapour phase.

Table 1.1. Trace elements distribution in coal.[11]

Affinity	Mineral group	Mineral type	Elements
Inorganic	Clay minerals and feldspars	Kaolinite Montmorillonite	Al, Ba, Bi, Cr, Cs, Cu, Ga, K, Li, Mg, Na, Ni, P, Pb, Rb, Sn, Sr, Ta, Th, Ti, U, V, Y and rare earth elements
	Iron sulfides	Pyrite Sphalerite	As, Cd, Co, Cu, Fe, Hg, Mo, Ni, Pb S, Sb, Se, Ti, W and Zn
	Carbonates	Calcite, Dolomite, Ankertie	Ca, Co and Mn
	Sulfates	-	Ba, Ca, Fe and S
	Heavy minerals	Tourmaline	B
Organic	N, S, Be, B, Ge, V, W and Zr (B exhibits partial association with tourmaline in the heavy fraction, and V with clay minerals).		

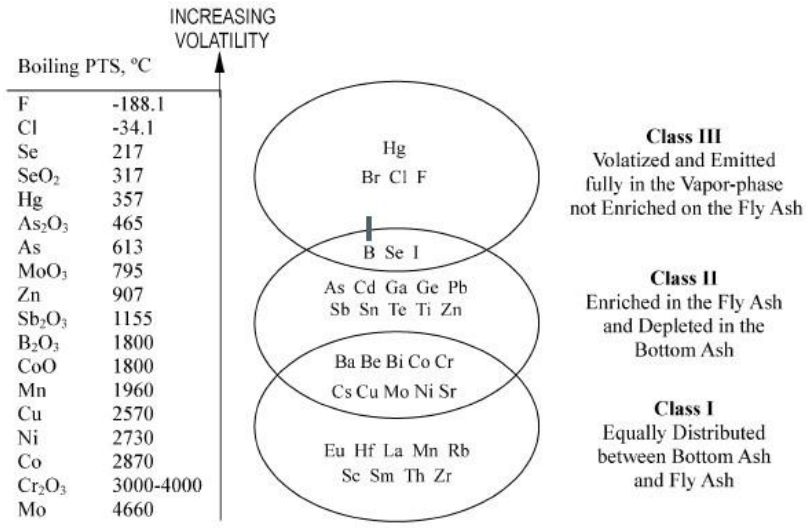

Figure 1.2. Categorization of trace elements based on volatility behaviour.[23]

1.2.2 Mercury, Mercury Chemical Compounds and their toxicity

Among all the trace elements released from coal combustion, mercury accounts for the highest level of volatility and also the highest level of toxicity. The former property determines its resistance to flue gas clean devices or adsorbents, along with the toxicity, making mercury pollution one of the most serious problems derived from coal-fired power plants. Once released, mercury can cycle among air, soil, water and creatures for years. According to Clarkson and Magos (2006)'s report[24], it has various inorganic and organic forms in the environment (listed in Table 1.2) whereas the divalent mercury is responsible for the mercury toxicity as it is the product of biological metabolism.

Table 1.2. Mercury and its chemical compounds.[24]

Inorganic Mercury			Organic Mercury	
Hg Vapor	Mercurous	Mercuric	Short chain alkyl	Other organics
Hg^0 Amalgam	$Hg\text{-}Hg^{2+}$	Hg^{2+}	$CH_3(CH_2)_n\text{-}Hg^+$ (Methylmercury, Ethylmercury)	$(R\text{-}C\text{-}Hg^+)$ Phenyl Hg

In most cases, the toxicity of mercury refers to its other compound forms. But, it is still dangerous to inhale mercury vapour through the volatilization of liquid metallic mercury because the monatomic mercury can easily diffuse in cell membranes. Also, the mercury vapour can damage the central nervous as it can cross blood-brain barrier. Both mercurous and mercuric compounds are the pathogenesis of children's acrodynia or "pink disease". And the mercuric mercury can accumulate in the kidneys and bring kidney damage. Other symptoms like stomatitis, gastroenteritis and the inhibition of enzyme function or blockade of other cellular processes were reported by researchers in mercuric mercury intake. Except for inorganic mercury, the organic mercury cause serious health problems as well. Methylmercury ranks the most dangerous organic mercury, which exposed to human mainly through consumption of fish or marine mammals. Methylmercury has higher concentrations in higher tropic levels of the food chain as it undergoes a remarkable biomagnification process during its lifelong time. And it is fatal to central nervous system and may cause death for adult exposures, and is fatal to infant brain and cardiac for prenatal exposures. Ethylmercury is another organic form of mercury that threats human health which targets the central nervous system. Besides, it is a source of inorganic mercury through metabolism and therefore cause the damages as inorganic mercury.[24]

Considering the fatal toxicity of all forms of mercury, it is essential to eliminate and control the mercury from the industrial plants, especially the coal-fired power plant due to the large consumption of coal.

1.2.3 Worldwide Emissions of Mercury and its Concentrations in Coals

Considering the extremely toxicity of mercury to both human beings and other living creature, it is necessary to have a comprehensive knowledge of the mercury concentrations of coals for subsequent assessing, monitoring and analysis.

Mercury is released primarily from anthropogenic activities and natural sources, such as coal and petroleum combustion, gold mining, volcanic fires, etc. On an annual basis of the mercury emissions assessments before 2010, natural sources liberate 5207 tonnes mercury to the atmosphere, part of which is reemission of the previously deposited mercury. Among the anthropogenic interferences, fossil-fuel combustion contributes most to the discharge of various forms of mercury[25]. That is 810 tonnes of the total 2320 tonnes each year. Other releasing are 400 tonnes, 310 tonnes, 236 tonnes, 187 tonnes, 163 tonnes from gold mining, manufacturing, cement production, waste disposal and soda production, respectively.[25]

The concentrations of mercury in coal are at levels between 0.03-3.3 mg/m^3, with an average value of 0.12 mg/kg[26]. After combustion, the concentration of mercury in flue gas will range from 0.3 $\mu g/m^3$ to 35 $\mu g/m^3$, while, the concentration of mercury in power plant flue gas desulfurization (FGD) sludge is around 4 - 26 mg/kg according to the researches done in 1991 to 2002[26, 27].[26, 27] The value can vary nowadays due to the update of the technologies.

Mercury concentrations differ from different coals. Take US coals (1999) as examples[28], the mean concentration was around 0.2 μg/g. Coals from San Juan River and Uinta had the lowest mercury level of 0.08 μg/g, while, the Gulf Coast provided coal with 0.22 μg/g mercury. Coals in Korea had the lowest mercury concentration level of 0.012-0.048 μg/g according to the summary of Pirrone et al., while Chinese coals showed the highest level of 0.19-1.95 μg/g.[25] Of the mercury in coals, a large proportion was found to be inorganically bound and a certain part was

associated with organic matter. Mercury was also found to have high affinity with pyrite in several reports.[28]

The conventional coal cleaning can reduce the mercury concentrations afterwards. Toole-O'Neil's work[28] summarized the mercury reduction extent in clean coal, the average of which reached 37 % with a range from 12 % to 78 % for coals from different regions. The variation of the reduction efficiency is due to the different occurrence of mercury in coals. In this regard, the first step of cleaning coal is advantageous for reducing the mercury entering the combustion system.

1.2.4 Mercury Behaviours during Coal Combustion and Its Post-Treatment

Mercury goes through various transformations[29] during the coal combustion as typically showed in Figure 1.3. It is reported that mercury is intimate with inorganic mineral compounds contain copper, pyrite and sulfur in coals.[29-31] As decomposition propels in the combustion process, mercury is liberated only in gas phase-elemental mercury (Hg^0) and then partly transfers into the other two main forms- divalent mercury (HgX(g)) and particulate bound mercury (Hg_p) later on. This transformation extent is significantly affected by the coal types as well as combustion conditions and will consequently and substantially affect the mercury removal efficiencies by the following APCDs treatment. The bituminous coals were found to respond to post-treatment of mercury more effective. In contrast, subbituminous coals and lignites were inactive to the cleaning technologies towards mercury.[30-32] These results were in large extent related to the chlorine content in coals and the unburned carbons in fly ash. Lots of researches have demonstrated the mercury chlorination after coal combustion. Hg^0 reacts with HCl or Cl_2 to form $HgCl_2$ which is considered to be the primary mechanism of mercury transformation behaviours[29, 30].[29, 30] The resulting $HgCl_2$ can either exist as flue gas or attach onto the ash

particles and then enter into the APCDs system. In reality, the mercury chlorination as a function of temperature largely determines the future destiny of mercury before final disposal of the coal combustion product.[33] Hg transfers between solid $HgSO_4$ and gaseous $HgO/HgCl_2$ or the solid and gas phase of HgO or the gaseous HgO and Hg^0 that depends on the flue gas temperature. Even theoretically Hg^0 can completely convert to oxidized forms at low temperature, the reality still showed quite a lot Hg^0 existed, owing to the inhibition impact from other elements. The individual existence of acid gases (e.g., SO_2, NO_x, HCl) can positively improve the mercury (excluding SO_2), however, coexist of two or more acidic gases may have negative effects[32, 34].[32, 34] And, the active reactions between calcium and chlorine consume chlorine and conversely reduce the available chlorine that can oxidize Hg.

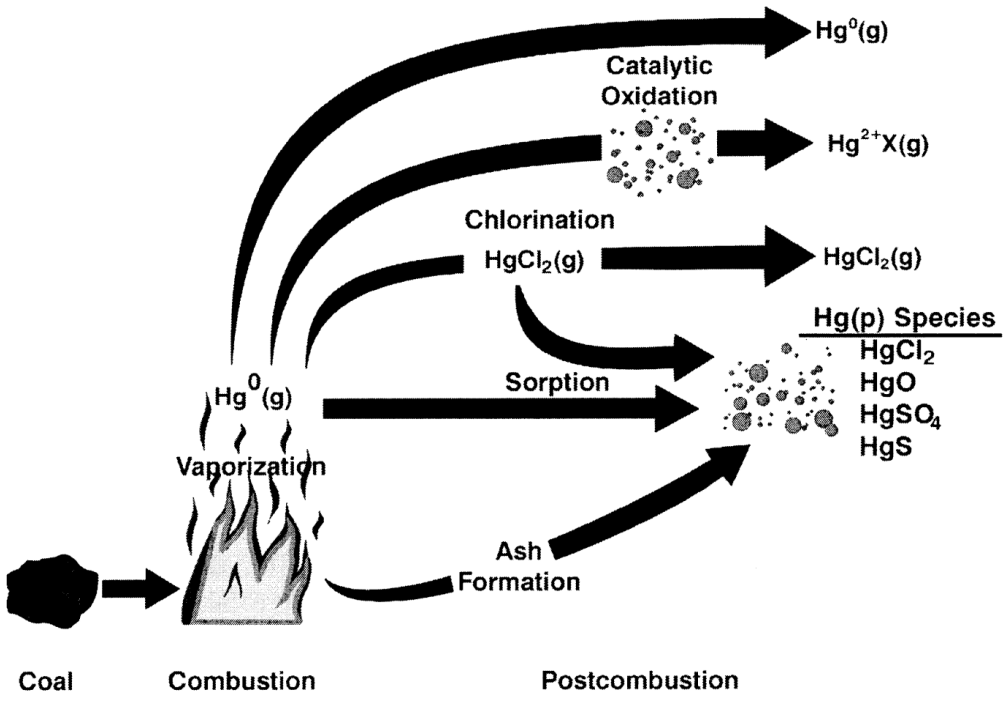

Figure 1.3. Mercury transformations during coal combustion.[29]

The transformed or transforming mercury will be sent with flue gas and fly ash to the clean devices. Mercury in different forms is going to experience different fates in the APCDs. As

discussed before, the particulate control devices will capture most of the particles discharged as pulverized fuel ash, correspondingly, most of the Hg_p species. SCRs are also effective in oxidizing Hg although the mechanism is unclear. The FGD gypsum, the sludge and the effluent of the wastewater treatment plant were found to carry some mercury, however, only Hg^{2+}, indicating the high ability of mercury capture of FGD system. The highest mercury removal efficiency of Coal-fired power plants equipped with ESP/FF, FGD and SCR systems reached 90 %. But this value varied for different coals. Table 1.3[31, 35, 36] extracted from the EPA reports listed the average mercury capture of the three coals by the different pollution control devices. In the end, it will still have a certain extent of mercury emitted as waste gas.[31]

Table 1.3. Average mercury capture of three types of coals by different APCD systems.[31, 35, 36]

Postcombustion control strategy	Postcombustion emission control device conFigureuration	Coal burned in PC-fired boiler unit		
		Bituminous (%)	Subbituminous (%)	Lignite (%)
Particulate matter (PM) control only	CS-ESP	36	9	1
	HS-ESP	14	7	/
	FF	90	72	/
	PS	/	9	/
PM control and spray dryer absorber (SDA)	SDA+ESP	/	43	/
	SDA+FF	98	25	2
	SDA+FF+SCR	98	/	/
PM control and wet flue gas desulfurization (FGD)	PS+FGD	12	10	/
	CS-ESP+FGD	81	29	48
	HS-ESP+FGD	46	20	/
	FF+FGD	98	/	/

From Kilgroe[35], et al. (2002), Staudt and Jozewicz[36] (2003).

CS-ESP, cold-side ESP; HS-ESP, hot-side ESP; PS, particle scrubber; FF, fabric filter.

1.2.5 Treatments for Mercury

Mercury treatment technologies develop based on the mercury source and mercury transformation mechanisms. Selective coal mining can minimize mercury from the original resources.[31] All the coals more or less contain mercury. Thus, selective coal mining is just a better choice instead of a treatment method. Coal cleaning is a necessary procedure to reduce many kinds of trace element emission before coal commbustion which has been discussed above. According the mercury behaviours in APCDs, the more Hg is oxidized, the higher the Hg capture efficiency will be. Combustion modification is therefore an influential factor for the total mercury removal outcome. Effective modifications of the combustion can result in higher mercury oxidization or higher quality fly ash.

Other technologies (APCDs) are classified as post-treatment methods. Even the APCDs contribute a lot to the mercury capture, the escaping mercury remains to be a terrible threat. Sorbent injection[31, 32, 37] is widely utilized either upstream or downstream as the compensation strategy. The most general used sorbents include activated carbon (ACs)/treated ACs, calcium based sorbents, petroleum coke and zeolites. All of these sorbents capture elemental mercury or catalyze mercury oxidization by means of active surface chemicals. Although sorbent injection is highly potential and applicable, its disadvantages should also be considered. The sorbents may pollute the by-products (e.g., fly ash, gypsum, fertilizer) if injected upstream of the ESP or FGD. Some sorbents may bring secondary pollution brought by the introduced contaminative or toxic elements. Therefore, more efforts should be made to develop more functional, safe and economic sorbents.

1.3 Sorbents for Elemental Mercury Removal

1.3.1 Adsorption mechanism

The large releasing of mercury from large consumption of coal and the incompletely capture of mercury during the post-treatment of the coal combustion residues determine that other means for mercury removal are needed. Over the past few decades, lots of sorbents aim at elemental mercury capture have been created, studies and optimized. All the sorbents adsorb elemental mercury through three mechanisms: physicsorption, chemisorption and amalgamation.

Elemental mercury can be physically bounded by electrostatic force and Van de Waals force onto the sorbent active sites.[30] This type of binding is not strong enough to resist the reverse release when the temperature increases. As for chemisorption, active chemicals or functional groups[38] on the sorbents can oxidize or catalyze the oxidization of elemental mercury to its mercurous or mercuric forms which are solvable and attachable, as a result, lowering the difficulty of removal. Compared to physisorption, chemisorption is more reliable and stable. The most active sites in the findings[39, 40] so far are halogen, S^{2-}, some metal oxides like iron oxides and vanadium pentoxide, etc. Huggins[41] studied the mercury adhered surface centers through X-ray absorption fine structure (XAFS) and X-ray Absorption Near Edge Structure (XANES) scanning which implied that only Hg^{2+} is adsorbed. Anionic groups such as I^-, Cl^-, S^{2-}, O^{2-}, and Se^{2-} donate electrons for incorporation with Hg^{2+}. In addition to physisorption and chemisorption, the special capacity of forming amalgamation with some noble metals enables the third adsorption method of capturing mercury.[42] The difference between physisorption and amalgamation is that the former one is weak and the temperature barrier is very low. However, amalgamation provides strong binding and allows the release of the mercury at high temperature

(at least above 300 °C) for recycling. The most effective noble metals include gold, silver, platinum, palladium, etc.

1.3.2 Efficient Sorbents for Elemental Mercury Capture

The choosing of sorbents usually take three aspects into account: cost, selectivity for mercury during the short residence time and the environmental concerns. So far, lots of findings[32, 37, 43] use activated carbons, carbon-based materials, calcium-based materials, coke, fly ash, zeolites, porous silicon as the carriers of the active chemicals or groups for elemental mercury removal. These materials have two common characters: porosity and large surface area, which are considered to be advantageous for high removal efficiencies.

ACs and treated ACs have long been applied in industries for toxic chemicals and heavy metals adsorption. They are generally injected upstream of the ESPs or FF baghouse and then are collected in the hoppers. Surface functional groups (e.g., OH, C−O, C=O, COOH) or groups containing inorganic elements (e.g., Cl, Br, S) on the moisture-containing ACs contribute a lot to the reactions with Hg^0 as well as the binding for Hg^0 that both physisorption and chemisorption take place.[37] However, chemisorption is the dominant process. Besides, ACs were also found to serve as the electrode if the Hg^0 adsorption involves electron transfer reaction. Even though ACs are favourable for Hg^0 elimination, the efficiencies of ACs vary in a wide range as the elemental mercury transformations are highly changeable over the coal types, combustion regime, flue gas temperature and compositions, etc. And the cost for ACs is very high in the coal plants. Therefore, novel ACs are impregnated with effective materials to enhance the performance, such as chlorine[44], bromine[45] and sulfur[46] impregnated ACs, metal chlorides[47] (e.g., $ZnCl_2$, $CoCl_2$, $MnCl_2$) modified ACs, metal oxides[48] (e.g., Co_3O_4, MnO_2) modified ACs, etc. All these modified ACs showed significant improvement in simulated flue gas Hg^0 capture compared to

virgin commercial ACs. In Shen et al.'s study[47], metal chlorides demonstrated better mercury adsorption capacities over the same metal oxides.

Other carbon-based sorbents like coke are being developed in the past few years to lower down the high cost of ACs. Activated coke[12, 49], for instance, pyrolyzed petroleum coke, is used as sorbent for Hg^0. The contained sulfur shifts from inside to the surface during the activation, and plays the main role of capturing mercury. Although the capacity of activated coke is lower than ACs, it costs much less than ACs. Hence, activated coke has been used as cheap resource to be modified to enhance the capability for Hg^0 removal. Hua et al.[50] introduced CeO_2 into the activated coke which achieved high efficiencies at room temperature in simulated flue gases. $CeCl_3$ was utilized by Tao et al.[51] to improve the activated coke performance also in the simulated flue gases but at higher temperatures and showed better mercury capture as expected. Based on the influence brought by different flue gases, activated coke can be applied for some coals specifically.

Fly ash produced during the coal combustion can also serve as the Hg^0 sorbent. Due to the differences in the coals and combustion conditions, the components of fly ash are quite complicated. Dunham[39] investigated the interactions between $Hg^0/HgCl_2$ and the 16 different fly ashes in fixed-bed simulated flue gases at 121 and 177 °C. Not all the fly ash had the $Hg^0/HgCl_2$ selectivity. Since well performed fly ashes were found to be rich in carbon and iron oxides while poor performed fly ashes did not contain much of these components, the neglectable mercury capture ability was suggested to be attributed to the lack of active catalyzers like carbon and iron oxides in the fly ashes. Besides, large surface area was another positive influential factor of both the physisorption and chemisorption of $Hg^0/HgCl_2$. Massive source of fly ash from coal-fired power plants makes it a potential material for mercury capture. But, extra burden to the APCDs

system brought by fly ash sorbent injection should be considered. Efforts are still needed to create the more effective fly ash so as to reduce the dosage.

Calcium-based sorbents are proposed for co-adsorption of SO_2 and mercury as hydrated lime is largely used in the FGD system. Original hydrated lime is weak in mercury adsorption so that adding active sites and oxidative catalyzers is necessary. Ghorishi et al.[52] incorporated lime with four different oxidants to simultaneously react with SO_2 and oxidize Hg^0. These kind of technologies can save the cost for sorbent injection but are still under upgrade.

Zeolites are natural aluminosilicates that also carry other atoms like Ca, Fe, Cu, etc. The special tetrahedral structure makes them famous for their gas separation capacities. Natural zeolites are cheap, safe, with large surface areas, and are easy to be modified through ion exchange or direct deposition. Novel zeolites[53, 54] are therefore treated to activate the abundant metal or metal oxides to remove Hg^0. So far, silver modified zeolites, sulfur modified zeolites and so on have been tested for their attraction towards Hg^0.

In addition to the conventional sorbents, novel sorbents are developed to fulfill the requirements current and future demands of mercury releasing. For examples, Qu et al.[55] studied bromine chloride (BrCl) and employed the material under simulated flue gas conditions. Pitoniak et al.[56] investigated the photocatalytic oxidation effect of Hg^0 by SiO_2-TiO_2 composites. Moreover, there are more and more researches try to create multipollutant control sorbents which target Hg^0 and other pollutants. V_2O_5-ACs[43] was able to simultaneously remove SO_2, NO_2 and Hg^0 in the flue gases. $V_2O_5(WO_3)/TiO_2$ was developed to capture Hg^0 and also reduce the NO[57]. Even great progress has been made for Hg^0 removal, the more effective, environmental friendly, and cost-efficient sorbents need to be developed.

1.3.3 Grphene Oxide for Hg^0 Adsorption

Graphene oxide (GO) derived from graphite is the graphene sheets with oxygen containing functional groups (e.g., hydroxyl groups, carbolic acid groups) on the basal planes and edges.[58] A typical model of GO structure is shown in Figure 1.4.[59] GO is famous for its outstanding properties, such as large surface area and good electrical conductivity, which make it a popular support material nowadays.[60] By far, the performance of graphene oxide is found to be enhanced by functionalization with various materials. Graphene oxide has been previously utilized as the host material for both organic and inorganic catalysts in water purification.[61] For instance, an effective polypyrrole-reduced GO (RGO) composite is developed by Chandra and Kim to treat the Hg^{2+} polluted water and achieved maximum 980 mg/g adsorption ability.[62]

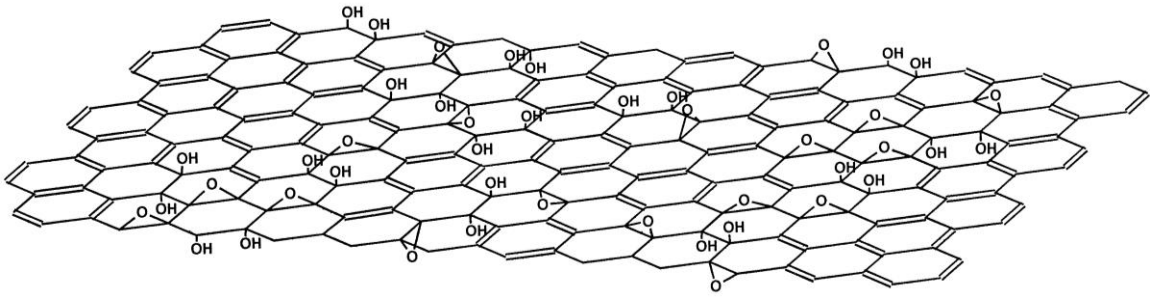

Figure 1.4. Structure model of graphene oxide.[59]

However, to my best knowledge, there is no report about applying GO or functionalized GO in gas purification, especially Hg^0 treatment. As GO has large specific surface area and abundant surface oxygen-containing functional groups which may facilitate further functionalization, it should be suitable to be applied as the alternative adsorbent substrate. Based on the previous discussion, active Hg^0 adsorption reagents can be combine with GO to create novel adsorbents. To create cost-efficient and effective adsorbents, recycling of the adsorbents is recommended.

1.4 Objectives and Thesis Outline

The industry still needs efficient and cost-efficient adsorbents for Hg^0 removal. However, only a few researches have been conducted on the recycling of the injected adsorbents. Additionally, the graphene oxide has not been explored for its Hg^0 adsorption capability before. In this regard, the project objectives mainly include three aspects, including creating novel effective adsorbents (based on GO) for Hg^0 adsorption, realizing the adsorbent separation as well as adsorbent regeneration, and investigating the influential factors for the Hg^0 adsorption performance.

With the three main objectives listed above, the outline of this thesis is very clear. Chapter 1 provides an overall and comprehensive introduction of the mercury emissions from coal-fired power plant, the toxicity of mercury, the transformation and destiny of mercury in the APCDs, and the treatment applied on mercury control so far. Chapter 2 and Chapter 3 present the efforts made to achieve the project objectives: In Chapter 2, composites of Ag nanoparticles, magnetic ferrite nanoparticles and GO were synthesized for efficient Hg^0 adsorption and adsorbent regeneration; Chapter 3 explores the Hg^0 adsorption performance of three metal oxides modified adsorbents and their adsorption capabilities. Chapter 4 is a summary of the work which also suggests the perspectives of the future development.

1.5 Reference

(1) Chauhan, D. S.; Srivastava, S. K., *Non-Conventional Energy Resources.* 2 ed.; New Age International: 2007; p 2-17.

(2) Bhattacharyya, S. C., *Energy Economics*

Concepts, Issues, Markets and Governance. 1 ed.; Springer: 2011; p 9-11.

(3) Shafiee, S.; Topal, E. An Econometrics View of Worldwide Fossil Fuel Consumption and the Role of US. *Energy. Policy.* **2008,** *36* (2), 775-786.

(4) Patzek, T. W.; Croft, G. D. A Global Coal Production Forecast with Multi-Hubbert Cycle Analysis. *Energy.* **2010,** *35* (8), 3109-3122.

(5) Teske, S.; Pregger, T.; Simon, S.; Naegler, T.; Graus, W.; Lins, C. Energy [R] Evolution 2010-a Sustainable World Energy Outlook. *Energy Efficiency* **2010,** *4* (3), 409-433.

(6) Liu, C. H.; Zhou, Z. D.; Yu, X.; Lv, B. Q.; Mao, J. F.; Xiao, D. Preparation and Characterization of Fe_3O_4/Ag Composite Magnetic Nanoparticles. *Inorg. Mater.* **2008,** *44* (3), 291-295.

(7) Meij, R.; te Winkel, B. The Emissions and Environmental Impact of PM10 and Trace Elements from a Modern Coal-Fired Power Plant Equipped with ESP and Wet FGD. *Fuel Process. Technol.* **2004,** *85* (6-7), 641-656.

(8) Chen, J.-C.; Liu, Z.-S.; Huang, J.-S. Emission Characteristics of Coal Combustion in Different O_2/N_2, O_2/CO_2 and O_2/RFG Atmosphere. *J. Hazard. Mater.* **2007,** *142* (1-2), 266-271.

(9) Bose, A. C.; Dannecker, K. M.; Wendt, J. O. L. Coal Composition Effects on Mechanisms Governing the Destruction of Nitric Oxide and Other Nitrogenous Species during Fuel-Rich Combustion. *Energy. Fuels.* **1988,** *2* (30), 301-308.

(10) Chagué-G, C.; Fyfe, W. S. Geochemical and Petrographical Characteristics of a Domed Bog, Nova Scotia a Modern Analogue for Temperature Coal Deposits. *Org. Geochem.* **1996,** *24* (2), 141-158.

(11) Vejahati, F.; Xu, Z.; Gupta, R. Trace Elements in Coal: Associations with Coal and Minerals and Their Behavior during Coal Utilization-A review. *Fuel.* **2010,** *89* (4), 904-911.

(12) Lee, S.; Rhim, Y.; Cho, S.; Baek, J. Carbon-Based Novel Sorbent for Removing Gas-Phase Mercury. *Fuel.* **2006,** *85* (2), 219-226.

(13) Carlson, C. L.; Adriano, D. C. Environmental Impacts of Coal Combustion Residues. *J. Environ. Qual.* **1993,** *22* (2), 227-247.

(14) Skorek-Osikowska, A.; Kotowicz, J.; Janusz-Szymańska, K. Comparison of the Energy Intensity of the Selected CO_2 Capture Methods Applied in the Ultra-Supercritical Coal Power Plants. *Energ. Fuel.* **2012,** *26* (11), 6509-6517.

(15) Finkelman, R. B.; Orem, W.; Castranova, V.; Tatu, C. A.; Belkin, H. E.; Zheng, B.; Lerch, H. E.; Maharaj, S. V.; Bates, A. L. Health Impacts of Coal and Coal Use Possible Solutions. *Int. J. Coal Geol.* **2002,** *50* (1-4), 425-443.

(16) Finkelman, R. B. Trace Elements in Coal. *Biol. Trace Elem. Res.* **1999,** *67* (3), 197-204.

(17) News Releases from Headquarters. http://yosemite.epa.gov/opa/admpress.nsf/bd4379a92ceceeac8525735900400c27/5bb6d20668b9a18485257ceb00490c98!OpenDocument (accessed July 19, 2014).

(18) Alberta Energy: Coal Acts and Regulations. http://www.energy.alberta.ca/coal/664.asp (accessed July 19, 2014).

(19) Jaworek, A.; Krupa, A.; Czech, T. Modern Electrostatic Devices and Methods for Exhaust Gas Cleaning: A Brief Review. *J. Electrostat.* **2007,** *65* (3), 133-155.

(20) Srivastava, R. K.; Jozewicz, W. Flue Gas Desulfurization: The State of the Art. *J. Air. Waste. Manage.* **2001,** *51* (12), 1676-1688.

(21) Srivastava, R. K.; Hall, R. E.; Khan, S.; Culligan, K.; Lani, B. W. Nitrogen Oxides Emission Control Options for Coal-Fired Electric Utility Boilers. *J. Air & Waste Manage. Assoc.* **2005,** *55* (9), 1367-1388.

(22) Barman, S.; Philip, L. Integrated System for the Treatment of Oxides of Nitrogen from Flue Gasea. *Environ. Sci. Technol.* **2006,** *40* (3), 1035-1041.

(23) Xu, M. Status of Trace Element Emission in a Coal Combustion Process: A Review. *Fuel Process. Technol.* **2004,** *85* (2-3), 215-237.

(24) Clarkson, T. W.; Magos, L. The Toxicology of Mercury and Its Chemical Compounds. *Crit. Rev. Toxicol.* **2006,** *36* (8), 609-662.

(25) Pirrone, N.; Cinnirella, S.; Feng, X.; Finkelman, R. B.; Friedli, H. R.; Leaner, J.; Mason, R.; Mukherjee, A. B.; Stracher, G. B.; Streets, D. G.; Telmer, K. Global Mercury

Emissions to the Atmosphere from Anthropogenic and Natural Sources. *Atmos. Chem. Phys.* **2010,** *10* (13), 5951-5964.

(26) Meij, R.; Vredenbregt, L. H. J.; Winkel, H. t. The Fate and Behavior of Mercury in Coal-Fired Power Plants. *J. Air. Waste. Manage.* **2002,** *52* (8), 912-917.

(27) Meij, R. The Fate of Mercury in Coal-Fired Power Plants and the Influence of Wet Flue-Gas Desulphurization. *Water, Air, Soil Pollut.* **1991,** *56* (1), 21-33.

(28) Toole-O'Neil, B.; Tewalt, S. J.; Finkelman, R. B.; Akers, D. J. Mercury Concentration in Coal-Unraveling the Puzzle. *Fuel.* **1999,** *78* (1), 47-54.

(29) Galbreath, K. C.; Zygarlicke, C. J. Mercury Transformations in Coal Combustion Flue Gas. *Fuel Process. Technol.* **2000,** *65-66*, 289-310.

(30) Pavlish, J. H.; Sondreal, E. A.; Mann, M. D.; Olson, E. S.; Galbreath, K. C.; Laudal, D. L.; Benson, S. A. Status Review of Mercury Control Options for Coal-Fired Power Plants. *Fuel Process. Technol* **2003,** *82* (2-3), 89-165.

(31) Yudovich, Y. E.; Ketris, M. P. Mercury in Coal: A Review Part 2. Coal Use and Environmental Problems. *Int. J. Coal. Geol.* **2005,** *62* (3), 135-165.

(32) Yang, H.; Xu, Z.; Fan, M.; Bland, A. E.; Judkins, R. R. Adsorbents for Capturing Mercury in Coal-Fired Boiler Flue Gas. *J. Hazard. Mater.* **2007,** *146* (1-2), 1-11.

(33) Senior, C. L.; Sarofim, A. F.; Zeng, T.; Helble, J. J.; Mamani-Paco, R. Gas-phase Transformations of Mercury in Coal-Fired Power Plants. *Fuel Process. Technol.* **2000,** *63* (2), 197-213.

(34) Hsi, H.-C.; Chen, C.-T. Influences of Acidic/Oxidizing Gases on Elemental Mercury Adsorption Equilibrium and Kinetics of Sulfur-Impregnated Activated Carbon. *Fuel.* **2012,** *98*, 229-235.

(35) Kilgroe, J. D.; Sedman, C. B.; Srivastava, R. K.; Ryan, J. V.; Lee, C. W.; Thorneloe, S. A. *Control of Mercury Emissions from Coal-Fired Electric Utility Boilers: Interim Report. U.S.*; 2002.

(36) Staudt, J. E.; Jozewicz, W. *Performance and Cost of Mercury and Multipollutant Emission Control Technology Applications on Electric Utility Boilers.*; 2003.

(37) Reddy, B. M.; Durgasri, N.; Kumar, T. V.; Bhargava, S. K. Abatement of Gas-Phase Mercury-Recent Developments. *Catal. Rev.* **2012,** *54* (3), 344-398.

(38) Sun, X.; Hwang, J.-Y.; Xie, S. Density Functional Study of Elemental Mercury Adsorption on Surfactants. *Fuel.* **2011,** *90* (3), 1061-1068.

(39) Dunham, G. E.; DeWall, R. A.; Senior, C. L. Fixed-Bed Studies of the Interactions between Mercury and Coal Combustion Fly Ash. *Fuel Process. Technol.* **2003,** *82* (2-3), 197-213.

(40) Dranga, B.-A.; Lazar, L.; Koeser, H. Oxidation Catalysts for Elemental Mercury in Flue Gases-A Review. *Catalysts.* **2012,** *2* (4), 139-170.

(41) Huggins, F. E.; Yap, N.; Huffman, G. P.; Senior, C. L. XAFS Characterization of Mercury Captured from Combustion Gases on Sorbents at Low Temperatures. *Fuel Process. Technol.* **2003,** *82* (2-3), 167-196.

(42) Presto, A. A.; Granite, E. J. Noble Metal Catalysts for Mercury Oxidation in Utility Flue Gas. *Platinum Met. Rev*. **2008,** *52* (3), 144-154.

(43) Liu, Y.; Bisson, T. M.; Yang, H.; Xu, Z. Recent Developments in Novel Sorbents for Flue Gas Clean Up. *Fuel Process. Technol* **2010,** *91* (10), 1175-1197.

(44) Ghorishi, S. B.; Keeney, B. K. Development of a Cl-Impregnated Activated Carbon for Entrained-Flow Capture of Elemental Mercury. *Environ. Sci. Technol.* **2002,** *36* (20), 4454-4459.

(45) Hutson, N.; Atwood, B.; Scheckel, K. XAS and XPS Characterization of Mercury Binding on Brominated Activated Carbon. *Environ Sci. Technol.* **2007,** *41* (5), 1747-1752.

(46) Hsi, H.-C.; Rood, M. J.; Rostam-Abadi, M.; Chen, S.; Chang, R. Effects of Sulfur Impregnation Temperature on the Properties and Mercury Adsorption Capacities of Activated Carbon Fibers (ACFs). *Environ Sci. Technol.* **2001,** *35* (13), 2785-2791.

(47) Shen, Z.; Ma, J.; Mei, Z.; Zhang, J. Metal Chlorides Loaded on Activated Carbon to Capture Elemental Mercury. *J. Environ. Sci.* **2010,** *22* (11), 1814-1819.

(48) Mei, Z.; Shen, Z.; Zhao, Q.; Wang, W.; Zhang, Y. Removal and Recovery of Gas-Phase Element Mercury by Metal Oxide-Loaded Activated Carbon. *J. Hazard. Mater.* **2008,** *152* (2), 721-729.

(49) Olson, D. G.; Tsuji, K.; Shiraishi, I. The Reduction of Gas Phase Air Toxics from Combustion and Incineration Sources Using the MET-Mitsui-BF Activated Coke Process. *Fuel Process. Technol.* **2000,** *65-66*, 393-405.

(50) Hua, X.-y.; Zhou, J.-s.; Li, Q.; Luo, Z.-y.; Cen, K.-f. Gas-Phase Elemental Mercury Removal by CeO_2 Impregnated Activated Coke. *Energ. Fuel.* **2010,** *24* (10), 5426-5431.

(51) Tao, S.; Li, C.; Fan, X.; Zeng, G.; Lu, P.; Zhang, X.; Wen, Q.; Zhao, W.; Luo, D.; Fan, C. Activated Coke Impregnated with Cerium Chloride Used for Elemental Mercury Removal from Simulated Flue Gas. *Chem. Eng. J.* **2012,** *210*, 547-556.

(52) Ghorishi, S. B.; Singer, C. F.; Jozewicz, W. S.; Sedman, C. B.; Srivastava, R. K. Simultaneous Control of Hg^0, SO_2, and NO_x by Novel Oxidized Calcium-Based Sorbents. *J. Air. Waste. Manage.* **2002,** *52* (3), 273-278.

(53) Hsi, H.-C.; Rood, M. J.; Rostam-Abadi, M.; Chen, S.; Chang, R. Mercury Adsorption Properties of Sulfur-Impregnated Adsorbents. *J. Environ. Eng.* **2002,** *128* (11), 1080-1089.

(54) Liu, Y.; Kelly, D. J. A.; Yang, H.; Lin, C. C. H.; Kuznicki, S. M.; Xu, Z. Novel Regenerable Sorbent for Mercury Capture from Flue Gases of Coal-Fired Power Plant. *Environ. Sci. Technol.* **2008,** *42* (16), 6205-6210.

(55) Qu, Z.; Yan, N.; Liu, P.; Chi, Y.; Jia, J. Bromine Chloride as an Oxidant to Improve Elemental Mercury Removal from Coal-Fired Flue Gas. *Environ. Sci. Technol.* **2009,** *43* (22), 8610-8615.

(56) Pitoniak, E.; Wu, C.-Y.; Londeree, D.; Mazyck, D.; Bonzongo, J.-C.; Powers, K.; Sigmund, W. Nanostructured Silica-Gel Doped with TiO_2 for Mercury Vapor Control. *J. Nanopart. Res.* **2003,** *5* (3-4), 281-292.

(57) Kamata, H.; Ueno, S.-i.; Naito, T.; Yukimura, A. Mercury Oxidation Over the V_2O_5 (WO_3)/TiO_2 Commercial SCR Catalyst. *Ind. Eng. Chem. Res.* **2008,** *47* (21), 8136-8141.

(58) Dreyer, D. R.; Park, S.; Bielawski, C. W.; Ruoff, R. S. The Chemistry of Graphene Oxide. *Chem. Soc. Rev.* **2010,** *39* (1), 228.

(59) He, H.; Klinowskia, J.; Forsterb, M.; Lerf, A. A New Structural Model for Graphite Oxide. *Chem. Phys. Lett.* **1998,** *287* (1-2), 53-56.

(60) Xu, C.; Wang, X. Fabrication of Flexible Metal-Nanoparticle Films Using Graphene Oxide Sheets as Substrates. *Small.* **2009,** *5* (19), 2212-2217.

(61) Sreeprasad, T. S.; Maliyekkal, S. M.; Lisha, K. P.; Pradeep, T. Reduced Graphene Oxide-Metal/Metal Oxide Composites: Facile Synthesis and Application in Water Purification. *J. Hazard. Mater.* **2011,** *186* (1), 921-931.

(62) Chandra, V.; Kim, K. S. Highly Selective Adsorption of Hg^{2+} by a Polypyrrole-Reduced Graphene Oxide Composite. *Chem. Commun.* **2011,** *47* (13), 3942.

CHAPTER 2 Composites of Graphene Oxide, Ag Nanoparticles, and Magnetic Ferrite Nanoparticles for Elemental Mercury (Hg^0) Removal[i]

2.1 Abstract

Mercury emission from combustion flue gas causes considerable environmental challenges and serious adverse health threats, and elemental mercury (Hg^0) is the most challenging chemical form for removal. In this work, four types of graphene oxide (GO) based composite adsorbents were successfully synthesized by depositing Ag nanoparticles (NPs) and/or magnetic ferrite NPs on GO sheets (denoted as GO, GO-Ag, MGO and MGO-Ag), characterized and applied for the removal of Hg^0 for the first time. The presence of Ag NPs on GO greatly enhances the Hg^0 removal capability of GO-Ag and MGO-Ag as compared to that of pure GO, which is mainly attributed to the amalgamation of Hg^0 on Ag NPs. MGO-Ag shows the best Hg^0 removal performance and thermal tolerance among the four types of adsorbents developed, which can effectively capture Hg^0 up to 150-200 ^oC in simulated flue gas environment and can be also effectively recycled and reused. Our results indicate that the graphene oxide based composites (i.e. MGO-Ag) have significant potential applications for mercury emission control in coal-fired power plant.

Key words: Graphene oxide, Hg^0 adsorption, Ag nanoparticles, Magnetic nanoparticle, Adsorbents

[i]A version of this chapter has been submitted to *ACS Applied Materials & Interfaces* in 2014.

2.2 Introduction

As one of the most abundant fossil fuels, coal is the dominant energy source for production of electricity and heat through coal-fired power plants worldwide. However, coal combustion causes considerable environmental challenges and serious health threats by emissions of particulate matters (< 10 μm) and toxic trace elements (especially mercury).[1-3] Mercury finds its way out in emissions through precipitation and bioaccumulation, which results in serious health problems.[4, 5] Mercury presents as three major chemical forms in combustion flue gas: elemental (Hg^0), particulate-bound (Hg_p) and oxidized (Hg^{2+}) form.[6-9] Hg^{2+} and Hg_p can be relatively easily eliminated by air pollution control devices (APCDs). However, Hg^0 is much more difficult to be removed, due to its high equilibrium vapor pressure and low water solubility.[7, 10-12] Generally, a considerable proportion (20%-85%) of Hg^0 remained in the flue gas released from post-treatment systems,[9] resulting in an intractable challenge for Hg^0 removal.

Much effort has been devoted to the development of efficient adsorbents to remove mercury from combustion flue gas. To be efficient and qualified adsorbents, some basic prerequisites need to be satisfied: large specific surface area which ensures sufficient contact between adsorbents and mercury, high degree of surface reactivity to guarantee a suitable mercury adsorption capacity. Therefore, porous materials[13-16] such as activated carbons, zeolite, and mesoporous silica have been extensive explored as scaffolds to impregnate active chemicals including chlorine, sulfur, bromide, iodine and notable metals, and are employed as adsorbents.[13, 17, 18] However, most of these sorbents are difficult to regenerate due to the strong chemical interactions involved in mercury adsorption, thereby incurring high operating costs. Therefore, it will be of paramount benefit to explore a novel scaffold and develop an efficient mercury adsorbent with feasible recycling ability under suitable regeneration temperature, which will not

only greatly enhance the mercury removal performance but also significantly reduce the operation cost of sorbent injection.

Graphene oxide (GO) derived from graphene has received much attention over the past few years as a novel adsorbent substrate for various applications due to its outstanding features,[19] such as large specific surface area, high water dispersibility, and good surface functionalization feasibility. Taking advantage of their abundant functional groups and large surface areas, various functionalized GO composites, such as polypyrrole-reduced GO (RGO), RGO-MnO_2, RGO-Ag and RGO-SnO_2 composites, have been applied for removal of Hg^{2+} in water treatment and detection of Hg^{2+}.[20, 21] According to previous reports,[22-24] metal or metal oxide nanoparticles are some of the most intensively-studied Hg^0 adsorbents. In particular, notable nanoparticles, such as silver and gold, are the most intriguing ones,[19, 23, 25] which can efficiently capture mercury vapour by forming Ag-Hg or Au-Hg amalgam at a temperature close to flue gas conditions and can be regenerated by release of captured mercury through thermal treatment, providing a feasible way to regenerate mercury adsorbents. Meanwhile, surface functional groups (e.g., hydroxyl, epoxy, carboxyl) on adsorbents have been reported as active sites for Hg^0 adsorption.[26] Thus, GO composites decorated with notable nanoparticles are expected to have great potential in mercury removal from coal flue gas. Yet, to date, no study has been reported on exploitation of GO based composites to remove mercury from flue gases.

Herein, we explored the possibility of applying GO as a new scaffold to develop a regenerable mercury sorbent for the first time. By incorporating silver and magnetic nanoparticles on GO surfaces, GO and several GO based composites including magnetic nanoparticle-GO (MGO), silver nanoparticle-GO (GO-Ag), and MGO-Ag were synthesized, characterized and applied to remove Hg^0 under various temperatures. The recyclability of MGO-

Ag was investigated and its Hg^0 adsorption capacity was also explored in simulated combustion gases.

2.3 Experiment Section

2.3.1 Materials

Graphite flakes with a median of 7-10 micron, sulfuric acid (H_2SO_4, 95.0-98.0 wt.%), sodium nitrate ($NaNO_3$), hydrogen peroxide (H_2O_2, 29-32% w/w aq.) and poly(-*N*-vinyl-2-pyrrolidone) (PVP, average M.W. 58000) were purchased from Alfa Aesar. α-D-Glucose (96%), iron (III) chloride hexahydrate ($FeCl_3 \cdot 6H_2O$) and iron (II) chloride tetrahydrate ($FeCl_2 \cdot 4H_2O$) were supplied by Sigma-Aldrich. Potassium permanganate ($KMnO_4$), ammonia solution (29.5 wt.%) and silver nitrate ($AgNO_3$) were provided by Fisher Scientific.

2.3.2 Synthesis of GO

GO was prepared according to Hummer's method.[27] Firstly, H_2SO_4 (98 wt.%, 150 mL) was added to a three-neck flask with graphite powder (2 g) and $NaNO_3$ (1.5 g) in an ice bath, then $KMnO_4$ (9.1 g) was gradually added and vigorously stirred for 5 days. Afterwards, H_2O_2 (30 wt.%, 6 mL) was added directly and the resulted solution was slowly diluted with a mixture of 500 mL deionization (DI) water, H_2SO_4 (98%, 15 mL) and H_2O_2 (30 wt.%, 8.35 mL), in which the color of the suspension would change to brilliant yellow. Then, the resultant was centrifuged and washed several times with DI water, followed by dialysis against 2 L DI water with water exchange every 4 hours for 2 days. Finally, loose brownish black powders were obtained after freeze drying.

2.3.3 Synthesis of GO-Ag

GO-Ag composites were synthesized according to a revised procedure based on a previous report[28] and briefly described as follows: a homogeneous aqueous mixture of GO (0.5 mg/mL, 100 mL) was obtained after 45 min ultrasonical exfoliation. Then, PVP solution (4 mg/mL, 20 mL) and glucose (1.6 g) were added sequentially under vigorous stirring. Afterwards, a silver-ammonia aqueous solution (18.7 mg/mL, 20mL) was added to the above mixture at 60 °C. The reaction was held at this temperature for 7 min. Finally, GO-Ag composites were collected by centrifuging and purified with thoroughly washing with ethanol and DI water for several times. Followed by freeze drying, the dry GO-Ag composites were reclaimed as grey black powders.

2.3.4 Synthesis of MGO and MGO-Ag

MGO composites were synthesized following a modified procedure based on a recent report[29] and the details were shown as follows. An aqueous solution of $FeCl_3$ and $FeCl_2$ in 2:1 mole ratio was added to a homogenous aqueous solution of GO (5 mg/mL, 50 mL) prepared via 45 min ultrasonication treatment at room temperature. The whole system was heated to 90 °C, and pH of the mixture was adjusted to 10 by using 30 wt.% ammonia solution. After being vigorously stirred for 40 min, the solution was cooled down to room temperature. The resulting black composites were collected by a magnet and washed thoroughly with copious amount of DI water and then reclaimed by freeze drying, and the final product was denoted as MGO. MGO-Ag was synthesized by the same procedure as that for GO-Ag with MGO as the initial reactant.

2.3.5 Material Characterizations

The morphologies of the as-prepared GO and GO-nanoparticle composites were characterized by field emission-scanning electron microscopy (FE-SEM) using a JAMP-9500F

(Jeol, Japan) and transmission electron microscopy (TEM) using a Philips/FEI Morgagni microscope at 80 kV. The element compositions of all composites were analyzed by X-ray diffraction (XRD) on a Rigaku Ultima IV X-ray diffractometer using Cu Kα irradiation (k = 1.5406 Å) and X-ray photoelectron spectroscopy (XPS) on an AXIS 165 spectrometer (Kratos Analytical). Magnetic hysteresis measurements were performed on a Quantum Design 9T-PPMS magnetometer at 300K under an applied field of 5000 Oe. Thermal gravimetric analysis (TGA) was conducted on a TA instrument SDT Q600 to measure the thermal properties of GO.

2.3.6 Mercury Breakthrough Test

The mercury breakthrough experiments were carried out by using a Tekran 2500 Cold Vapor Atomic Fluorescence Spectrophotometer (CVAFS).[23] The details about CVAFS measurement setup are given in Scheme 2.1 (Supporting Information). 15 mg GO based adsorbents were precisely weighed and loaded into a borosilicate glass u-tube with an inner diameter of 4 mm, held into a GC oven which was used to control the temperature for the adsorbents to capture Hg^0. 200μL of Hg^0 standard vapor at room temperature was injected into the system with an argon flow rate of 40 mL/min and exposed to loaded adsorbent in each test. A GB trap filled with gold beads (GB) and wrapped with a heating wire was applied to capture the Hg^0 escaped from the upstream adsorbent and would be heated later to release the Hg^0 to a downstream Hg^0 detector-CVAFS. The mercury breakthrough value was correspondingly calculated as the ratio between the amount of Hg^0 that has not been captured by the loaded composite adsorbent under designed experimental conditions and the total amount of Hg^0 injected.

2.4 Results and Discussions

2.4.1 Characterizations of the developed GO nanoparticle composites

The morphologies of the as-prepared GO, GO-Ag, MGO and MGO-Ag were characterized by FE-SEM and TEM. The FE-SEM and TEM images of GO (Figure 2.1a and Figure 2.8e in Supporting Information) show a typical morphology of thin sheets with some wrinkles that is consistent with previous reports.[30, 31] A relatively uniform distribution of Ag NPs with an average particle size of 50 nm on GO surfaces can be observed and shown in the FE-SEM (Figure 2.1b) and TEM images of GO-Ag (Figure 2.1c). It should be noted that by tuning the initial concentration of $[Ag(NH_3)_2]OH$ added, Ag-GO composites with different silver loadings could be easily achieved (see Figure 2.8a and Figure 2.8b in Supporting Information) while would not lead to significant size variation of the Ag NPs deposited. Figure 2.1e shows TEM image of as-prepared MGO-Ag which exhibits massive ultra-fine magnetic nanoparticles around 10 nm uniformly dispersed with Ag NPs on GO substrates, indicating the successful deposition of both Ag and magnetic NPs on GO surfaces, as further confirmed by TEM coupled with energy dispersive X-ray spectroscopy (TEM-EDX) showing a homogeneous and dense mapping of Fe and Ag elements on GO sheets in Figure 2.1f.

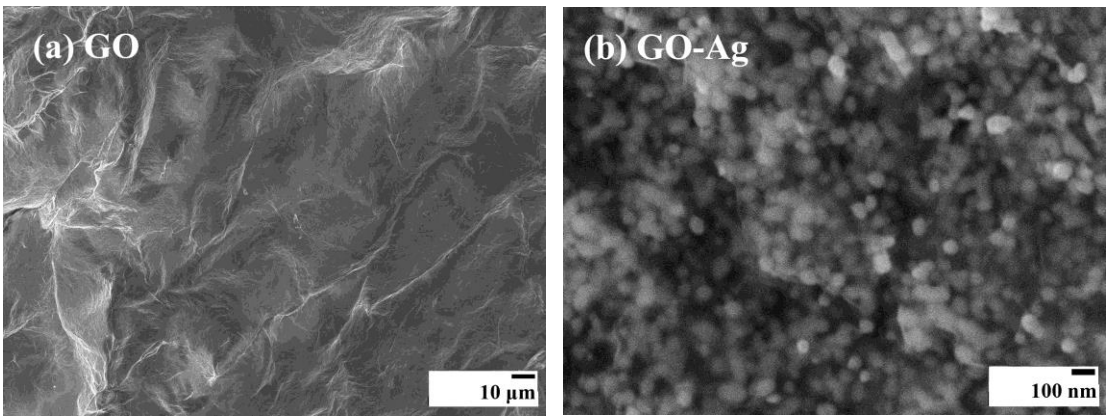

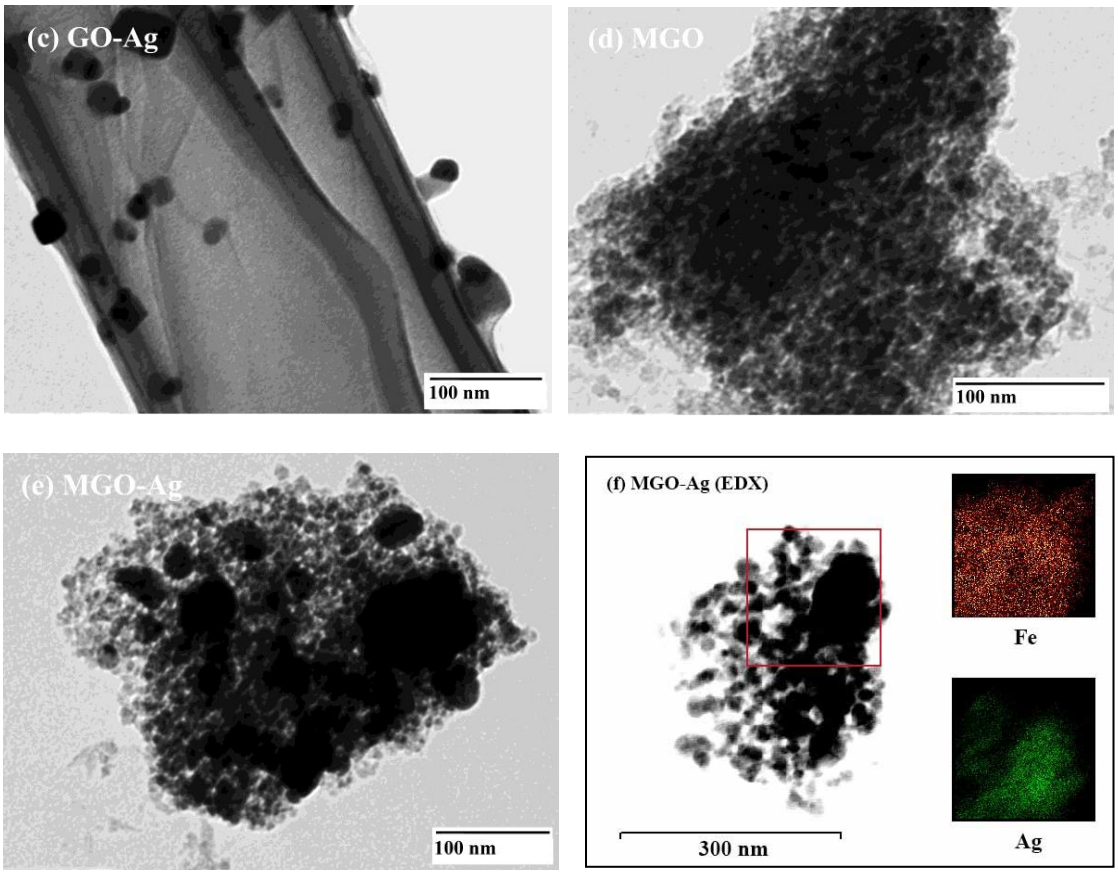

Figure 2.1. FE-SEM images of (a) GO, (b) GO-Ag. TEM images of (c) GO-Ag, (d) MGO, (e) MGO-Ag, and (f) TEM-EDX spectra of Fe, Ag on MGO-Ag.

To further verify the successful synthesis of the GO composites and evaluate the compositions of the NPs, XRD and XPS characterizations were conducted. The XRD patterns of GO, GO-Ag, GO-1/2Ag, GO-1/4Ag, MGO and MGO-Ag are displayed in Figure 2.2a. GO shows a clear diffraction peak at 9.92°, indicating an expanded GO interlayer spacing of 0.89 nm calculated from Bragg Equation. Compared with the ~0.34 nm d-spacing of the pristine graphite, the d-spacing of GO is much larger due to the addition of surface oxygen-containing functional groups.[31, 32] Comparing the XRD spectra of GO and GO-nanoparticle composites, a typical diffraction peak for GO at 9.92° was absent in the GO-nanoparticle composites, revealing further

exfoliation of GO sheets by ultrasonication,[32] which leads to the effective dispersion of Ag NPs and magnetic NPs during synthesis. The diffraction peaks shown in the XRD spectra of GO-Ag and MGO-Ag at 2θ = 38.2°, 44.3°, 64.5°, 77.5° and 81.6° can be assigned to (1 1 1), (2 0 0), (2 2 0), (3 1 1) and (2 2 2) crystallographic planes of face centered cubic (fcc) silver nanoparticles (in good agreement with No. 04-0783 JCPDS Card), supporting the successful synthesis of Ag NPs on GO surfaces. In addition, the XRD data of MGO and MGO-Ag displays the diffraction peaks originating from both cubic Fe_3O_4 (JCPDS Card No. 75-0449) and cubic γ-Fe_2O_3 (JCPDS Card No. 39-1346), indicating that the co-precipitation method results in simultaneous formation of Fe_3O_4 and γ-Fe_2O_3 on GO surfaces.

The XPS spectra of all the synthesized composites are shown in Figure 2.9a (Supporting Information) which display the major element peaks of C1s, O1s, Ag 3d and Fe 2p. The C1s XPS spectrum of GO (Figure 2.2b) can be fitted with five curves located at 284.6 eV (C=C/C-C), 285.5 eV (C-OH), 286.9 eV (C-O-C), 287.8 eV (C=O) and 288.9 eV (COOH), respectively, confirming the successful synthesis of GO. The C1s XPS spectra of the GO-nanoparticle composites with similar peaks are shown in Figure 2.9b-f (Supporting Information). After the deposition of silver and magnetic nanoparticles, sharp XPS peaks at 368.2 eV and at 374.2 eV assigned to Ag $3d_{5/2}$ and Ag $3d_{3/2}$ were clearly detected on GO-Ag and MGO-Ag composites, which are in accordance with the reported binding energy of metallic silver.[33, 34] Furthermore, a small satellite peak of Fe $2p_{3/2}$ at ~718 eV appears on the Fe XPS spectra (Fig 2.2d) of both MGO and MGO-Ag, indicating the coexistence of γ-Fe_2O_3 and cubic Fe_3O_4 on GO surfaces (consistent with XRD measurements in Figure 2.2a).[35] All the above results demonstrate the successful synthesis of GO-nanoparticle composites.

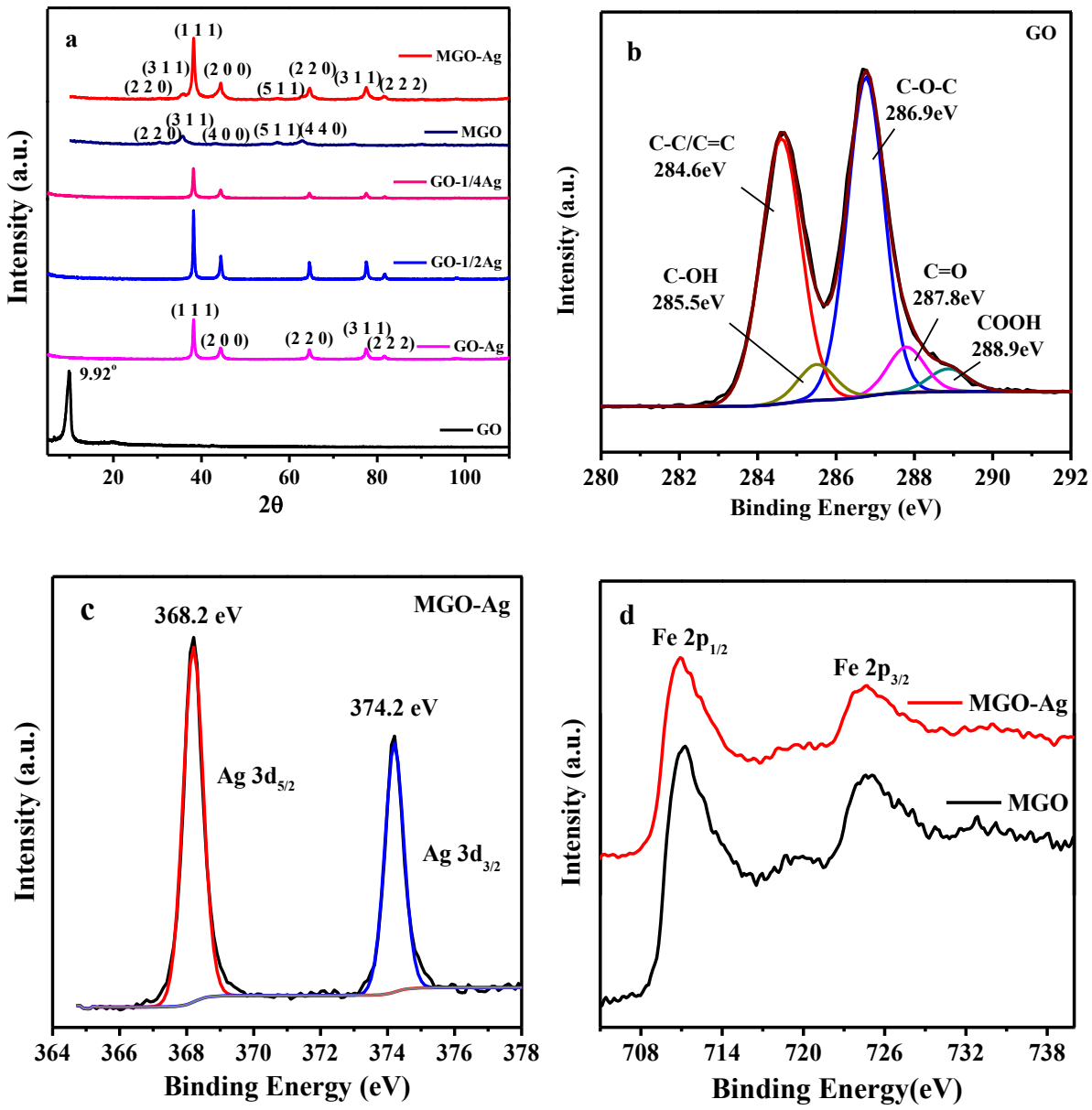

Figure 2.2. (a) XRD spectra of GO, GO-Ag, GO-1/2Ag, GO-1/4Ag, MGO and MGO-Ag composites. XPS survey scans of (b) C on GO, (c) Ag on MGO-Ag and (d) Fe on MGO and MGO-Ag.

In order to test the possibility of recycling the developed MGO and MGO-Ag composites via applying an external magnetic field, the magnetism of the as-prepared MGO and MGO-Ag

was evaluated by magnetic hysteresis measurements. As shown in Figure 2.3, both MGO and MGO-Ag display typical superparamagnetism with no hysteresis loops, which guarantees a convenient reclamation of MGO and MGO-Ag composites after mercury adsorption and re-dispersion of these composites via withdrawal of the magnetic field for recycling. Saturation magnetizations of 14.9 emu/g and 13.4 emu/g were measured for MGO-Ag and MGO, respectively, which are comparable to that of ultrafine magnetic nanoparticles reported previously[36, 37] and strong enough for easy separation of the MGO and MGO-Ag composites (see inset graph in Figure 2.3). It should be noted that a slightly higher saturation magnetization was obtained for MGO-Ag than that of MGO, which is most likely attributed to the magnetic moment change induced by the dipolar interactions between ferrite and Ag nanoparticles.[38]

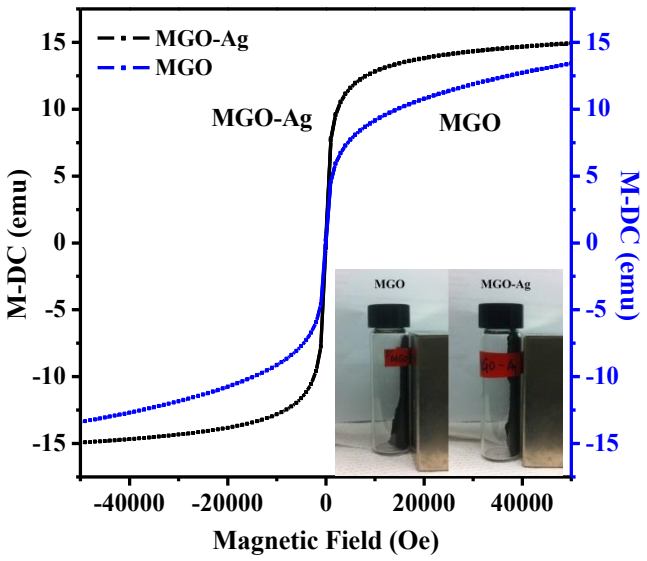

Figure 2.3. Magnetization curves of MGO and MGO-Ag. The inset photographs: separation of MGO and MGO-Ag by a magnet.

2.4.2 Mercury adsorption of GO nanoparticle composites

To investigate the Hg^0 adsorption capability of the developed GO composites including GO, GO-Ag, MGO and MGO-Ag, the mercury breakthrough were examined over a wide temperature range from 50 °C to 250 °C. As shown in Figure 2.4, GO displays a mercury breakthrough of 50% at low temperature (i.e. 50 °C) and an excellent mercury capturing performance with the nearly complete mercury capture at the tested temperatures of 100 ℃ and 150 ℃ , but the Hg^0 adsorption capabilities were totally deteriorated once the temperature reached above 200 °C. Previous study showed that surface moisture and low temperature could significantly lower the adsorption capability of Hg^0 on AC,[39] which most likely leads to the low mercury removal (~50%) of GO at 50 °C observed here. The high Hg^0 adsorption capability of GO at 100-150 °C is probably attributed to abundant surface functional groups (e.g., hydroxyl, epoxy, carboxyl) on GO surfaces, which have been demonstrated as active sites for Hg^0 adsorption.[26] To test our hypothesis, a control experiment was carried out: GO was exposed to thermal treatment at 350 °C to remove all the functional groups (as verified by TGA measurement shown in Figure 2.11, Supporting Information), and the treated GO was then applied for mercury breakthrough measurement. It was found that GO composites lost the Hg^0 adsorption capability after thermal treatment at 350 °C (Figure 2.12, Supporting Information), thereby supporting that functional groups on GO determine its Hg^0 adsorption performance. Hence, it might be challenging to regenerate GO composites after releasing Hg^0 via a thermal treatment at high temperature. However, compared to the conventional widely-applied carbon based adsorbents with a very weak adsorption of Hg^0 above 50 °C (<20% under similar experimental conditions to the current work, and further losing Hg^0 adsorption capability at higher temperature),[18] GO composites are

expected to still bear great advantages as activated adsorbent for Hg^0 removal in coal combustion flue gas, particularly with the addition of Ag nanoparticles and magnetic nanoparticles.

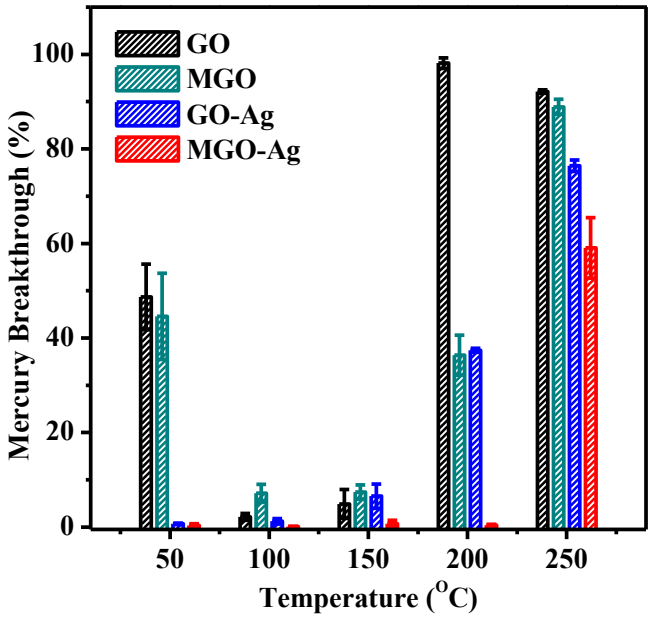

Figure 2.4. Mercury breakthrough at different temperatures on various composite materials: GO, GO-Ag, MGO and MGO-Ag.

As shown in Figure 2.4, with the incorporation of Ag NPs, the as-prepared GO-Ag composites exhibit enhanced Hg^0 adsorption capability as compared to that of GO as evident from the lower mercury breakthrough, especially at high temperatures, which is mainly due to a stable Ag-Hg amalgam formed.[17, 18, 23, 24] The Hg^0 adsorption capability of GO-Ag could be further enhanced by increasing the silver content loaded on GO surfaces. The results shown in Figure 2.5 clearly displays that increasing Ag loading on GO-Ag composites strengthens their Hg^0 adsorption capability as evident from the low mercury breakthrough at 150-250 °C, i.e., Hg^0 breakthrough of GO-Ag < GO-1/2Ag < GO-1/4Ag. Because mercury could be reversibly released from Ag-Hg amalgam, the GO-Ag composites could be easily regenerated after a

thermal treatment at a high temperature. As shown in Figure 2.13 (Supporting Information), unlike GO composites, GO-Ag composites could nearly fully recover its Hg^0 adsorption capability after thermal treatment at 350 °C, indicating that the GO-Ag based composites are highly regenerable.

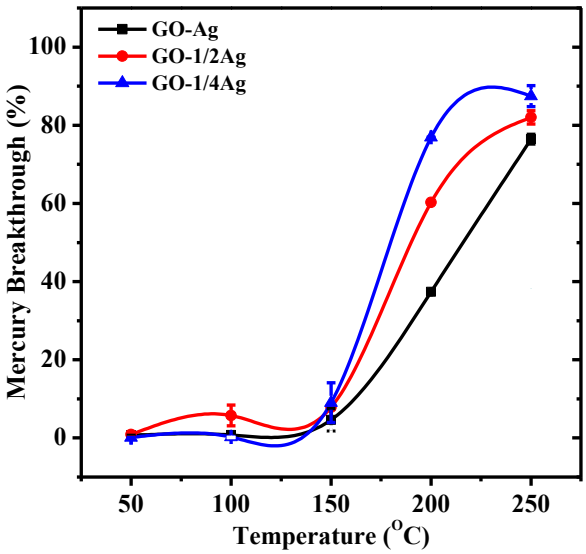

Figure 2.5. Mercury breakthrough at different temperatures for GO-Ag, GO-1/2Ag, and GO-1/4Ag.

In order to confer the feasible reclamation ability of the GO-Ag composites during recycling, magnetic nanoparticles were introduced onto the GO composites, which allows the MGO-Ag to be easily separated under an external magnetic field (as shown in Figure 2.3). The impact of the addition of magnetic nanoparticles on the Hg^0 adsorption capability of MGO and MGO-Ag composites was shown in Figure 2.4. Overall, the incorporation of magnetic nanoparticles does not weaken the Hg^0 adsorption capability of MGO composites as compared to that of GO over the whole temperature range studied (50-250 °C). The further addition of Ag NPs significantly enhanced the Hg^0 adsorption capability of MGO-Ag, which shows the best Hg^0

removal performance among all the four composites (i.e. GO, GO-Ag, MGO, and MGO-Ag) particularly at high temperature (150-250 °C) as shown in Figure 2.4, indicating the best tolerance at high temperature. The above results indicate that the deposition of both Ag NPs and magnetic iron oxide NPs on GO could synergistically enhance the Hg^0 capturing capability and temperature tolerance of the MGO-Ag composites, which shows significant potential for the removal of Hg^0 from flue gases. This synergic performance is most likely achieved through Ag-Hg amalgamation coupled with chemi-sorption and amalgamation of Hg^0 on ferrite oxide NPs via certain active sites reported previously.[13, 24, 40]

To explore the recyclability of MGO-Ag, the mercury breakthrough recycling test was carried out at 200 °C, and the regeneration of the MGO-Ag composite was achieved by thermal treatment at 370°C as detected by CVAFS. Figure 2.6 shows that MGO-Ag could maintain almost 100% of the Hg^0 adsorption capability (equivalent to 0% breakthrough) even after 5 cycles of reuse. Meanwhile, the TEM, TEM-EDX and XPS results of the MGO-Ag composites after recycling test (see Figure 2.14 and Figure 2.15 in Supporting Information) show that the composites maintain their physical and chemical structures after recycling, demonstrating excellent stability. The above results further demonstrate that the MGO-Ag composites could be regenerated after a thermal treatment at high temperature (i.e. 370 °C) without significant destruction of MGO-Ag and deterioration of Hg^0 adsorption capability, suggesting that the as-prepared MGO-Ag has great potential application in Hg^0 removal from practical flue gases.

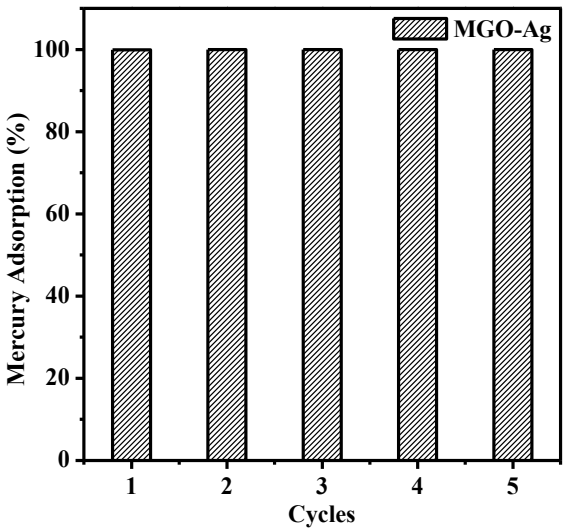

Figure 2.6. Hg^0 adsorption recycling tests for regenerated MGO-Ag at 200 ℃ .

The Hg^0 adsorption capacity of MGO-Ag was further tested by continuous exposure to simulated flue gases (consisted of 4% O_2, 12% CO_2, 400 ppm SO_2, 300 ppm NO and 75 μg/m^3 Hg^0 that is two times higher than the Hg^0 concentration in real flue gases[41, 42]) at a flow rate of 1.2 L/min for 0.5 h to explore its potential practical mercury removal capability in coal combustion flue gases, and the inlet and outlet Hg^0 concentrations of the gas flow were monitored by a VM-3000 Mercury Vapour Detector. Figure 2.7 shows that MGO-Ag exhibits Hg^0 capture capacity of about 60 μg/g (w/w, adsorbed Hg^0/adsorbent) at 100 to 150 °C, which is much higher than Hg^0 capture capacity of previously reported adsorbents such as fly ash (10-30 μg/g at 135 °C)[43] and magnetic zeolite silver composites (13.3-40 μg/g at 150 °C)[17] under similar experimental conditions. Furthermore, it demonstrates a faster Hg^0 adsorption rate in the simulated flue gases: ~4.5 ppm Hg^0 (w/w, Figure 2.16 in Supporting Information) was captured by 15 mg MGO-Ag in the first 5 min over the whole temperature range (100-200 °C), which outperforms the previously reported Ag NPs based composites within the same exposure time (~140 ppb of chabazite-based Ag composite and ~30 ppb of magnetic zeolite silver composite).[23,

[44] All the above results indicate that the MGO-Ag composites could be used as potential adsorbents for mercury emission control in the practical downstream flue gas (typically with temperature ~150 °C) of coal-fired power plant. It is also noted that the Hg^0 capture capacity of MGO-Ag dramatically drops to ~7 μg/g as the temperature of simulated flue gases increases to 200 °C, similar to that in Ar environment in the CVAFS test.

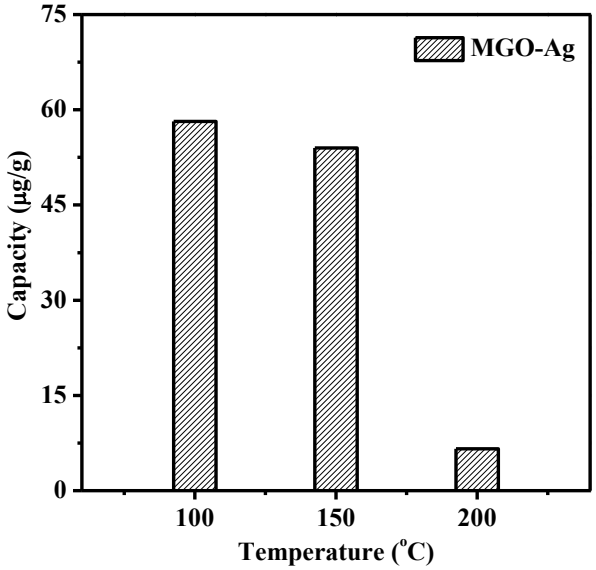

Figure 2.7. The Hg^0 adsorption capacity of MGO-Ag under continuous exposure to simulated flue gases for 0.5 h from 100 °C to 200 °C.

2.5 Conclusions

In this work, four types of novel adsorbents based on graphene oxide (i.e. GO, GO-Ag, MGO and MGO-Ag) were successfully synthesized, characterized and applied for the adsorption of elemental mercury (Hg^0) for the first time. The deposition of Ag NPs on GO enhances the Hg^0 removal capability of GO-Ag as compared to that of pure GO, mainly due to amalgamation between Ag NPs and Hg^0. The addition of magnetic ferrite NPs on GO does not show a negative

impact on the Hg^0 removal capability of MGO. The deposition of both Ag NPs and magnetic NPs on GO makes the MGO-Ag composites possess the best Hg^0 removal capability and thermal tolerance among the four types of adsorbents tested. MGO-Ag composites are able to effectively capture Hg^0 up to 150-200 ^oC in simulated flue gas environment, which can be also effectively recycled and reused with excellent thermal stability. Our results indicate that the graphene oxide based composites (i.e. MGO-Ag) have significant potential applications for mercury emission control in coal-fired power plant.

2.6 Acknowledgment

The authors are grateful for the financial support from the Helmholtz-Alberta Initiative - Energy & Environment (HAI-E&E) program and Natural Sciences and Engineering Research Council of Canada (NSERC).

2.7 Reference

(1) Environmental Impacts of Coal Power: Air Pollution. http://www.ucsusa.org/clean_energy/coalvswind/c02c.html

(2) Carlson, C. L.; Adriano, D. C. Environmental Impacts of Coal Combustion Residues. *J. Environ. Qual.* **1993,** *22* (2), 227-247.

(3) Finkelman, R. B.; Orem, W.; Castranova, V.; Tatu, C. A.; Belkin, H. E.; Zheng, B.; Lerch, H. E.; Maharaj, S. V.; Bates, A. L. Health Impacts of Coal and Coal Use Possible Solutions. *Int. J. Coal Geol.* **2002,** *50* (1-4), 425-443.

(4) Fitzgerald, W. F. Is Mercury Increasing in the Atmosphere? The Need for an Atmospheric Mercury Network (AMNET). *Water, Air, Soil Pollut.* **1995,** *80* (1-4), 245-254.

(5) Dastoor, A. P.; Larocque, Y. Global Circulation of Atmospheric Mercury: A Modelling Study. *Atmos. Environ.* **2004,** *38* (1), 147-161.

(6) Galbreath, K. C. Z., C J. Mercury Speciation in Coal Combustion and Gasification Flue Gases. *Environ. Sci. Technol.* **1996,** *30* (8), 2421-2426.

(7) Galbreath, K. C.; Zygarlicke, C. J. Mercury Transformations in Coal Combustion Flue Gas. *Fuel Process. Technol.* **2000,** *65-66*, 289-310.

(8) Pavlish, J. H.; Sondreal, E. A.; Mann, M. D.; Olson, E. S.; Galbreath, K. C.; Laudal, D. L.; Benson, S. A. Status Review of Mercury Control Options for Coal-Fired Power Plants. *Fuel Process. Technol* **2003,** *82* (2-3), 89-165.

(9) Yang, H.; Xu, Z.; Fan, M.; Bland, A. E.; Judkins, R. R. Adsorbents for Capturing Mercury in Coal-Fired Boiler Flue Gas. *J. Hazard. Mater.* **2007,** *146* (1-2), 1-11.

(10) Lindqvist, O.; Johansson, K.; Aastrup, M.; Anderson, A.; Bringmark, L.; Hovsenius, G. Mercury in the Swedish Environment-Recent Research on Causes, Consequences and Corrective Methods. *Water, Air, Soil Pollut.* **1991,** *55* (1-2), 1-261.

(11) Liu, Y.; Bisson, T. M.; Yang, H.; Xu, Z. Recent Developments in Novel Sorbents for Flue Gas Clean Up. *Fuel Process. Technol* **2010,** *91* (10), 1175-1197.

(12) Reddy, B. M.; Durgasri, N.; Kumar, T. V.; Bhargava, S. K. Abatement of Gas-Phase Mercury-Recent Developments. *Cat. Rev: Sci. Eng.* **2012,** *54* (3), 344-398.

(13) Granite, E. J.; Pennline, H. W.; Hargis, R. A. Novel Sorbents for Mercury Removal from Flue Gas. *Ind. Eng. Chem. Res.* **2000,** *39* (4), 1020-1029.

(14) Zeng, H.; Jin, F.; Guo, J. Removal of Elemental Mercury from Coal Combustion Flue Gas by Chloride-Impregnated Activated Carbon. *Fuel.* **2004,** *83* (1), 143-146.

(15) Worathanakul, P.; Kongkachuichay, P.; Noel, J. D.; Suriyawong, A.; Giammar, D. E.; Biswas, P. Evaluation of Nanostructured Sorbents in Differential Bed Reactors for Elemental Mercury Capture. *Environ. Eng. Sci.* **2008,** *25* (7), 1061-1070.

(16) Abu-Daabes, M. A.; Pinto, N. G. Synthesis and Characterization of a Nano-Structured Sorbent for the Direct Removal of Mercury Vapor from Flue Gases by Chelation. *Chem. Eng. Sci.* **2005,** *60* (7), 1901-1910.

(17) Dong, J.; Xu, Z.; Kuznicki, S. M. Magnetic Multi-Functional Nano Composites for Environmental Applications. *Adv. Funct. Mater.* **2009,** *19* (8), 1268-1275.

(18) Luo, G.; Yao, H.; Xu, M.; Cui, X.; Chen, W.; Gupta, R.; Xu, Z. Carbon Nanotube-Silver Composite for Mercury Capture and Analysis. *Energ. Fuel.* **2010,** *24* (1), 419-426.

(19) Zhu, Y.; Murali, S.; Cai, W.; Li, X.; Suk, J. W.; Potts, J. R.; Ruoff, R. S. Graphene and Graphene Oxide: Synthesis, Properties, and Applications. *Adv. Mater.* **2010,** *22* (35), 3906-3924.

(20) Chandra, V.; Kim, K. S. Highly Selective Adsorption of Hg^{2+} by a Polypyrrole-Reduced Graphene Oxide Composite. *Chem. Commun.* **2011,** *47* (13), 3942.

(21) Sreeprasad, T. S.; Maliyekkal, S. M.; Lisha, K. P.; Pradeep, T. Reduced Graphene Oxide-Metal/Metal Oxide Composites: Facile Synthesis and Application in Water Purification. *J. Hazard. Mater.* **2011,** *186* (1), 921-931.

(22) Poulston, S.; Granite, E. J.; Pennline, H. W.; Myers, C. R.; Stanko, D. P.; Hamilton, H.; Rowsell, L.; Smith, A. W. J.; Ilkenhans, T.; Chu, W. Metal Sorbents for High Temperature Mercury Capture from Fuel Gas. *Fuel.* **2007,** *86* (14), 2201-2203.

(23) Liu, Y.; Kelly, D. J. A.; Yang, H.; Lin, C. C. H.; Kuznicki, S. M.; Xu, Z. Novel Regenerable Sorbent for Mercury Capture from Flue Gases of Coal-Fired Power Plant. *Environ. Sci. Technol.* **2008,** *42* (16), 6205-6210.

(24) Wilcox, J.; Rupp, E.; Ying, S. C.; Lim, D.-H.; Negreira, A. S.; Kirchofer, A.; Feng, F.; Lee, K. Mercury Adsorption and Oxidation in Coal Combustion and Gasification Processes. *Int. J. Coal. Geol.* **2012,** *90-91*, 4-20.

(25) Yan, T. Y. A Novel Process for Hg Removal from Gases. *Ind. Eng. Chem. Res.* **1994,** *33* (12), 3010-3014.

(26) Li, Y. H.; Lee, C. W.; Gullett, B. K. Importance of Activated Carbon's Oxygen Surface Functional Groups on Elemental Mercury Adsorption. *Fuel.* **2003,** *82* (4), 451-457.

(27) Shen, J.; Hu, Y.; Shi, M.; Li, N.; Ma, H.; Ye, M. One Step Synthesis of Graphene Oxide-Magnetic Nanoparticle Composite. *J. Phys. Chem. C.* **2010,** *114* (3), 1498-1503.

(28) Tang, X.-Z.; Li, X.; Cao, Z.; Yang, J.; Wang, H.; Pu, X.; Yu, Z.-Z. Synthesis of Graphene Decorated with Silver Nanoparticles by Simultaneous Reduction of Graphene Oxide and Silver Ions with Glucose. *Carbon.* **2013,** *59*, 93-99.

(29) Kassaee, M. Z.; Motamedi, E.; Majdi, M. Magnetic Fe_3O_4-Graphene Oxide/Polystyrene: Fabrication and Characterization of a Promising Nanocomposite. *Chem. Eng. J.* **2011,** *172* (1), 540-549.

(30) Hou, C.; Zhang, Q.; Zhu, M.; Li, Y.; Wang, H. One-Step Synthesis of Magnetically-Functionalized Reduced Graphite Sheets and Their Use in Hydrogels. *Carbon.* **2011,** *49* (1), 47-53.

(31) Fu, Y.; Wang, J.; Liu, Q.; Zeng, H. Water-Dispersible Magnetic Nanoparticle-Graphene Oxide Composites for Selenium Removal. *Carbon* **2014,** *77*, 710-721.

(32) Liu, L.; Liu, J.; Wang, Y.; Yan, X.; Sun, D. D. Facile Synthesis of Monodispersed Silver Nanoparticles on Graphene Oxide Sheets with Enhanced Antibacterial Activity. *New J. Chem.* **2011,** *35* (7), 1418.

(33) Weaver, J. F.; Hoflund, G. B. Surface Characterization Study of the Thermal Decomposition of Ag_2O. *Chem. Mater.* **1994,** *6* (10), 1693-1699.

(34) Heister, K.; Zharnikov, M.; Grunze, M. Adsorption of Alkanethiols and Biphenylthiols on Au and Ag Substrates: A High-Resolution X-Ray Photoelectron Spectroscopy Study. *J. Phys. Chem. B.* **2001,** *105* (19), 4058-4061.

(35) Yamashita, T.; Hayes, P. Analysis of XPS Spectra of Fe^{2+} and Fe^{3+} Ions in Oxide Materials. *Appl. Surf. Sci.* **2008,** *254* (8), 2441-2449.

(36) Han, D. H.; Wang, J. P.; Luo, H. L. Crystallite Size Effect on Saturation Magnetization of Fine Ferrimagnetic Particles. *J. Magn. Magn. Mater.* **1994,** *136* (1-2), 176-182.

(37) Ai, Z. D., K.; Wan, Q.; Zhang, L.; Lee, S. Facile Microwave-Assisted Synthesis and Magnetic and Gas Sensing Properties of Fe_3O_4 Nanoroses. *J. Phys. Chem. C.* **2010,** *114* (14), 6237-6242.

(38) Liu, C. H.; Zhou, Z. D.; Yu, X.; Lv, B. Q.; Mao, J. F.; Xiao, D. Preparation and Characterization of Fe_3O_4/Ag Composite Magnetic Nanoparticles. *Inorg. Mater.* **2008,** *44* (3), 291-295.

(39) Li, Y. H.; Lee, C. W.; Gullett, B. K. The Effect of Activated Carbon Surface Moisture on Low Temperature Mercury Adsorption. *Carbon.* **2002,** *40* (1), 65-72.

(40) Wu, S.; Oya, N.; Ozaki, M.; Kawakami, J.; Uddin, M. A.; Sasaoka, E. Development of Iron Oxide Sorbents for Hg^0 Removal from Coal Derived Fuel Gas: Sulfidation Characteristics of Iron Oxide Sorbents and Activity for COS Formation during Hg^0 Removal. *Fuel.* **2007,** *86* (17-18), 2857-2863.

(41) Meij, R. The Fate of Mercury in Coal-Fired Power Plants and the Influence of Wet Flue-Gas Desulphurization. *Water, Air, Soil Pollut.* **1991,** *56* (1), 21-33.

(42) Pirrone, N.; Cinnirella, S.; Feng, X.; Finkelman, R. B.; Friedli, H. R.; Leaner, J.; Mason, R.; Mukherjee, A. B.; Stracher, G. B.; Streets, D. G.; Telmer, K. Global Mercury Emissions to the Atmosphere from Anthropogenic and Natural Sources. *Atmos. Chem. Phys.* **2010,** *10* (13), 5951-5964.

(43) Carey, T. R.; Richardson, C. F. Assessing Sorbent Injection Mercury Control Effectiveness in Flue Gas Streams. *Environ. Progress.* **2004,** *19* (3), 167-174.

(44) Dong, J.; Xu, Z.; Kuznicki, S. M. Mercury Removal from Flue Gases by Novel Regenerable Magnetic Nanocomposite Sorbents. *Advan. Funct. Mater* **2009,** *19*, 1268-1275.

2.8 Supporting Information

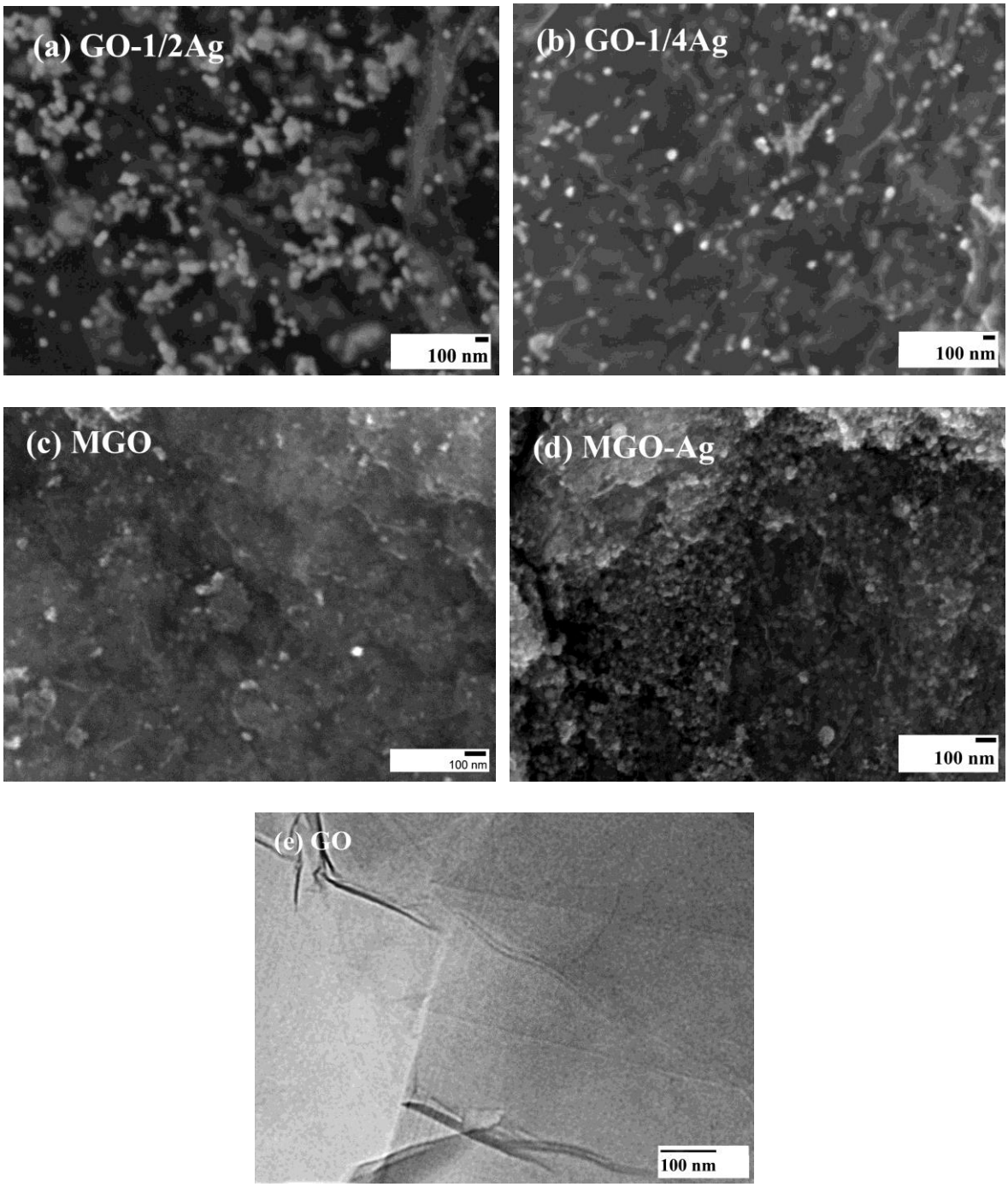

Figure 2.8 FE-SEM images of (a) GO-1/2Ag, (b) GO-1/4Ag, (c) MGO and (d) MGO-Ag. TEM image of (e) GO.

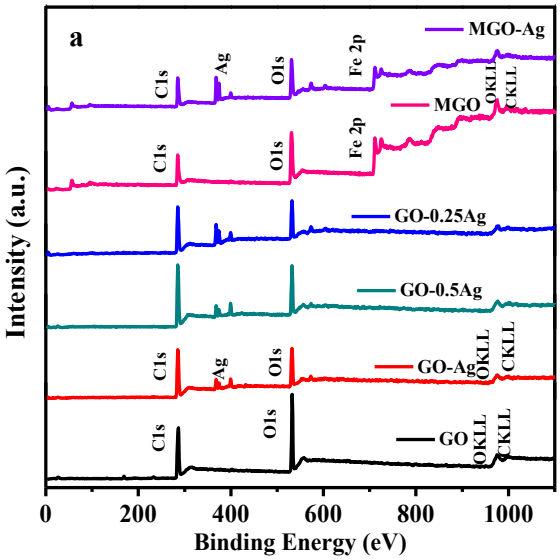
a
MGO-Ag
MGO
GO-0.25Ag
GO-0.5Ag
GO-Ag
GO
C1s
Ag
O1s
Fe 2p
OKLL
CKLL
Intensity (a.u.)
0
200
400
600
800
1000
Binding Energy (eV)

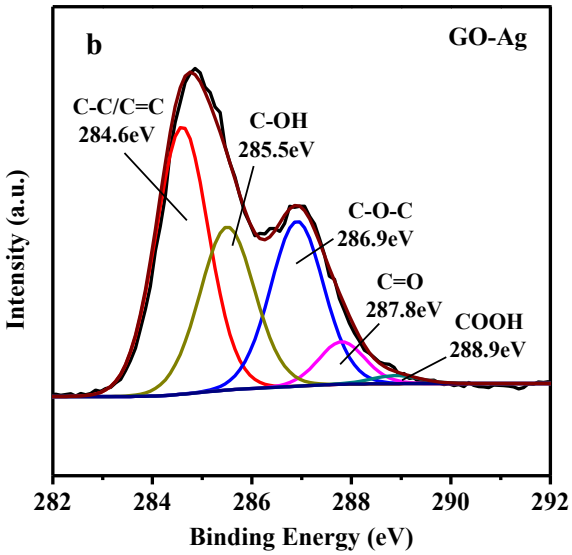
b
GO-Ag
C-C/C=C
284.6eV
C-OH
285.5eV
C-O-C
286.9eV
C=O
287.8eV
COOH
288.9eV
Intensity (a.u.)
282
284
286
288
290
292
Binding Energy (eV)

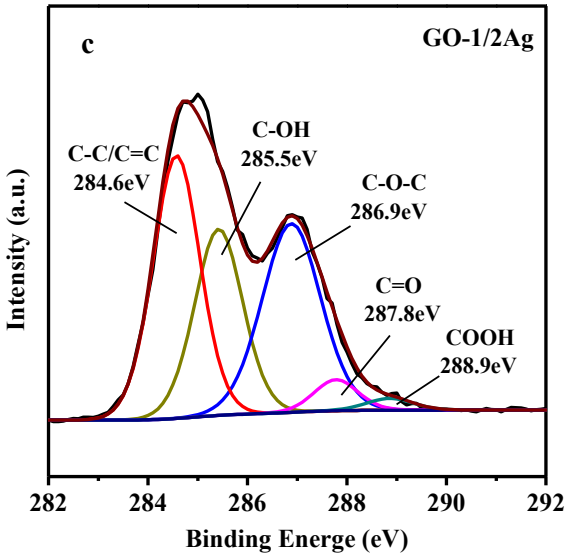
c
GO-1/2Ag
C-C/C=C
284.6eV
C-OH
285.5eV
C-O-C
286.9eV
C=O
287.8eV
COOH
288.9eV
Intensity (a.u.)
282
284
286
288
290
292
Binding Energe (eV)

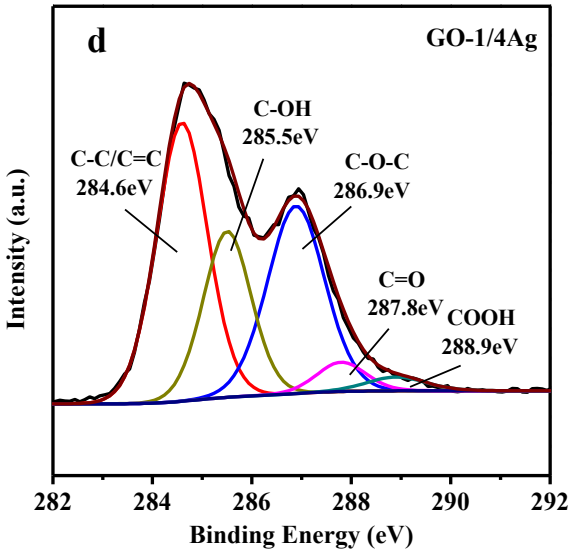
d
GO-1/4Ag
C-C/C=C
284.6eV
C-OH
285.5eV
C-O-C
286.9eV
C=O
287.8eV
COOH
288.9eV
Intensity (a.u.)
282
284
286
288
290
292
Binding Energy (eV)

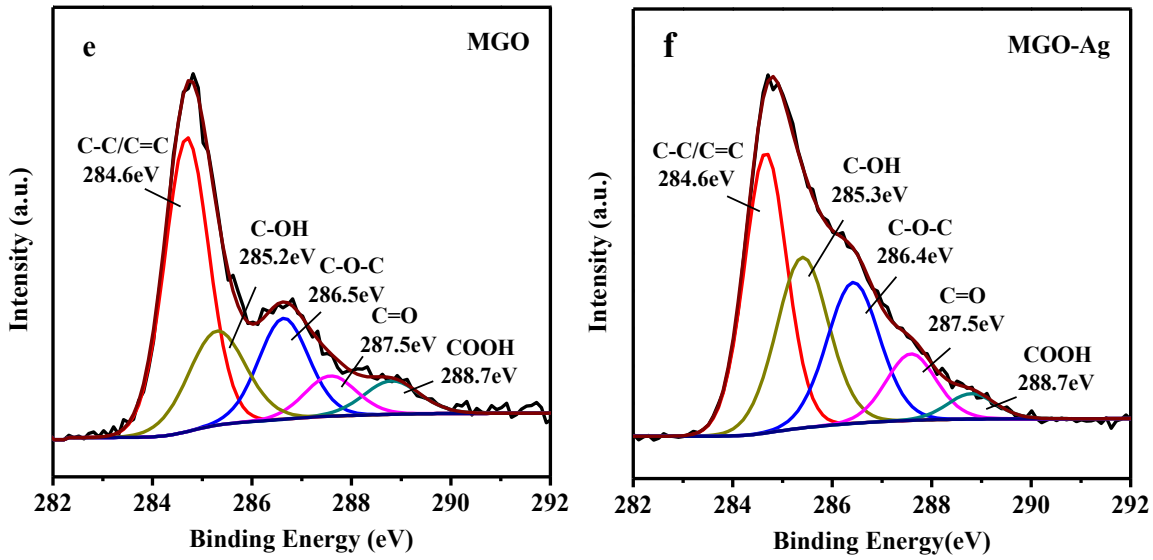

Figure 2.9. (a) XPS patterns of GO, GO-Ag, GO-1/2Ag, GO-1/4Ag, MGO and MGO-Ag. XPS spectra of C1s of (b) GO-Ag, (c) GO-1/2Ag, (d) GO-1/4Ag, (e) MGO and (f) MGO-Ag.

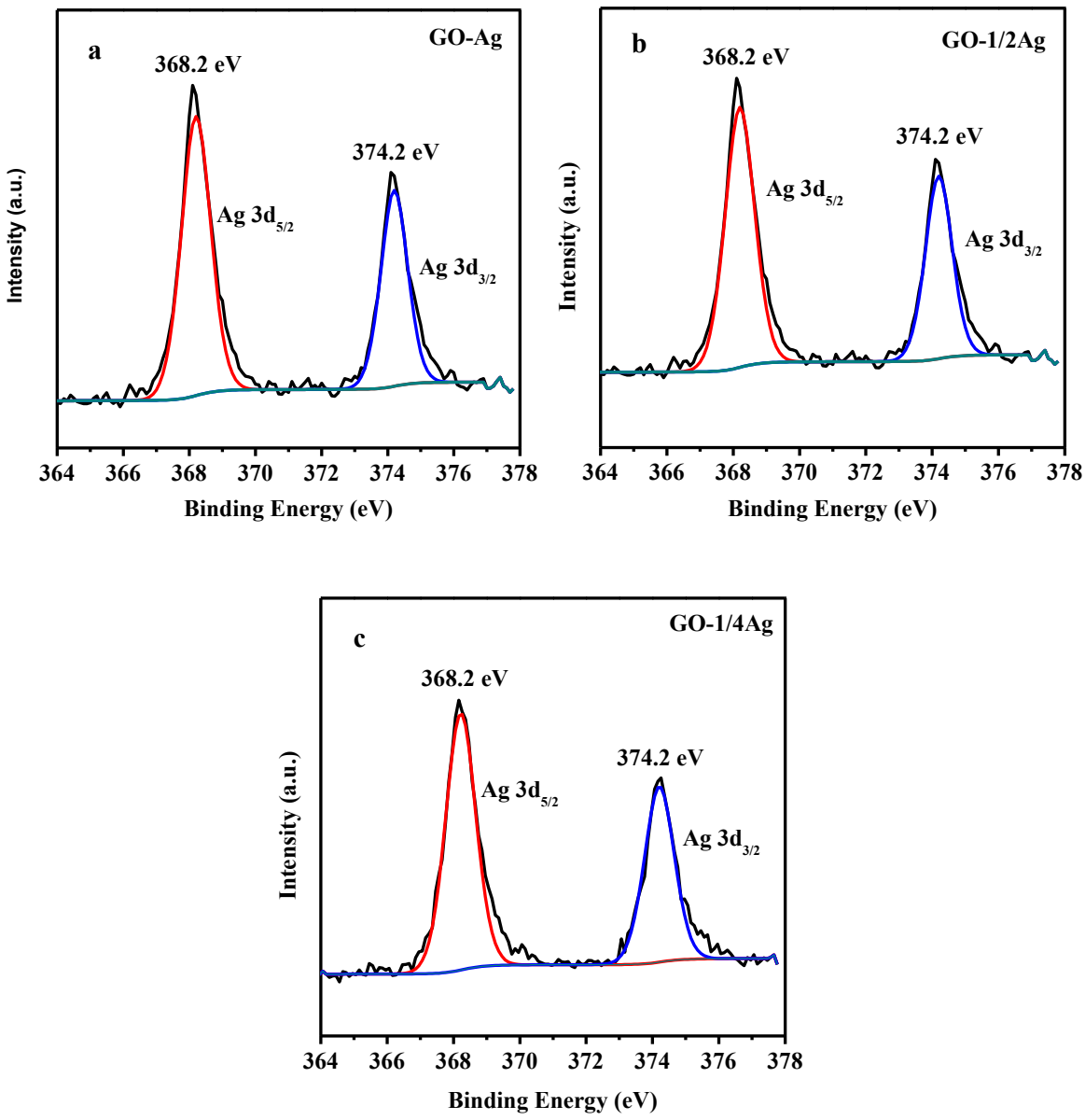

Figure 2.10. XPS spectra of silver of (a) GO-Ag, (b) GO-1/2Ag and (c) GO-1/4Ag.

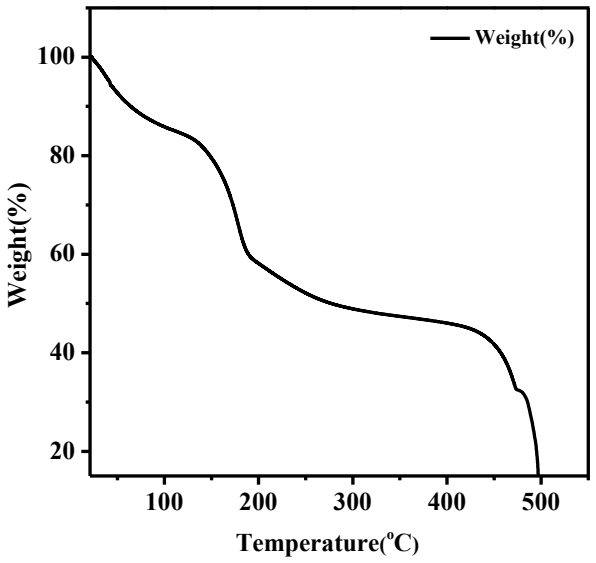

Figure 2.11. TGA curves of GO from room temperature to 550 °C: ~15% mass loss below 100 °C, a sharp mass loss (~25%) at ~150 °C, and an additional ~10% mass loss from ~200 °C to ~300 °C.

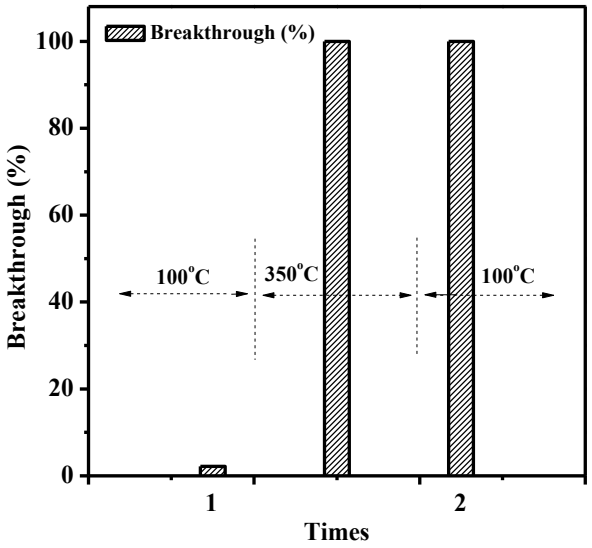

Figure 2.12. GO mercury breakthrough before and after thermal treatment at 350 °C. The mercury breakthrough remains almost 100% after the thermal treatment indicating the GO lost its mercury removal capability after thermal treatment.

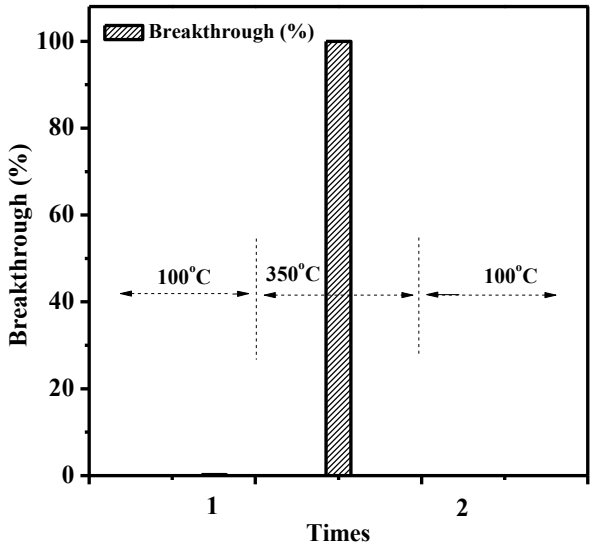

Figure 2.13. GO-Ag mercury breakthrough before and after thermal treatment at 350 °C. The mercury breakthrough remains almost 0% after the thermal treatment indicating the GO-Ag fully recovered its mercury removal capability after thermal treatment.

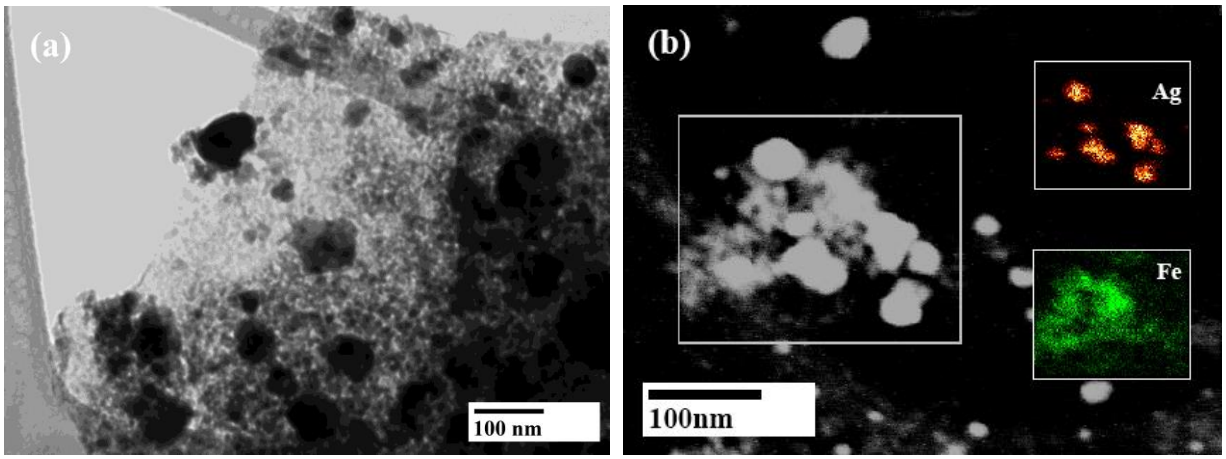

Figure 2.14. (a) TEM image of MGO-Ag after recycling test. (b) TEM-EDX image of MGO-Ag after recycling test.

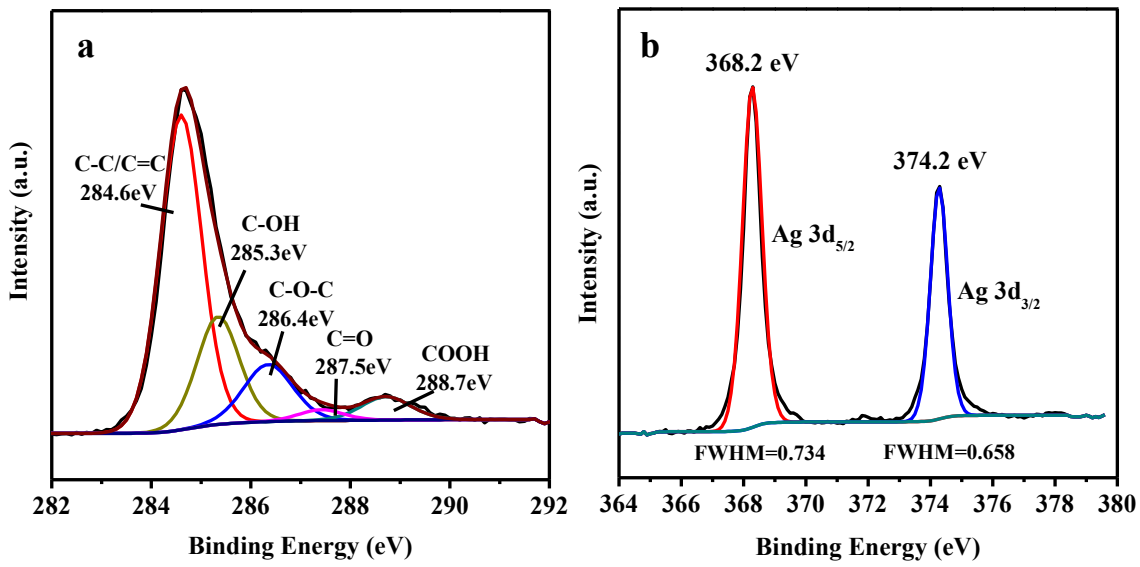

Figure 2.15. XPS spectra of (a) C of MGO-Ag and (b) Ag of MGO-Ag after recycling test.

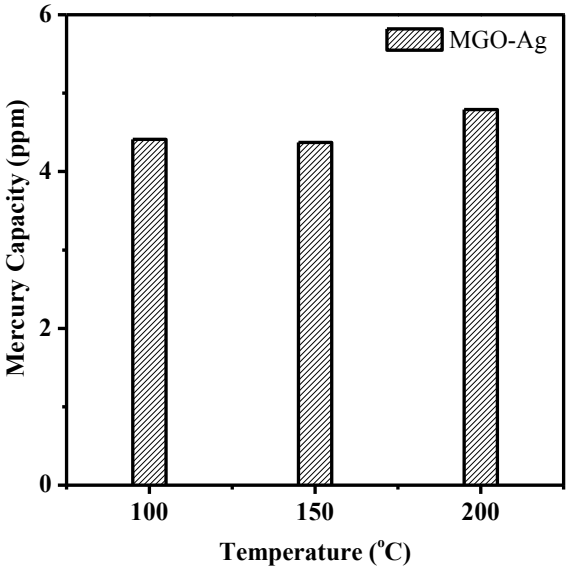

Figure 2.16. The Hg^0 adsorption capacity of MGO-Ag in continuous simulated flue gases over 5 min from 100 °C to 200 °C.

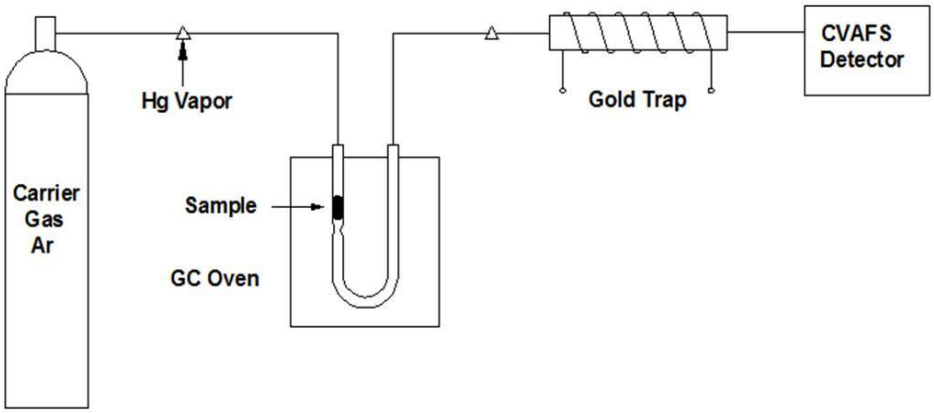

Scheme 2.1. Experiment setup for mercury breakthrough test (15 mg GO/GO-Ag/MGO/MGO-Ag and 200μL of Hg^0 standard vapor injection at room temperature were applied for each test).

CHAPTER 3 Enhanced Elemental Mercury Adsorption Capability by Metal Oxide Nanoparticles-Modified Graphene Oxide

3.1 Abstract

Mercury is an extremely toxic element, released primarily from anthropogenic activities and natural sources. Controlling the emissions of Hg, especially from coal combustion flue gas, is practical important for protecting the environment and preventing healthy risks for human beings.

In the present work, three metal oxides (MnO_2, CuO, ZnO) loaded graphene oxide (GO) sorbents (designated as GO-MnO_2, GO-CuO, GO-ZnO) have been developed. All the three kinds of adsorbents were successfully synthesized, and well characterized by the scanning electron microscopy (SEM), transmission electron microscopy (TEM), X-ray diffraction (XRD) and X-ray photoelectron spectroscopy (XPS). The results indicated that all the metal oxides nanoparticles (NPs) have been successfully deposited on GO. The elemental mercury (Hg^0) adsorption abilities of the three sorbents have been subsequently evaluated by means of a cold vapour atomic fluorescence spectrophotometry (CVAFS) with Argon as a carrier gas for mercury detection. The testing temperature ranged from 50 °C to 200 °C with intervals of 50 °C. GO-MnO_2 presented an excellent Hg^0 adsorption capacity through chemisorption from 50-150 °C and as high as 85% efficiency even at 200 °C. However, the Hg^0 adsorption capacity on the adsorbents decreased when temperature increased. Both GO-CuO and GO-ZnO did not perform efficient mercury adsorption. This work revealed that MnO_2-NPs modified GO is highly applicable for enhancing the gas phase elemental mercury removal.

3.2 Introduction

Mercury emission has long been a serious problem in energy production industries, especially elemental mercury (Hg^0) in flue gases released from coal-fired power plants and coal gasification power plants.[1, 2] Since the Hg^0 can be transformed into a highly toxic compound-methylmercury through biosystem and eventually accumulate in human body through the consumption of sea foods,[3, 4] which will cause serious damage to nerve system and organs, the removal of Hg^0 from the flue gases and coal combustion/gasification is of great importance. The flue gas constituents HCl, SO_2 and NO_x along with the air pollution control devices (APCD), such as electrostatic precipitator (ESP), wet scrubber, flue gas desulfurization (FGD), can help partialy oxidize Hg^0 into divalent mercury (Hg^{2+}),[5, 6] which may enter into the desulfurization sludge.[7] However, due to the special properties of Hg^0 (e.g., high volatility and insolubility in water), it is very difficult to eliminate the Hg^0 by these devices to meet the standard requirements compared to the other two forms of mercury-Hg^{2+} and particulate bounded mercury (Hg_p). Around 25 % of the mercury in coal will still be emitted as the gaseous Hg.[6]

To minimize the elemental mercury emission, adsorbent injection has been widely used and studied as the supplemental method. Adsorbents can be injected into the combustion gas upstream or downstream of the APCD to react with Hg^0 by physic-sorption/chemi-sorption and/or amalgamation.[8] So far, various adsorbents, such as treated activated carbon,[9, 10] treated zeolites,[11, 12] calcium based adsorbent[13, 14] and many novel sorbents have been developed. Some researchers also used the coal-fired power plant by-product fly ash[15, 16] and activated coke[17] as the modification alternative substrates. These materials usually have large specific surface area that can facilitate the surface modification and maximize the collision among the target atoms and the reactors as well. Recently, graphene oxide derived from graphite has been progressively

applied in pollution treatment (e.g., trace element in industrial wastewater[18, 19] and dyestuff[20]) that benefits from its two-dimension structure, large specific surface area and abundant surface functional groups.

Bare materials described above only have unstable and weak attraction for Hg^0. In this regard, active medium are needed to be introduced. Halogen elements, S, metal oxides, etc. were found to be active towards Hg^0 and were thereby grafted onto large surface area materials for flue gas clean-up.[9, 10, 21] Ghorishi[9] chemically impregnated ACs with chlorine and tested the Cl containing ACs in nitrogen and simulated flue gas at 100-200 °C. Boosted capabilities (around 70 %) were observed as compared to virgin ACs, and more meaningfully, Cl-ACs did not weaken much in simulated flue gas. Even progresses have been made, some potential problems emerged accordingly. Halogen elements and S could bring secondary pollution once the sorbents are disposed or attach to fly ash. As a consequence, to avoid the potential safety issues, nanosize metal/metal oxides are generalized for removing Hg^0 as they can be efficient, safe and multi-functional. Dong[12] modified zeolite with silver nanoparticles and magnetic nanoparticles (MagZ-Ag) and found out the MagZ-Ag presented highly positive impact in Hg^0 adsorption tests. More interestingly, the magnetism enabled the separation of the sorbent from fly ash. Metal oxides like MnO_2, TiO_2, CuO, V_2O_5 and so on were likewise effective for Hg^0 capture.[22-25] Nevertheless, none of them have been combined with graphene oxide as sorbents so far.

Therefore, for enhancing the Hg^0 adsorption capacity on graphene oxides, metal oxides (CuO, MnO_2, ZnO) modified graphene oxide were developed and evaluated to explore the combination impact for capturing gaseous mercury in the present work. The characteristics of the adsorbents and Hg^0 adsorption mechanisms were analyzed in details, and the Hg^0 adsorption

performance were compared among the metal oxides modified GO, GO and thermal treated GO. Results indicate that GO-MnO_2 is highly capable for Hg^0 capture.

3.3 Experiment Section

3.3.1 Materials

Graphite flakes, sulfuric acid (H_2SO_4, 95.0-98.0 %), sodium nitrate ($NaNO_3$) and hydrogen peroxide (H_2O_2, 29-32 % w/w aq.) were all purchased from Alfa Aesar. The manganous nitrate hydrate ($Mn(NO_3)_2 \cdot xH_2O$), copper acetate hydrate ($Cu(Ac)_2H_2O$) and zinc nitrate hexahydrate ($Zn(NO_3)_2 \cdot 6H_2O$) were supplied by Sigma-Aldrich. Potassium permanganate ($KMnO_4$), isopropyl alcohol and sodium hydroxide (NaOH) were provided by Fisher Scientific Canada.

3.3.2 Synthesis of GO-MnO_2

GO was prepared as described previously and the modification of MnO_2 nanoparticles was based on Chen's research.[26] GO (100 mg) and $Mn(NO_3)_2 \cdot xH_2O$ (1.79 g) were dispersed and ultrasonically exfoliated in isopropyl alcohol (100 mL) to make a brown suspension. The mixture was afterwards heated to 83 °C and vigorously stirred in a round-bottomed flask with a condenser. 30 mL $KMnO_4$ (0.92 g) dissolved deionized (DI) water was then added rapidly into the refluxing system. After being kept for half an hour, the black mixture designated as GO-MnO_2 was cooled, washed, freeze dried and was finally treated under 200 ºC for 2 hours.

3.3.3 Synthesis of GO-CuO

The copper oxide nanoparticles was synthesized according to Zhu's work[27] as follows: Firstly, $Cu(Ac)_2H_2O$ was mixed with a GO slurry obtained by sonicating GO (100 mg) in isopropyl alcohol (100 mL) for 1 hour. The resulting dispersion was then heated to 83 °C and refluxed in a round-bottomed flask with vigorous stirring. After 30 minutes, 10 mL deionized

(DI) water was rapidly added and the mixture was maintained in stirring and refluxing for another 30 min. During this process, the dispersion color gradually turned darker. Finally, the product was cooled, centrifuged, and washed with ethanol and DI water for a few times, and was designated as GO-CuO after freeze drying and then 200 ºC drying for 2 hours.

3.3.4 Synthesis of GO-ZnO

The method used for the deposition of zinc oxide nanoparticles were based on Chen's report.[28] $Zn(NO_3)_2 \cdot 6H_2O$ (2.97 g) and GO (100 mg) were dissolved in distilled water (100 mL) and were ultra-sonicated for 1 hour. Then, the suspension was kept in an ice-bath with vigorous stirring for 20 hours after rising the mixture PH to 8.5 by adding NaOH solution. The obtaining product-$Zn(OH)_2$/GO composite was subsequently centrifuged, washed and freeze dried to get a grey black powder. Afterwards, the grey black powders were heated at 200 °C for 2 h to remove generate ZnO which led the color finally turn into black. The resultant black powder was designated as GO-ZnO.

3.3.5 Adsorbents Characterization

In this work, FE-SEM (field emission-SEM) obtained through JAMP-9500F (Jeol, Japan) and TEM scaned by a Philips/FEI Morgagni microscope at 80 kV were utilized to character the morphologies of the synthesized materials. XRD conducted by Rigaku Ultima IV X-ray diffractometer under Cu Kα irradiation (k = 1.5406 Å) and XPS operated by AXIS 165 spectrometer (Kratos Analytical) were applied to further evaluate the compositions of the deposited particles.

3.3.6 Mercury Breakthrough Test

Elemental mercury removal adsorption capacity on both tGO/GO and the metal oxide loaded GO were tested from 50 to 200 °C, respectively. And the Hg^0 was detected by using a Tekran 2500 Cold Vapor Atomic Fluorescence Spectrophotometry (CVAFS). The percentage of mercury breakthrough stands for the part of elemental mercury that has not been adsorbed by the adsorbent.

3.4 Results and Discussions

3.4.1 Characterization of composites

Figure 3.1 shows the virgin transparent GO sheets with a few wrinkles, and the distribution and particle morphologies of the three metal oxides on GO layers. As clearly shown in Figure 3.1b and Figure 3.1d, the MnO_2 and ZnO nanoparticles are around 20 nm. While, two different sizes of CuO particles can be apparently found in Figure 3.1c: a few nanoparticles around 100 nm scatter with the dominating 20 nm nanoparticles on the substrate. Since the growth of the CuO-NPs derived from the hydrolysis reaction between the $Cu(Ac)_2$ and later added water, it is suggested that the appearance of large nanoparticles can be dated back to the earliest hydrolysis brought by the few containing H_2O molecules from copper acetate hydrate and the isopropyl alcohol. In addition, almost no aggregation exist, in other words, all the three metal oxide nanoparticles are uniformly distributed on the GO substrates which will facilitate their future utilization as adsorbents.

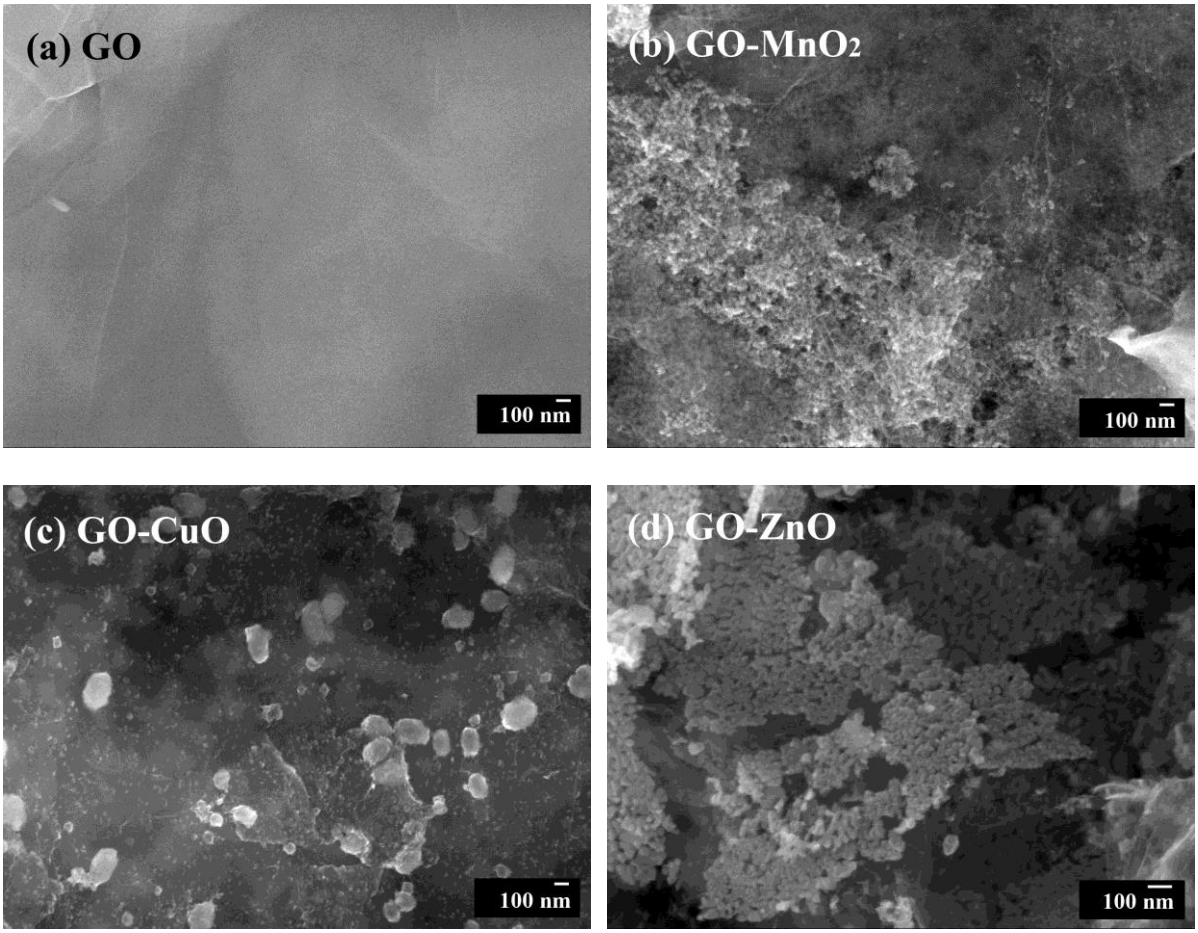

Figure 3.1. FE-SEM images of (a) GO, (b) GO-MnO_2, (c) GO-CuO and (d) GO-ZnO composites.

TEM was further employed to confirm the morphology of the metal oxides. The graphene oxide sheets are lucid and crumpled in all the three images, indicating that the deposition of metal oxides will not affect much to the original morphology of GO. In Figure 3.2a, two shapes of nanoparticles are scattered on the GO layers: the sphere-like nanoparticles and the needle-like nanoparticles. According to the referred paper,[26] the H_2O molecules would preferentially react with the O atoms in the (0 0 1) direction and therefore grew faster in this specific direction in the presence of H_2O, resulting in the needle-like nanoparticles. Meanwhile, the isopropyl alcohol would lead the development of the spherical particles. Consequently, the water/isopropyl alcohol ratio would decide the final overall morphologies of the coexistence of both the spherical

particles and the acicular particles of MnO_2. Figure 3.2b presents both large and small rough spherical particles with different extent of aggregations, highly in accordance with the FE-SEM image of GO-CuO. From Figure 3.2c, ZnO nanoparticles showed spindle shapes which are similar with Chen's work.[28] No ZnO nanoparticle is located outside the borders of GO, indicating the successful incorporation of ZnO onto GO surfaces. To further confirm the particle compositions, TEM-EDX was scanned as illustrated in Figure 3.2d from which Mn and Zn are clearly mapped. The EDX distribution and intensity of K, Mn and O on GO-MnO_2 as well as Zn and O on GO-ZnO are also given in supporting information (Figure 3.7, Supporting Information). Overall, from the FE-SEM and TEM measurements, it is obvious that nanoparticles containing Mn, Zn and Cu were successfully deposited on GO surfaces, respectively.

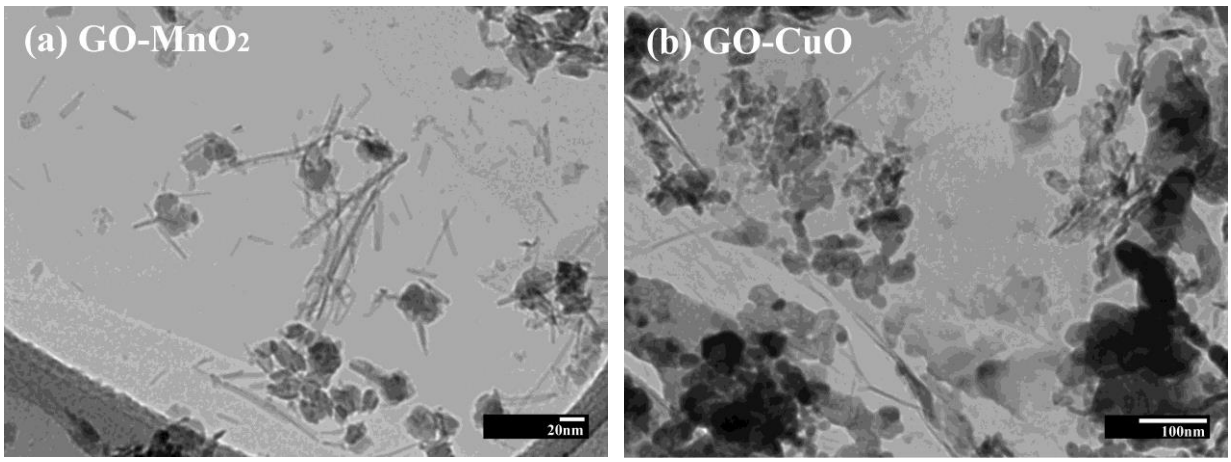

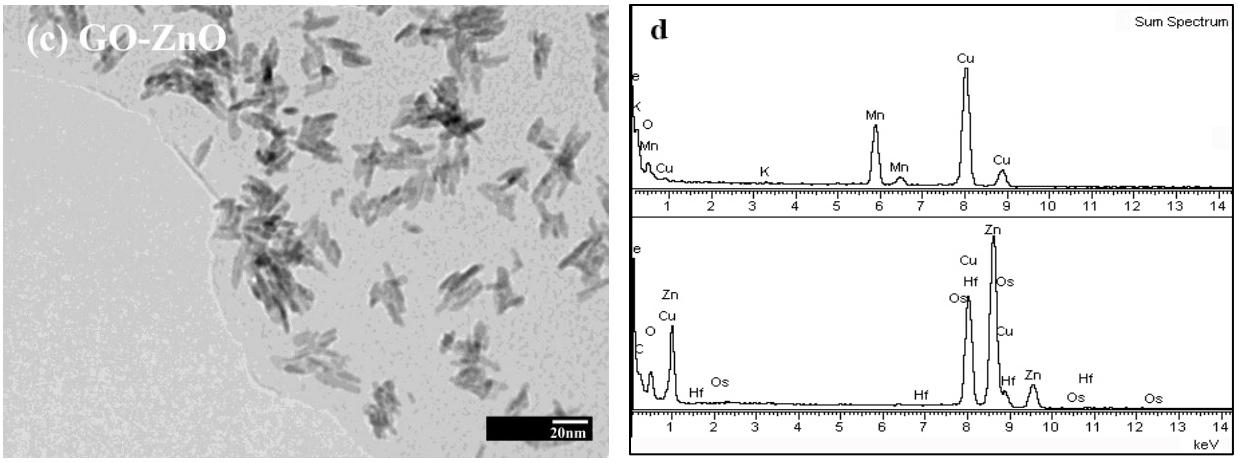

Figure 3.2. TEM images of (a) GO-MnO_2, (b) GO-CuO, (c) GO-ZnO and (d) TEM-EDX spectrum for GO-MnO_2 and GO-ZnO using the carbon-film coated copper mesh.

The exact compositions of the metal oxides were analyzed through both XRD and XPS characterizations. In this work, pristine GO and GO treated at 200 °C for 2 hours (tGO) were prepared and characterized for comparison. XRD patterns of GO, tGO and the metal oxide GO are displayed in Figure 3.3. The typical intensive peak of GO at 10.9° turns to a weak peak at 23.5° after 200 °C thermal treatment, indicating the interlayer spacing of GO reduced from 0.811 nm (close to the reported data[29]) to 0.378 nm (close to the 0.34 nm graphite d-spacing [30]) as calculated from the Bragg Equation ($2d\sin\theta=\lambda$). Curves of other metal oxide modified GO do not present any obvious peak of small θ (large d-spacing), which can be all explained by the exfoliation GO layers. The diffraction peaks of the modified GO matched well with the data from JCPDS card No. 36-1451, No. 30-0820 and No. 78-0428 for ZnO, MnO_2 and CuO, respectively. Since ZnO was obtained by dehydration of the precursor-$Zn(OH)_2$, the XRD patterns manifested the complete dehydration as no peak of $Zn(OH)_2$ is showed in the the figure. However, the existing forms of Cu and Mn are much more complicated to be analyzed and are needed to be further confirmed.

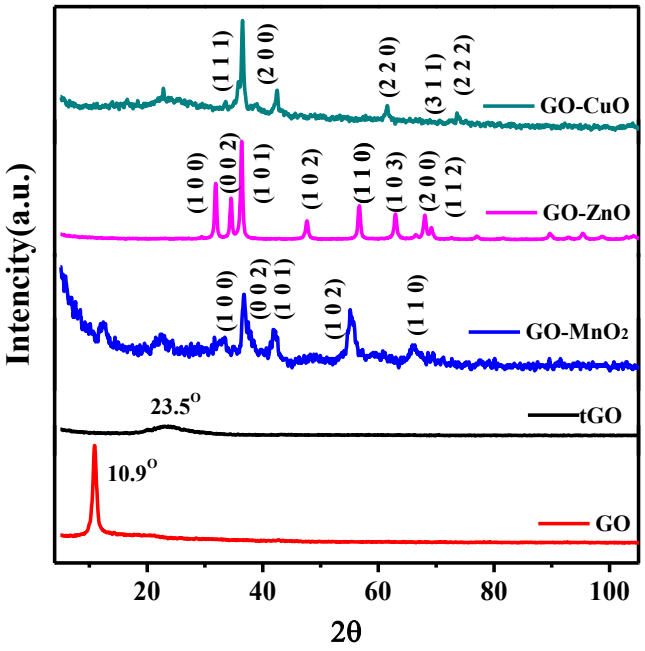

Figure 3.3. XRD spectra of GO, tGO, GO-MnO_2, GO-ZnO and GO-CuO.

Figure 3.4 displays the XPS characterization results. Figure 3.4a summary the full spectrum of GO, tGO and the metal oxides loaded GO that apparently presented the existence of Cu, Mn and Zn. The GO-MnO_2 curve (Figure 3.4b) shows a 4.97eV energy gap between the two peaks of the 3s spin orbit doublet which is in agreement with the reported data of MnO_2 XPS characterization.[31] In Figure 4d, peaks located at 934.23 eV, 945.0 eV, 954.33 eV and 962.73 eV can fit well with the CuO curve reported in Tahir's research[32] in which a comprehensive comparison of the Cu, Cu_2O and CuO XPS patterns was provided. Moreover, comparing the changes of the GO surface carbon-oxygen bonding before and after the 200 °C thermal treatment (Figure 3.8a and 3.8b, Supporting Information), it can be found that only C-O-C group is seriously reduced which probably results from the weakening effect of the incorporation methods used for MnO_2 and CuO deposition (Figure 3.8c-d, Supporting Information). However, the loading of Zn on GO greatly affects the C-OH groups instead of the C-O-C groups as shown in

Figure 3.8e (Supporting Information). Associated with the XRD results, the XPS demonstrated the loaded nanoparticles on GO are ZnO, CuO and MnO_2.

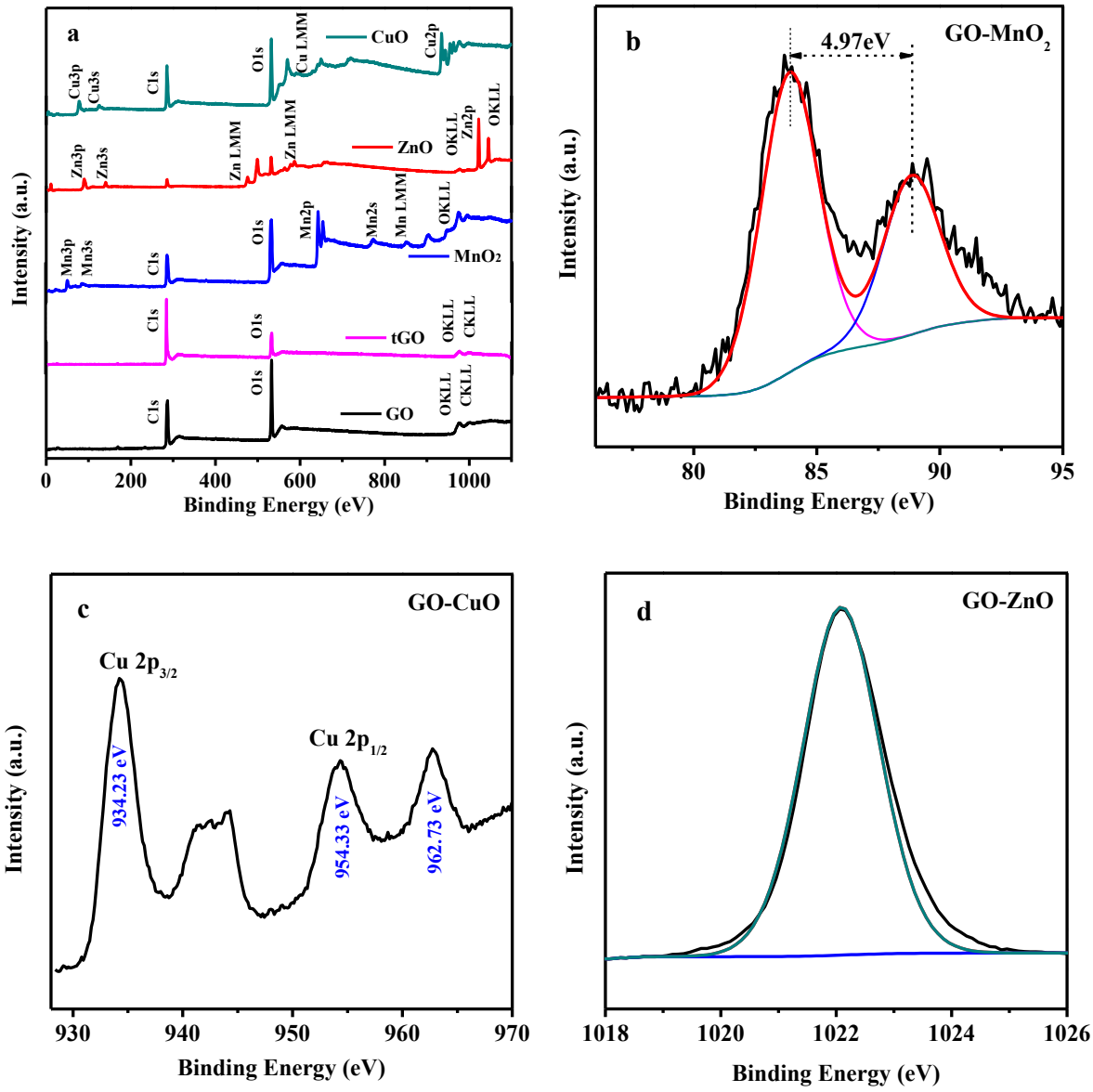

Figure 3.4. (a) XPS survey scan of GO, tGO, GO-MnO_2, GO-ZnO and GO-CuO, and XPS spectrum of (b) GO-MnO_2, (c) GO-CuO and (d) GO-ZnO.

3.4.2 Mercury Adsorption Capability of Composites

As shown in Figure 3.5, the virgin graphene oxide and the 2h 200 °C treated graphene oxide are compared to study the difference brought by the thermal treatment. The virgin GO has strong attraction towards Hg^0 at 100-150 °C which has already been analyzed in our previous work. However, after the exfoliation of the functional groups (mainly C-O-C group as indicated by XPS result), GO almost lost its Hg^0 adsorption capacity at the temperature range of 100-150 °C and at 50 °C as well, correspondingly confirming the assumption proposed before. Therefore, the mercury adsorption results of the metal oxide modified GO presented in Figure 3.6 primarily reflect the pure effect of the metal oxides towards Hg^0 as the C-O-C group partly retained for GO-MnO_2 and GO-CuO and C-OH group increased for GO-ZnO.

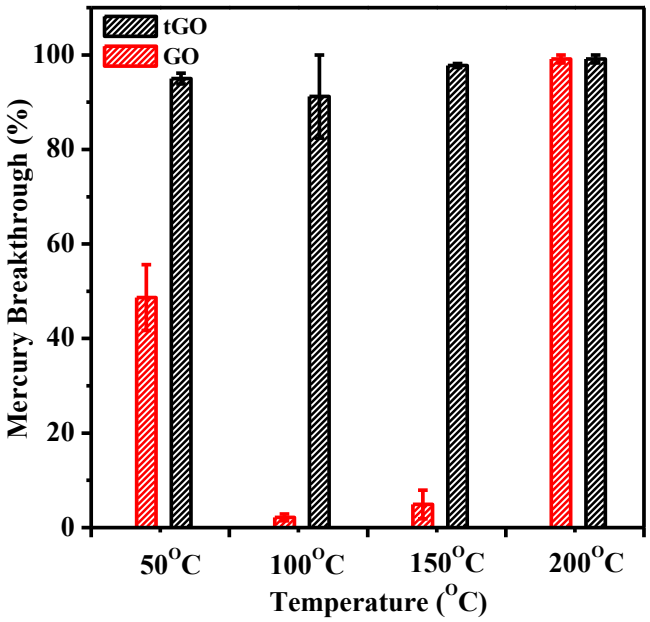

Figure 3.5. Hg^0 breakthrough of tGO and GO from 50 °C to 100 °C.

As is clearly presented in Figure 3.6, GO-MnO_2 performs excellent Hg^0 removal ability from 50 to 200 °C, viz., around 100% from 50 to 150 °C and around 83% at 200 °C of the 200

μL Hg^0 with only 15 mg sample loadings. Compared to the titania supported MnO_2 that tested at 175 °C by Ji,[22] this ability is normal. Hence, the incorporation of GO neither promote nor impede the catalysis of the MnO_2 nanoparticles towards Hg^0. Previous researches[22, 33] indicate that MnO_2 reacted with Hg^0 in two steps: Firstly, Hg^0 was oxidized to HgO by the manganese dioxide after the contact with the GO-MnO_2 surfaces. Meanwhile, the manganese dioxide was reduced to manganese oxide. Subsequently, a binary oxide-$HgMnO_3$-could form as the oxidized HgO continually combined with MnO_2 or MnO. Therefore, the total capacity of the material will be significantly determined by the MnO_2 loading amount. Additionally, with reposefully maintained mercury breakthrough from 50 to 200 °C, it can be evaluated that this chemi-sorption mechanism is very stable. Expectedly, magnetism can be introduced in future work into GO-MnO_2 to enhance the function.

Oppositely, the mercury breakthrough of GO-ZnO does not show much difference with the tGO, nearly perform no selectivity for Hg^0. The ineffectiveness of ZnO-NPs is in consistent with the literature data.[2, 34] Even though, it is found that the coexistence of H_2S and ZnO could dramatically promote the Hg^0 adsorption in which ZnO acted as the oxidizer of S^{2-} and the obtained S^0 consequently contributed to the oxidation of Hg^0.[34] Considering the H_2S in the flue gas and the utilization of ZnO on desulfurization, GO-ZnO still has potential application on simultaneous Hg^0 removal in flue gas. We would further conduct the Hg removal experiment in the flue gas for GO-ZnO.

Besides, GO-CuO just manifests a little bit adsorption effect (less than 10%) which deviates from the data reported by Yamaguchi.[25] The Cu atoms on (1 1 0) faces of CuO crystal was found to be able to bond the mercury molecules strongly. Thus, the mercury removal capability of GO-CuO is in large extent related to the crystallization of the CuO nanoparticles. Unless stable

synthesis and growth methods of CuO can be found, otherwise the GO-CuO is not capable to be applied as the Hg^0 adsorption adsorbent.

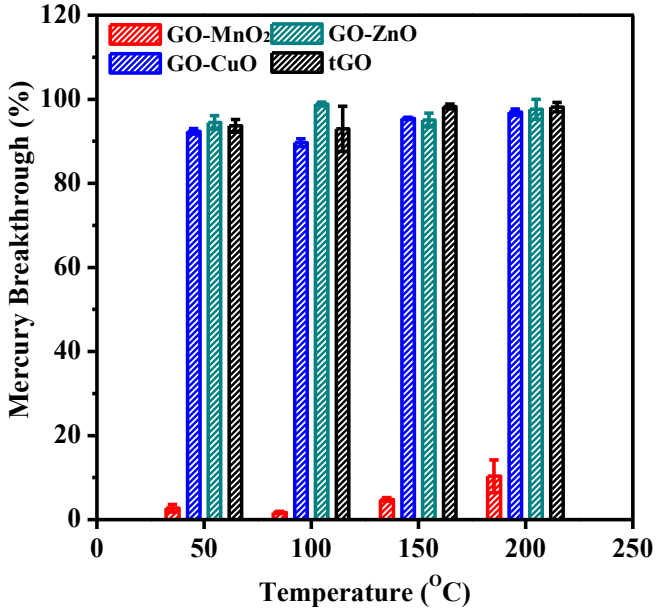

Figure 3.6. Hg^0 breakthrough of tGO, GO-MnO_2, GO-ZnO and GO-CuO from 50 °C to 100 °C.

3.5 Conclusions

Three kinds of metal oxides-MnO_2, CuO and ZnO nanoparticles were successfully deposited on GO substrates by using facile methods for enhancing the gas phase Hg adsorption capacity. All the composites were characterized with FE-SEM, TEM, XRD and XPS to investigate the particle sizes and morphologies, and to testify the compositions of the particles. It can be found that metal oxides, including ZnO, CuO and MnO_2 are successfully loaded on the GO. The spherical/acicular MnO_2-NPs and the spindle ZnO-NPs are around 30 nm while both the 100 nm and the 30 nm size CuO-NPs can be obtained. The following mercury breakthrough results demonstrate that the virgin GO has strong attraction towards Hg^0 at 100-150 °C because of the surface oxygen containing active sites. However, after the exfoliation of the functional

groups (mainly C-O-C group as indicated by XPS result), GO almost lost its Hg^0 adsorption capacity. The loading of MnO_2 on the GO obviously enhances its Hg^0 adsorption capacity- around 100% at low and medium temperatures and around 83% at 200 °C. While, the CuO and ZnO did not show visible effect in Argon carried vapour mercury.

3.6 Acknowledgement

The authors are grateful for the financial support for this work from the Helmholtz-Alberta Initiative - Energy & Environment (HAI-E&E) program and Natural Sciences and Engineering Research Council of Canada (NSERC).

3.7 Reference

(1) Galbreath, K. C.; Zygarlicke, C. J. Mercury Speciation in Coal Combustion and Gasification Flue Gases. *Environ. Sci. Technol.* **1996,** *30* (8), 2421-2426.

(2) Jadhav, R. A.; Howard, M. S.; Winecki, S. *Evaluation of Nanocrystalline Sorbents for Mercury Removal from Coal Gasifier Fuel Gas//2005AIChE Annual Meeting and Fall Showcase.*; Cincinnati, USA, 2005; pp 5526-5531.

(3) Clarkson, T. W.; Magos, L. The Toxicology of Mercury and Its Chemical Compounds. *Crit. Rev. Toxicol.* **2006,** *36* (8), 609-662.

(4) Zheng, Y.; Jensen, A. D.; Windelin, C.; Jensen, F. Review of Technologies for Mercury Removal from Flue Gas from Cement Production Processes. *Prog. Energ. Combust.* **2012,** *38* (5), 599-629.

(5) Meij, R.; Vredenbregt, L. H. J.; Winkel, H. t. The Fate and Behavior of Mercury in Coal-Fired Power Plants. *J. Air. Waste. Manage.* **2002,** *52* (8), 912-917.

(6) Wang, Y.; Duan, Y.; Yang, L.; Zhao, C.; Shen, X.; Zhang, M.; Zhuo, Y.; Chen, C. Experimental Study on Mercury Transformation and Removal in Coal-Fired Boiler Flue Gases. *Fuel Process. Technol* **2009,** *90* (5), 643-651.

(7) Huang, Y. H.; Peddi, P. K.; Tang, C.; Zeng, H.; Teng, X. Hybrid Zero-Valent Iron Process for Removing Heavy Metals and Nitrate from Flue-Gas-Desulfurization Wastewater. *Sep. Purif. Technol.* **2013,** *118*, 690-698.

(8) Yang, H.; Xu, Z.; Fan, M.; Bland, A. E.; Judkins, R. R. Adsorbents for Capturing Mercury in Coal-Fired Boiler Flue Gas. *J. Hazard. Mater.* **2007,** *146* (1-2), 1-11.

(9) Ghorishi, S. B.; Keeney, R. M. Development of a Cl-Impregnated Activated Carbon for Entrained-Flow Capture of Elemental Mercury. *Environ. Sci. Technol.* **2002,** *36* (20), 4454-4459.

(10) Lee, S. Removal of Gas-Phase Elemental Mercury by Iodine- and Chlorine-Impregnated Activated Carbons. *Atmos. Environ.* **2004,** *38* (29), 4887-4893.

(11) Chojnacki, A.; Chojnacka, K.; Hoffmann, J.; Górecki, H. The Application of Natural Zeolites for Mercury Removal: From Laboratory Tests to Industrial Scale. *Miner. Eng.* **2004,** *17* (7-8), 933-937.

(12) Dong, J.; Xu, Z.; Kuznicki, S. M. Mercury Removal from Flue Gases by Novel Regenerable Magnetic Nanocomposite Sorbents. *Environ. Sci. Technol.* **2009,** *43* (9), 3266-3271.

(13) Ghorishi, B.; Gullett, B. K. Sorption of Mercury Species by Activated Carbons and Calcium-Based Sorbents: Effect of Temperature, Mercury Concentration and Acid Gases. *Waste. Manage. Res.* **1998,** *16* (6), 582-593.

(14) Wang, Y. J.; Duan, Y. F.; Huang, Z. J.; Meng, S. L.; Yang, L. G.; Zhao, C. S. Vapor-Phase Elemental Mercury Adsorption by $Ca(OH)_2$ Impregnated with MnO_2 and Ag in Fixed-Bed System. *Asia-Pac. J. Chem. Eng.* **2009,** *5* (3), 479-487.

(15) Maroto-Valer, M. M.; Zhang, Y.; Granite, E. J.; Tang, Z.; Pennline, H. W. Effect of Porous Structure and Surface Functionality on the Mercury Capacity of a Fly Ash Carbon and Its Activated Sample. *Fuel.* **2005,** *84* (1), 105-108.

(16) Zhao, P.; Guo, X.; Zheng, C. Removal of Elemental Mercury by Iodine-Modified Rice Husk Ash Sorbents. *J. Environ. Sci.* **2010,** *22* (10), 1629-1636.

(17) Hua, X.-y.; Zhou, J.-s.; Li, Q.; Luo, Z.-y.; Cen, K.-f. Gas-Phase Elemental Mercury Removal by CeO_2 Impregnated Activated Coke. *Energ. Fuel.* **2010,** *24* (10), 5426-5431.

(18) Sreeprasad, T. S.; Maliyekkal, S. M.; Lisha, K. P.; Pradeep, T. Reduced Graphene Oxide-Metal/Metal Oxide Composites: Facile Synthesis and Application in Water Purification. *J. Hazard. Mater.* **2011,** *186* (1), 921-931.

(19) Zhao, G.; Li, J.; Ren, X.; Chen, C.; Wang, X. Few-Layered Graphene Oxide Nanosheets As Superior Sorbents for Heavy Metal Ion Pollution Management. *Environ. Sci. Technol.* **2011,** *45* (24), 10454-10462.

(20) Jiang, G.; Lin, Z.; Chen, C.; Zhu, L.; Chang, Q.; Wang, N.; Wei, W.; Tang, H. TiO_2 Nanoparticles Assembled on Graphene Oxide Nanosheets with High Photocatalytic Activity for Removal of Pollutants. *Carbon.* **2011,** *49* (8), 2693-2701.

(21) Hutson, N. D.; Attwood, B. C.; Scheckel, K. G. XAS and XPS Characterization of Mercury Binding on Brominated Activated Carbon. *Environ. Sci. Technol.* **2007,** *41* (5), 1742-1752.

(22) Ji, L.; Sreekanth, P. M.; Smirniotis, P. G.; Thiel, S. W.; Pinto, N. G. Manganese Oxide Titania Materials for Removal of NO_x and Elemental Mercury from Flue Gas. *Energy Fuels.* **2008,** *22* (4), 2299-2306.

(23) Lee, W.; Bae, G.-N. Removal of Elemental Mercury (Hg(0)) by Nanosized V_2O_5/TiO_2 Catalysts. *Environ. Sci. Technol.* **2009,** *43* (5), 1522-1527.

(24) Pitoniak, E.; Wu, C.-Y.; Londeree, D.; Mazyck, D.; Bonzongo, J.-C.; Powers, K.; Sigmund, W. Nanostructured Silica-Gel Doped with TiO_2 for Mercury Vapor Control. *J. Nanopart. Res.* **2003,** *5* (3-4), 281-292.

(25) Yamaguchi, A.; Akiho, H.; Ito, S. Mercury Oxidation by Copper Oxides in Combustion Flue Gases. *Powder Technol.* **2008,** *180* (1-2), 222-226.

(26) Chen, S.; Zhu, J.; Wu, X.; Han, Q.; Wang, X. Graphene Oxide MnO_2 Nanocomposites for Supercapacitors. *ACS Nano*. **2010,** *4* (5), 2822-2830.

(27) Zhu, J.; Zeng, G.; Nie, F.; Xu, X.; Chen, S.; Han, Q.; Wang, X. Decorating Graphene Oxide with CuO Nanoparticles in a Water-Isopropanol System. *Nanoscale*. **2010,** *2* (6), 988.

(28) Chen, Y.-L.; Hu, Z.-A.; Chang, Y.-Q.; Wang, H.-W.; Zhang, Z.-Y.; Yang, Y.-Y.; Wu, H.-Y. Zinc Oxide/Reduced Graphene Oxide Composites and Electrochemical Capacitance Enhanced by Homogeneous Incorporation of Reduced Graphene Oxide Sheets in Zinc Oxide Matrix. *J. Phys. Chem. C* **2011,** *115* (5), 2563-2571.

(29) Dikin, D. A.; Stankovich, S.; Zimney, E. J.; Piner, R. D.; Dommett, G. H. B.; Evmenenko, G.; Nguyen, S. T.; Ruoff, R. S. Preparation and Characterization of Graphene Oxide Paper. *Nature*. **2007,** *448* (7152), 457-460.

(30) McAllister, M. J.; Li, J.-L.; Adamson, D. H.; Schniepp, H. C.; Abdala, A. A.; Liu, J.; Herrera-Alonso, M.; Milius, D. L.; Car, R.; Prud'homme, R. K.; Aksay, I. A. Single Sheet Functionalized Graphene by Oxidation and Thermal Expansion of Graphite. *Chem. Mater.* **2007,** *19* (18), 4396-4404.

(31) Wang, J.-G.; Yang, Y.; Huang, Z.-H.; Kang, F. Rational Synthesis of MnO_2/Conducting Polypyrrole@Carbon Nanofiber Triaxial Nano-Cables for High-Performance Supercapacitors. *J. Mater. Chem*. **2012,** *22* (33), 16943-16949.

(32) Tahir, D.; Tougaard, S. Electronic and Optical Properties of Cu, CuO and Cu_2O Studied by Electron Spectroscopy. *J. Phys.: Condens. Matter* **2012,** *24* (17), 175002.

(33) Granite, E. J.; Pennline, H. W.; Hargis, R. A. Novel Sorbents for Mercury Removal from Flue Gas. *Ind. Eng. Chem. Res.* **2000,** *39* (4), 1020-1029.

(34) Zhou, J.-s.; Qi, P.; Hou, W.-h.; You, S.-l.; Gao, X.; Luo, Z.-y. Elemental Mercury Removal from Syngas by Nano-ZnO Sorbent. *J. Fuel. Chem. Technol.* **2013,** *41* (11), 1371-1377.

3.8 Supporting Information

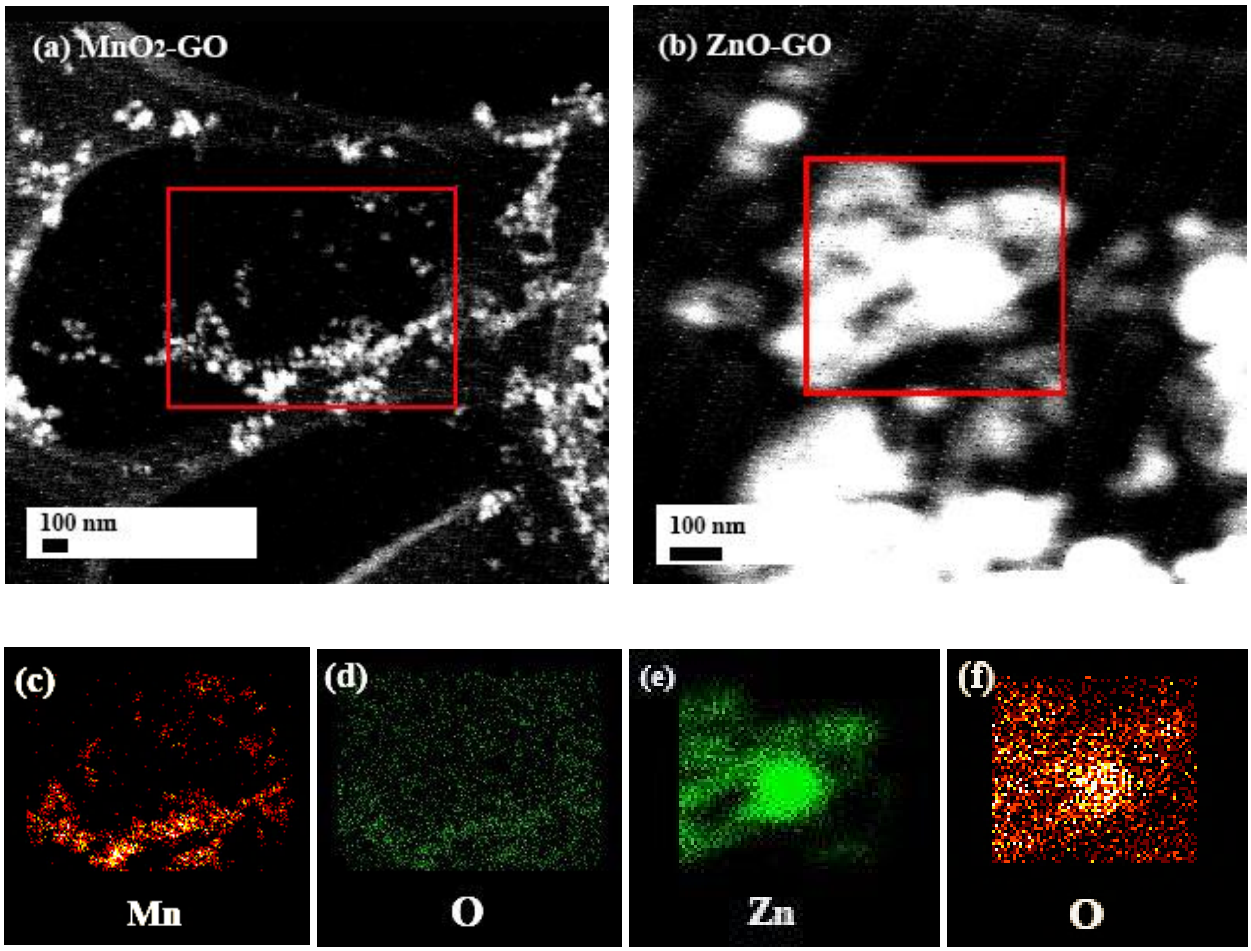

Figure 3.7. TEM-EDX survey scan of (a) GO-MnO_2, (b) GO-CuO and the element mapping of (c) Mn, (d) O on GO-MnO_2 and (e) Zn, (f) O on GO-ZnO.

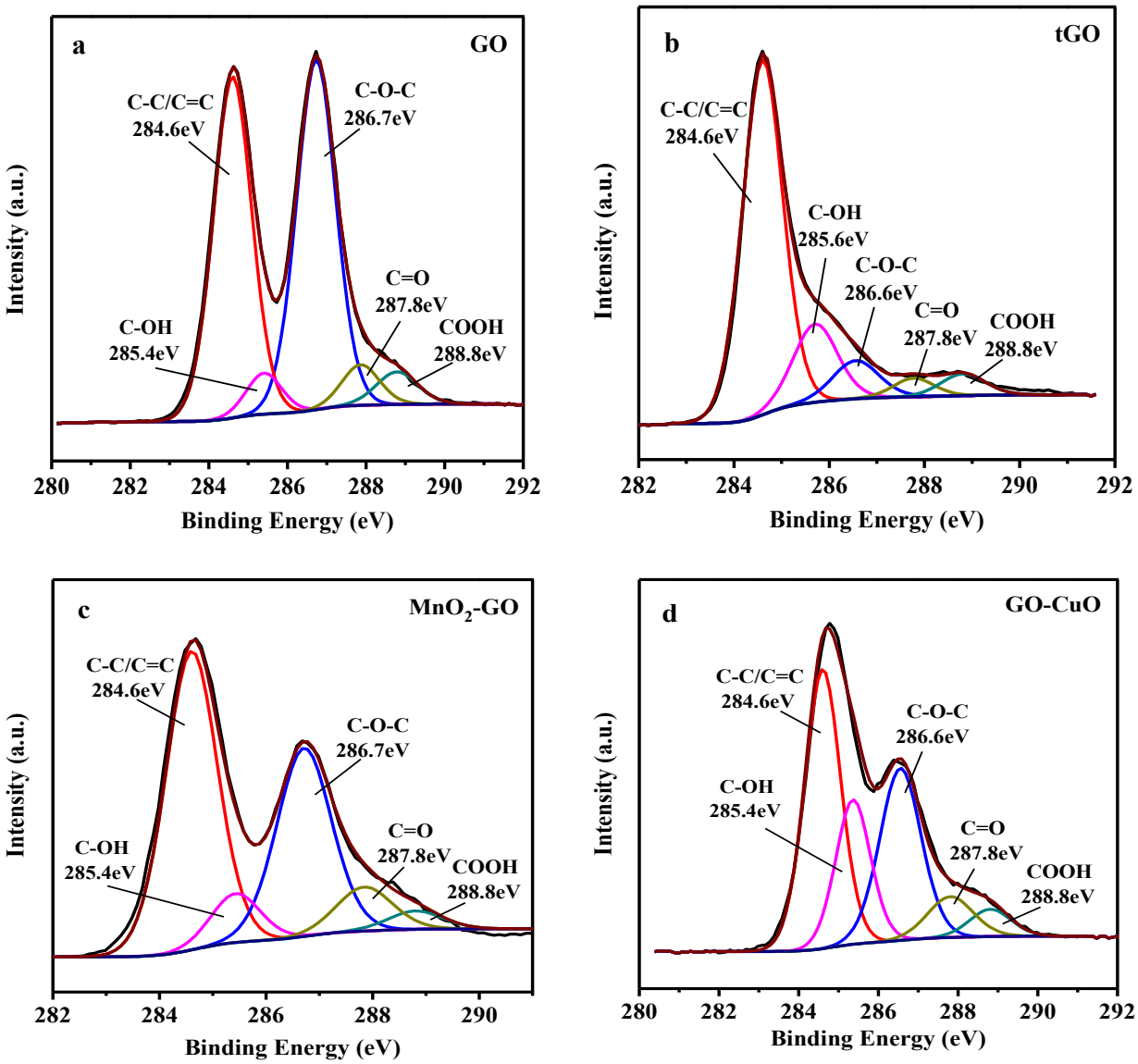
a
GO
C-C/C=C
284.6eV
C-O-C
286.7eV
C=O
287.8eV
COOH
288.8eV
C-OH
285.4eV
Intensity (a.u.)
Binding Energy (eV)
b
tGO
C-C/C=C
284.6eV
C-OH
285.6eV
C-O-C
286.6eV
C=O
287.8eV
COOH
288.8eV
Intensity (a.u.)
Binding Energy (eV)
c
MnO2-GO
C-C/C=C
284.6eV
C-O-C
286.7eV
C=O
287.8eV
COOH
288.8eV
C-OH
285.4eV
Intensity (a.u.)
Binding Energy (eV)
d
GO-CuO
C-C/C=C
284.6eV
C-O-C
286.6eV
C-OH
285.4eV
C=O
287.8eV
COOH
288.8eV
Intensity (a.u.)
Binding Energy (eV)

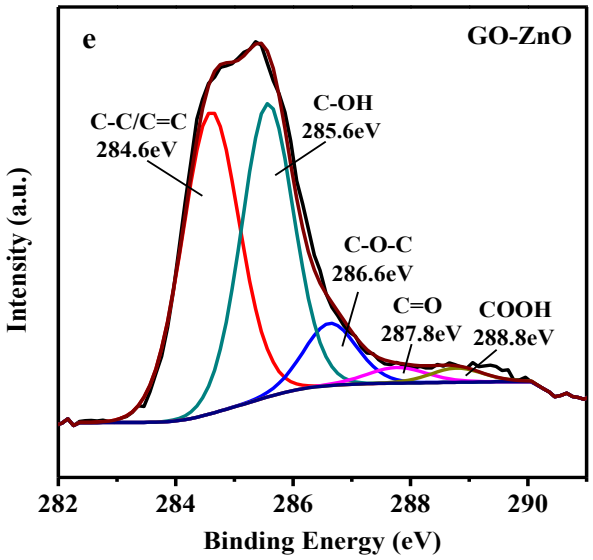

Figure 3.8. XPS spectra of carbon groups of (a) GO, (b) tGO, (c) GO-MnO_2, (d) GO-CuO and (e) GO-ZnO.

CHAPTER 4 CONCLUSIONS AND PROSPECTIVES

4.1 Conclusions

Several novel graphene oxide based composites were successfully synthesized and characterized in this work, and were applied for elemental mercury for the first time. The major findings and conclusions of this thesis work are summarized as follows:

1. By adding PVP and glucose, Ag-NPs (~50 nm) could be homogeneously deposited on GO and MGO sheets successfully. GO composites decorated with different amount of Ag NPs were obtained and characterized.
2. GO performed 50% Hg^0 adsorption at 50 ℃, around 100% Hg^0 adsorption at 100 and 150 °C possibly by oxygen-containing functional groups, and nearly no Hg^0 adsorption above 200 °C due to the loss of surface functional groups.
3. The deposition of Ag NPs on GO enhances the Hg^0 removal capability of GO-Ag as compared to that of pure GO, mainly due to amalgamation between Ag NPs and Hg^0.
4. The addition of magnetic ferrite NPs on GO shows similar mercury adsorption capability as GO at 50-150 ℃, but will enhance the Hg^0 removal capability of MGO to ~60% at 200 °C, and about ~20% at 250 °C.
5. Simultaneous existence of Ag and magnetic Fe will dramatically boost the Hg^0 adsorption to ~95% at 200 °C and ~40% at 250 °C. The results are better than the individual incorporation of Ag and Fe.
6. The silver content also affected the Hg^0 breakthrough results, higher silver content gets better removal efficiency.

7. MGO-Ag can be regenerated for reuse through a thermal treatment process, which shows great potential applications in Hg^0 removal from practical flue gas.
8. MnO_2 NPs could interact with Hg^0 through chemi-sorption, and GO-MnO_2 composites show excellent removal ability of Hg^0 even at high temperature (≥200 °C).
9. The addition of ZnO and CuO NPs does not significantly enhance the Hg^0 removal capability of GO composite.

4.2 Contributions to the Original Knowledge

Novel graphene oxide based composites were synthesized and systematically characterized in this work. Metal and metal oxides loaded graphene oxide composites were used in elemental mercury removal for the first time. Magnetism was also introduced for the purposes of recycling and fast separation. Some of composites developed show excellent Hg^0 removal efficiencies over a broad range of temperature which can be also regenerated for reuse, and they have great potential application for real flue gas clean-up.

4.3 Suggestions for Future Work

All the mercury adsorption tests in this thesis were conducted using pure mercury with Ar. To investigate the effect of other components in real flue gas, simulated flue gas is suggested to be applied for future experiments.

1. Hg^0 removal experiments in simulated flue gas at various temperatures for the synthesized composites
2. Hg^0 removal experiments in simulated flue gas with different contents of CO_2, O_2, NO_x, H_2O and SO_2.

BIBLIOGRAPHY

(1) Chauhan, D. S.; Srivastava, S. K., *Non-Conventional Energy Resources.* 2 ed.; New Age International: 2007; p 2-17.

(2) Bhattacharyya, S. C., *Energy Economics*

Concepts, Issues, Markets and Governance. 1 ed.; Springer: 2011; p 9-11.

(3) Shafiee, S.; Topal, E. An Econometrics View of Worldwide Fossil Fuel Consumption and the Role of US. *Energy. Policy.* **2008,** *36* (2), 775-786.

(4) Patzek, T. W.; Croft, G. D. A Global Coal Production Forecast with Multi-Hubbert Cycle Analysis. *Energy.* **2010,** *35* (8), 3109-3122.

(5) Teske, S.; Pregger, T.; Simon, S.; Naegler, T.; Graus, W.; Lins, C. Energy [R] Evolution 2010-a Sustainable World Energy Outlook. *Energy Efficiency* **2010,** *4* (3), 409-433.

(6) Liu, C. H.; Zhou, Z. D.; Yu, X.; Lv, B. Q.; Mao, J. F.; Xiao, D. Preparation and Characterization of Fe_3O_4/Ag Composite Magnetic Nanoparticles. *Inorg. Mater.* **2008,** *44* (3), 291-295.

(7) Meij, R.; te Winkel, B. The Emissions and Environmental Impact of PM10 and Trace Elements from a Modern Coal-Fired Power Plant Equipped with ESP and Wet FGD. *Fuel Process. Technol.* **2004,** *85* (6-7), 641-656.

(8) Chen, J.-C.; Liu, Z.-S.; Huang, J.-S. Emission Characteristics of Coal Combustion in Different O_2/N_2, O_2/CO_2 and O_2/RFG Atmosphere. *J. Hazard. Mater.* **2007,** *142* (1-2), 266-271.

(9) Bose, A. C.; Dannecker, K. M.; Wendt, J. O. L. Coal Composition Effects on Mechanisms Governing the Destruction of Nitric Oxide and Other Nitrogenous Species during Fuel-Rich Combustion. *Energy. Fuels.* **1988,** *2* (30), 301-308.

(10) Chagué-G, C.; Fyfe, W. S. Geochemical and Petrographical Characteristics of a Domed Bog, Nova Scotia a Modern Analogue for Temperature Coal Deposits. *Org. Geochem.* **1996,** *24* (2), 141-158.

(11) Vejahati, F.; Xu, Z.; Gupta, R. Trace Elements in Coal: Associations with Coal and Minerals and Their Behavior during Coal Utilization-A review. *Fuel.* **2010,** *89* (4), 904-911.

(12) Lee, S.; Rhim, Y.; Cho, S.; Baek, J. Carbon-Based Novel Sorbent for Removing Gas-Phase Mercury. *Fuel.* **2006,** *85* (2), 219-226.

(13) Carlson, C. L.; Adriano, D. C. Environmental Impacts of Coal Combustion Residues. *J. Environ. Qual.* **1993,** *22* (2), 227-247.

(14) Skorek-Osikowska, A.; Kotowicz, J.; Janusz-Szymańska, K. Comparison of the Energy Intensity of the Selected CO_2 Capture Methods Applied in the Ultra-Supercritical Coal Power Plants. *Energ. Fuel.* **2012,** *26* (11), 6509-6517.

(15) Finkelman, R. B.; Orem, W.; Castranova, V.; Tatu, C. A.; Belkin, H. E.; Zheng, B.; Lerch, H. E.; Maharaj, S. V.; Bates, A. L. Health Impacts of Coal and Coal Use Possible Solutions. *Int. J. Coal Geol.* **2002,** *50* (1-4), 425-443.

(16) Finkelman, R. B. Trace Elements in Coal. *Biol. Trace Elem. Res.* **1999,** *67* (3), 197-204.

(17) News Releases from Headquarters. http://yosemite.epa.gov/opa/admpress.nsf/bd4379a92ceceeac8525735900400c27/5bb6d20668b9a18485257ceb00490c98!OpenDocument (accessed July 19, 2014).

(18) Alberta Energy: Coal Acts and Regulations. http://www.energy.alberta.ca/coal/664.asp (accessed July 19, 2014).

(19) Jaworek, A.; Krupa, A.; Czech, T. Modern Electrostatic Devices and Methods for Exhaust Gas Cleaning: A Brief Review. *J. Electrostat.* **2007,** *65* (3), 133-155.

(20) Srivastava, R. K.; Jozewicz, W. Flue Gas Desulfurization: The State of the Art. *J. Air. Waste. Manage.* **2001,** *51* (12), 1676-1688.

(21) Srivastava, R. K.; Hall, R. E.; Khan, S.; Culligan, K.; Lani, B. W. Nitrogen Oxides Emission Control Options for Coal-Fired Electric Utility Boilers. *J. Air & Waste Manage. Assoc.* **2005,** *55* (9), 1367-1388.

(22) Barman, S.; Philip, L. Integrated System for the Treatment of Oxides of Nitrogen from Flue Gasea. *Environ. Sci. Technol.* **2006,** *40* (3), 1035-1041.

(23) Xu, M. Status of Trace Element Emission in a Coal Combustion Process: A Review. *Fuel Process. Technol.* **2004,** *85* (2-3), 215-237.

(24) Clarkson, T. W.; Magos, L. The Toxicology of Mercury and Its Chemical Compounds. *Crit. Rev. Toxicol.* **2006,** *36* (8), 609-662.

(25) Pirrone, N.; Cinnirella, S.; Feng, X.; Finkelman, R. B.; Friedli, H. R.; Leaner, J.; Mason, R.; Mukherjee, A. B.; Stracher, G. B.; Streets, D. G.; Telmer, K. Global Mercury

Emissions to the Atmosphere from Anthropogenic and Natural Sources. *Atmos. Chem. Phys.* **2010,** *10* (13), 5951-5964.

(26) Meij, R.; Vredenbregt, L. H. J.; Winkel, H. t. The Fate and Behavior of Mercury in Coal-Fired Power Plants. *J. Air. Waste. Manage.* **2002,** *52* (8), 912-917.

(27) Meij, R. The Fate of Mercury in Coal-Fired Power Plants and the Influence of Wet Flue-Gas Desulphurization. *Water, Air, Soil Pollut.* **1991,** *56* (1), 21-33.

(28) Toole-O'Neil, B.; Tewalt, S. J.; Finkelman, R. B.; Akers, D. J. Mercury Concentration in Coal-Unraveling the Puzzle. *Fuel.* **1999,** *78* (1), 47-54.

(29) Galbreath, K. C.; Zygarlicke, C. J. Mercury Transformations in Coal Combustion Flue Gas. *Fuel Process. Technol.* **2000,** *65-66*, 289-310.

(30) Pavlish, J. H.; Sondreal, E. A.; Mann, M. D.; Olson, E. S.; Galbreath, K. C.; Laudal, D. L.; Benson, S. A. Status Review of Mercury Control Options for Coal-Fired Power Plants. *Fuel Process. Technol* **2003,** *82* (2-3), 89-165.

(31) Yudovich, Y. E.; Ketris, M. P. Mercury in Coal: A Review Part 2. Coal Use and Environmental Problems. *Int. J. Coal. Geol.* **2005,** *62* (3), 135-165.

(32) Yang, H.; Xu, Z.; Fan, M.; Bland, A. E.; Judkins, R. R. Adsorbents for Capturing Mercury in Coal-Fired Boiler Flue Gas. *J. Hazard. Mater.* **2007,** *146* (1-2), 1-11.

(33) Senior, C. L.; Sarofim, A. F.; Zeng, T.; Helble, J. J.; Mamani-Paco, R. Gas-phase Transformations of Mercury in Coal-Fired Power Plants. *Fuel Process. Technol.* **2000,** *63* (2), 197-213.

(34) Hsi, H.-C.; Chen, C.-T. Influences of Acidic/Oxidizing Gases on Elemental Mercury Adsorption Equilibrium and Kinetics of Sulfur-Impregnated Activated Carbon. *Fuel.* **2012,** *98*, 229-235.

(35) Kilgroe, J. D.; Sedman, C. B.; Srivastava, R. K.; Ryan, J. V.; Lee, C. W.; Thorneloe, S. A. *Control of Mercury Emissions from Coal-Fired Electric Utility Boilers: Interim Report. U.S.*; 2002.

(36) Staudt, J. E.; Jozewicz, W. *Performance and Cost of Mercury and Multipollutant Emission Control Technology Applications on Electric Utility Boilers.*; 2003.

(37) Reddy, B. M.; Durgasri, N.; Kumar, T. V.; Bhargava, S. K. Abatement of Gas-Phase Mercury-Recent Developments. *Catal. Rev.* **2012,** *54* (3), 344-398.

(38) Sun, X.; Hwang, J.-Y.; Xie, S. Density Functional Study of Elemental Mercury Adsorption on Surfactants. *Fuel.* **2011,** *90* (3), 1061-1068.

(39) Dunham, G. E.; DeWall, R. A.; Senior, C. L. Fixed-Bed Studies of the Interactions between Mercury and Coal Combustion Fly Ash. *Fuel Process. Technol.* **2003,** *82* (2-3), 197-213.

(40) Dranga, B.-A.; Lazar, L.; Koeser, H. Oxidation Catalysts for Elemental Mercury in Flue Gases-A Review. *Catalysts.* **2012,** *2* (4), 139-170.

(41) Huggins, F. E.; Yap, N.; Huffman, G. P.; Senior, C. L. XAFS Characterization of Mercury Captured from Combustion Gases on Sorbents at Low Temperatures. *Fuel Process. Technol.* **2003,** *82* (2-3), 167-196.

(42) Presto, A. A.; Granite, E. J. Noble Metal Catalysts for Mercury Oxidation in Utility Flue Gas. *Platinum Met. Rev*. **2008,** *52* (3), 144-154.

(43) Liu, Y.; Bisson, T. M.; Yang, H.; Xu, Z. Recent Developments in Novel Sorbents for Flue Gas Clean Up. *Fuel Process. Technol* **2010,** *91* (10), 1175-1197.

(44) Ghorishi, S. B.; Keeney, B. K. Development of a Cl-Impregnated Activated Carbon for Entrained-Flow Capture of Elemental Mercury. *Environ. Sci. Technol.* **2002,** *36* (20), 4454-4459.

(45) Hutson, N.; Atwood, B.; Scheckel, K. XAS and XPS Characterization of Mercury Binding on Brominated Activated Carbon. *Environ Sci. Technol.* **2007,** *41* (5), 1747-1752.

(46) Hsi, H.-C.; Rood, M. J.; Rostam-Abadi, M.; Chen, S.; Chang, R. Effects of Sulfur Impregnation Temperature on the Properties and Mercury Adsorption Capacities of Activated Carbon Fibers (ACFs). *Environ Sci. Technol.* **2001,** *35* (13), 2785-2791.

(47) Shen, Z.; Ma, J.; Mei, Z.; Zhang, J. Metal Chlorides Loaded on Activated Carbon to Capture Elemental Mercury. *J. Environ. Sci.* **2010,** *22* (11), 1814-1819.

(48) Mei, Z.; Shen, Z.; Zhao, Q.; Wang, W.; Zhang, Y. Removal and Recovery of Gas-Phase Element Mercury by Metal Oxide-Loaded Activated Carbon. *J. Hazard. Mater.* **2008,** *152* (2), 721-729.

(49) Olson, D. G.; Tsuji, K.; Shiraishi, I. The Reduction of Gas Phase Air Toxics from Combustion and Incineration Sources Using the MET-Mitsui-BF Activated Coke Process. *Fuel Process. Technol.* **2000,** *65-66*, 393-405.

(50) Hua, X.-y.; Zhou, J.-s.; Li, Q.; Luo, Z.-y.; Cen, K.-f. Gas-Phase Elemental Mercury Removal by CeO_2 Impregnated Activated Coke. *Energ. Fuel.* **2010,** *24* (10), 5426-5431.

(51) Tao, S.; Li, C.; Fan, X.; Zeng, G.; Lu, P.; Zhang, X.; Wen, Q.; Zhao, W.; Luo, D.; Fan, C. Activated Coke Impregnated with Cerium Chloride Used for Elemental Mercury Removal from Simulated Flue Gas. *Chem. Eng. J.* **2012,** *210*, 547-556.

(52) Ghorishi, S. B.; Singer, C. F.; Jozewicz, W. S.; Sedman, C. B.; Srivastava, R. K. Simultaneous Control of Hg^0, SO_2, and NO_x by Novel Oxidized Calcium-Based Sorbents. *J. Air. Waste. Manage.* **2002,** *52* (3), 273-278.

(53) Hsi, H.-C.; Rood, M. J.; Rostam-Abadi, M.; Chen, S.; Chang, R. Mercury Adsorption Properties of Sulfur-Impregnated Adsorbents. *J. Environ. Eng.* **2002,** *128* (11), 1080-1089.

(54) Liu, Y.; Kelly, D. J. A.; Yang, H.; Lin, C. C. H.; Kuznicki, S. M.; Xu, Z. Novel Regenerable Sorbent for Mercury Capture from Flue Gases of Coal-Fired Power Plant. *Environ. Sci. Technol.* **2008,** *42* (16), 6205-6210.

(55) Qu, Z.; Yan, N.; Liu, P.; Chi, Y.; Jia, J. Bromine Chloride as an Oxidant to Improve Elemental Mercury Removal from Coal-Fired Flue Gas. *Environ. Sci. Technol.* **2009,** *43* (22), 8610-8615.

(56) Pitoniak, E.; Wu, C.-Y.; Londeree, D.; Mazyck, D.; Bonzongo, J.-C.; Powers, K.; Sigmund, W. Nanostructured Silica-Gel Doped with TiO_2 for Mercury Vapor Control. *J. Nanopart. Res.* **2003,** *5* (3-4), 281-292.

(57) Kamata, H.; Ueno, S.-i.; Naito, T.; Yukimura, A. Mercury Oxidation Over the V_2O_5 (WO_3)/TiO_2 Commercial SCR Catalyst. *Ind. Eng. Chem. Res.* **2008,** *47* (21), 8136-8141.

(58) Dreyer, D. R.; Park, S.; Bielawski, C. W.; Ruoff, R. S. The Chemistry of Graphene Oxide. *Chem. Soc. Rev.* **2010,** *39* (1), 228.

(59) He, H.; Klinowskia, J.; Forsterb, M.; Lerf, A. A New Structural Model for Graphite Oxide. *Chem. Phys. Lett.* **1998,** *287* (1-2), 53-56.

(60) Xu, C.; Wang, X. Fabrication of Flexible Metal-Nanoparticle Films Using Graphene Oxide Sheets as Substrates. *Small.* **2009,** *5* (19), 2212-2217.

(61) Sreeprasad, T. S.; Maliyekkal, S. M.; Lisha, K. P.; Pradeep, T. Reduced Graphene Oxide-Metal/Metal Oxide Composites: Facile Synthesis and Application in Water Purification. *J. Hazard. Mater.* **2011,** *186* (1), 921-931.

(62) Chandra, V.; Kim, K. S. Highly Selective Adsorption of Hg^{2+} by a Polypyrrole-Reduced Graphene Oxide Composite. *Chem. Commun.* **2011,** *47* (13), 3942.

(63) Environmental Impacts of Coal Power: Air Pollution. http://www.ucsusa.org/clean_energy/coalvswind/c02c.html

(64) Fitzgerald, W. F. Is Mercury Increasing in the Atmosphere? The Need for an Atmospheric Mercury Network (AMNET). *Water, Air, Soil Pollut.* **1995,** *80* (1-4), 245-254.

(65) Dastoor, A. P.; Larocque, Y. Global Circulation of Atmospheric Mercury: A Modelling Study. *Atmos. Environ.* **2004,** *38* (1), 147-161.

(66) Galbreath, K. C. Z., C J. Mercury Speciation in Coal Combustion and Gasification Flue Gases. *Environ. Sci. Technol.* **1996,** *30* (8), 2421-2426.

(67) Lindqvist, O.; Johansson, K.; Aastrup, M.; Anderson, A.; Bringmark, L.; Hovsenius, G. Mercury in the Swedish Environment-Recent Research on Causes, Consequences and Corrective Methods. *Water, Air, Soil Pollut.* **1991,** *55* (1-2), 1-261.

(68) Reddy, B. M.; Durgasri, N.; Kumar, T. V.; Bhargava, S. K. Abatement of Gas-Phase Mercury-Recent Developments. *Cat. Rev: Sci. Eng.* **2012,** *54* (3), 344-398.

(69) Granite, E. J.; Pennline, H. W.; Hargis, R. A. Novel Sorbents for Mercury Removal from Flue Gas. *Ind. Eng. Chem. Res.* **2000,** *39* (4), 1020-1029.

(70) Zeng, H.; Jin, F.; Guo, J. Removal of Elemental Mercury from Coal Combustion Flue Gas by Chloride-Impregnated Activated Carbon. *Fuel.* **2004,** *83* (1), 143-146.

(71) Worathanakul, P.; Kongkachuichay, P.; Noel, J. D.; Suriyawong, A.; Giammar, D. E.; Biswas, P. Evaluation of Nanostructured Sorbents in Differential Bed Reactors for Elemental Mercury Capture. *Environ. Eng. Sci.* **2008,** *25* (7), 1061-1070.

(72) Abu-Daabes, M. A.; Pinto, N. G. Synthesis and Characterization of a Nano-Structured Sorbent for the Direct Removal of Mercury Vapor from Flue Gases by Chelation. *Chem. Eng. Sci.* **2005,** *60* (7), 1901-1910.

(73) Dong, J.; Xu, Z.; Kuznicki, S. M. Magnetic Multi-Functional Nano Composites for Environmental Applications. *Adv. Funct. Mater.* **2009,** *19* (8), 1268-1275.

(74) Luo, G.; Yao, H.; Xu, M.; Cui, X.; Chen, W.; Gupta, R.; Xu, Z. Carbon Nanotube-Silver Composite for Mercury Capture and Analysis. *Energ. Fuel.* **2010,** *24* (1), 419-426.

(75) Zhu, Y.; Murali, S.; Cai, W.; Li, X.; Suk, J. W.; Potts, J. R.; Ruoff, R. S. Graphene and Graphene Oxide: Synthesis, Properties, and Applications. *Adv. Mater.* **2010,** *22* (35), 3906-3924.

(76) Poulston, S.; Granite, E. J.; Pennline, H. W.; Myers, C. R.; Stanko, D. P.; Hamilton, H.; Rowsell, L.; Smith, A. W. J.; Ilkenhans, T.; Chu, W. Metal Sorbents for High Temperature Mercury Capture from Fuel Gas. *Fuel.* **2007,** *86* (14), 2201-2203.

(77) Wilcox, J.; Rupp, E.; Ying, S. C.; Lim, D.-H.; Negreira, A. S.; Kirchofer, A.; Feng, F.; Lee, K. Mercury Adsorption and Oxidation in Coal Combustion and Gasification Processes. *Int. J. Coal. Geol.* **2012,** *90-91*, 4-20.

(78) Yan, T. Y. A Novel Process for Hg Removal from Gases. *Ind. Eng. Chem. Res.* **1994,** *33* (12), 3010-3014.

(79) Li, Y. H.; Lee, C. W.; Gullett, B. K. Importance of Activated Carbon's Oxygen Surface Functional Groups on Elemental Mercury Adsorption. *Fuel.* **2003,** *82* (4), 451-457.

(80) Shen, J.; Hu, Y.; Shi, M.; Li, N.; Ma, H.; Ye, M. One Step Synthesis of Graphene Oxide-Magnetic Nanoparticle Composite. *J. Phys. Chem. C.* **2010,** *114* (3), 1498-1503.

(81) Tang, X.-Z.; Li, X.; Cao, Z.; Yang, J.; Wang, H.; Pu, X.; Yu, Z.-Z. Synthesis of Graphene Decorated with Silver Nanoparticles by Simultaneous Reduction of Graphene Oxide and Silver Ions with Glucose. *Carbon.* **2013,** *59*, 93-99.

(82) Kassaee, M. Z.; Motamedi, E.; Majdi, M. Magnetic Fe_3O_4-Graphene Oxide/Polystyrene: Fabrication and Characterization of a Promising Nanocomposite. *Chem. Eng. J.* **2011,** *172* (1), 540-549.

(83) Hou, C.; Zhang, Q.; Zhu, M.; Li, Y.; Wang, H. One-Step Synthesis of Magnetically-Functionalized Reduced Graphite Sheets and Their Use in Hydrogels. *Carbon.* **2011,** *49* (1), 47-53.

(84) Fu, Y.; Wang, J.; Liu, Q.; Zeng, H. Water-Dispersible Magnetic Nanoparticle-Graphene Oxide Composites for Selenium Removal. *Carbon* **2014,** *77*, 710-721.

(85) Liu, L.; Liu, J.; Wang, Y.; Yan, X.; Sun, D. D. Facile Synthesis of Monodispersed Silver Nanoparticles on Graphene Oxide Sheets with Enhanced Antibacterial Activity. *New J. Chem.* **2011,** *35* (7), 1418.

(86) Weaver, J. F.; Hoflund, G. B. Surface Characterization Study of the Thermal Decomposition of Ag_2O. *Chem. Mater.* **1994,** *6* (10), 1693-1699.

(87) Heister, K.; Zharnikov, M.; Grunze, M. Adsorption of Alkanethiols and Biphenylthiols on Au and Ag Substrates: A High-Resolution X-Ray Photoelectron Spectroscopy Study. *J. Phys. Chem. B.* **2001,** *105* (19), 4058-4061.

(88) Yamashita, T.; Hayes, P. Analysis of XPS Spectra of Fe^{2+} and Fe^{3+} Ions in Oxide Materials. *Appl. Surf. Sci.* **2008,** *254* (8), 2441-2449.

(89) Han, D. H.; Wang, J. P.; Luo, H. L. Crystallite Size Effect on Saturation Magnetization of Fine Ferrimagnetic Particles. *J. Magn. Magn. Mater.* **1994,** *136* (1-2), 176-182.

(90) Ai, Z. D., K.; Wan, Q.; Zhang, L.; Lee, S. Facile Microwave-Assisted Synthesis and Magnetic and Gas Sensing Properties of Fe_3O_4 Nanoroses. *J. Phys. Chem. C.* **2010,** *114* (14), 6237-6242.

(91) Li, Y. H.; Lee, C. W.; Gullett, B. K. The Effect of Activated Carbon Surface Moisture on Low Temperature Mercury Adsorption. *Carbon.* **2002,** *40* (1), 65-72.

(92) Wu, S.; Oya, N.; Ozaki, M.; Kawakami, J.; Uddin, M. A.; Sasaoka, E. Development of Iron Oxide Sorbents for Hg^0 Removal from Coal Derived Fuel Gas: Sulfidation Characteristics of Iron Oxide Sorbents and Activity for COS Formation during Hg^0 Removal. *Fuel.* **2007,** *86* (17-18), 2857-2863.

(93) Carey, T. R.; Richardson, C. F. Assessing Sorbent Injection Mercury Control Effectiveness in Flue Gas Streams. *Environ. Progress.* **2004,** *19* (3), 167-174.

(94) Dong, J.; Xu, Z.; Kuznicki, S. M. Mercury Removal from Flue Gases by Novel Regenerable Magnetic Nanocomposite Sorbents. *Advan. Funct. Mater* **2009,** *19*, 1268-1275.

(95) Galbreath, K. C.; Zygarlicke, C. J. Mercury Speciation in Coal Combustion and Gasification Flue Gases. *Environ. Sci. Technol.* **1996,** *30* (8), 2421-2426.

(96) Jadhav, R. A.; Howard, M. S.; Winecki, S. *Evaluation of Nanocrystalline Sorbents for Mercury Removal from Coal Gasifier Fuel Gas//2005AIChE Annual Meeting and Fall Showcase.*; Cincinnati, USA, 2005; pp 5526-5531.

(97) Clarkson, T. W.; Magos, L. The Toxicology of Mercury and Its Chemical Compounds. *Crit. Rev. Toxicol.* **2006,** *36* (8), 609-662.

(98) Zheng, Y.; Jensen, A. D.; Windelin, C.; Jensen, F. Review of Technologies for Mercury Removal from Flue Gas from Cement Production Processes. *Prog. Energ. Combust.* **2012,** *38* (5), 599-629.

(99) Wang, Y.; Duan, Y.; Yang, L.; Zhao, C.; Shen, X.; Zhang, M.; Zhuo, Y.; Chen, C. Experimental Study on Mercury Transformation and Removal in Coal-Fired Boiler Flue Gases. *Fuel Process. Technol* **2009,** *90* (5), 643-651.

(100) Huang, Y. H.; Peddi, P. K.; Tang, C.; Zeng, H.; Teng, X. Hybrid Zero-Valent Iron Process for Removing Heavy Metals and Nitrate from Flue-Gas-Desulfurization Wastewater. *Sep. Purif. Technol.* **2013,** *118*, 690-698.

(101) Ghorishi, S. B.; Keeney, R. M. Development of a Cl-Impregnated Activated Carbon for Entrained-Flow Capture of Elemental Mercury. *Environ. Sci. Technol.* **2002,** *36* (20), 4454-4459.

(102) Lee, S. Removal of Gas-Phase Elemental Mercury by Iodine- and Chlorine-Impregnated Activated Carbons. *Atmos. Environ.* **2004,** *38* (29), 4887-4893.

(103) Chojnacki, A.; Chojnacka, K.; Hoffmann, J.; Górecki, H. The Application of Natural Zeolites for Mercury Removal: From Laboratory Tests to Industrial Scale. *Miner. Eng.* **2004,** *17* (7-8), 933-937.

(104) Dong, J.; Xu, Z.; Kuznicki, S. M. Mercury Removal from Flue Gases by Novel Regenerable Magnetic Nanocomposite Sorbents. *Environ. Sci. Technol.* **2009,** *43* (9), 3266-3271.

(105) Ghorishi, B.; Gullett, B. K. Sorption of Mercury Species by Activated Carbons and Calcium-Based Sorbents: Effect of Temperature, Mercury Concentration and Acid Gases. *Waste. Manage. Res.* **1998,** *16* (6), 582-593.

(106) Wang, Y. J.; Duan, Y. F.; Huang, Z. J.; Meng, S. L.; Yang, L. G.; Zhao, C. S. Vapor-Phase Elemental Mercury Adsorption by $Ca(OH)_2$ Impregnated with MnO_2 and Ag in Fixed-Bed System. *Asia-Pac. J. Chem. Eng.* **2009,** *5* (3), 479-487.

(107) Maroto-Valer, M. M.; Zhang, Y.; Granite, E. J.; Tang, Z.; Pennline, H. W. Effect of Porous Structure and Surface Functionality on the Mercury Capacity of a Fly Ash Carbon and Its Activated Sample. *Fuel.* **2005,** *84* (1), 105-108.

(108) Zhao, P.; Guo, X.; Zheng, C. Removal of Elemental Mercury by Iodine-Modified Rice Husk Ash Sorbents. *J. Environ. Sci.* **2010,** *22* (10), 1629-1636.

(109) Hua, X.-y.; Zhou, J.-s.; Li, Q.; Luo, Z.-y.; Cen, K.-f. Gas-Phase Elemental Mercury Removal by CeO_2 Impregnated Activated Coke. *Energ. Fuel.* **2010,** *24* (10), 5426-5431.

(110) Zhao, G.; Li, J.; Ren, X.; Chen, C.; Wang, X. Few-Layered Graphene Oxide Nanosheets As Superior Sorbents for Heavy Metal Ion Pollution Management. *Environ. Sci. Technol.* **2011,** *45* (24), 10454-10462.

(111) Jiang, G.; Lin, Z.; Chen, C.; Zhu, L.; Chang, Q.; Wang, N.; Wei, W.; Tang, H. TiO_2 Nanoparticles Assembled on Graphene Oxide Nanosheets with High Photocatalytic Activity for Removal of Pollutants. *Carbon.* **2011,** *49* (8), 2693-2701.

(112) Hutson, N. D.; Attwood, B. C.; Scheckel, K. G. XAS and XPS Characterization of Mercury Binding on Brominated Activated Carbon. *Environ. Sci. Technol.* **2007,** *41* (5), 1742-1752.

(113) Ji, L.; Sreekanth, P. M.; Smirniotis, P. G.; Thiel, S. W.; Pinto, N. G. Manganese Oxide Titania Materials for Removal of NO_x and Elemental Mercury from Flue Gas. *Energy Fuels.* **2008,** *22* (4), 2299-2306.

(114) Lee, W.; Bae, G.-N. Removal of Elemental Mercury (Hg(0)) by Nanosized V_2O_5/TiO_2 Catalysts. *Environ. Sci. Technol.* **2009,** *43* (5), 1522-1527.

(115) Yamaguchi, A.; Akiho, H.; Ito, S. Mercury Oxidation by Copper Oxides in Combustion Flue Gases. *Powder Technol.* **2008,** *180* (1-2), 222-226.

(116) Chen, S.; Zhu, J.; Wu, X.; Han, Q.; Wang, X. Graphene Oxide MnO_2 Nanocomposites for Supercapacitors. *ACS Nano.* **2010,** *4* (5), 2822-2830.

(117) Zhu, J.; Zeng, G.; Nie, F.; Xu, X.; Chen, S.; Han, Q.; Wang, X. Decorating Graphene Oxide with CuO Nanoparticles in a Water-Isopropanol System. *Nanoscale.* **2010,** *2* (6), 988.

(118) Chen, Y.-L.; Hu, Z.-A.; Chang, Y.-Q.; Wang, H.-W.; Zhang, Z.-Y.; Yang, Y.-Y.; Wu, H.-Y. Zinc Oxide/Reduced Graphene Oxide Composites and Electrochemical Capacitance Enhanced by Homogeneous Incorporation of Reduced Graphene Oxide Sheets in Zinc Oxide Matrix. *J. Phys. Chem. C* **2011,** *115* (5), 2563-2571.

(119) Dikin, D. A.; Stankovich, S.; Zimney, E. J.; Piner, R. D.; Dommett, G. H. B.; Evmenenko, G.; Nguyen, S. T.; Ruoff, R. S. Preparation and Characterization of Graphene Oxide Paper. *Nature.* **2007,** *448* (7152), 457-460.

(120) McAllister, M. J.; Li, J.-L.; Adamson, D. H.; Schniepp, H. C.; Abdala, A. A.; Liu, J.; Herrera-Alonso, M.; Milius, D. L.; Car, R.; Prud'homme, R. K.; Aksay, I. A. Single Sheet Functionalized Graphene by Oxidation and Thermal Expansion of Graphite. *Chem. Mater.* **2007,** *19* (18), 4396-4404.

(121) Wang, J.-G.; Yang, Y.; Huang, Z.-H.; Kang, F. Rational Synthesis of MnO_2/Conducting Polypyrrole@Carbon Nanofiber Triaxial Nano-Cables for High-Performance Supercapacitors. *J. Mater. Chem.* **2012,** *22* (33), 16943-16949.

(122) Tahir, D.; Tougaard, S. Electronic and Optical Properties of Cu, CuO and Cu_2O Studied by Electron Spectroscopy. *J. Phys.: Condens. Matter* **2012,** *24* (17), 175002.

(123) Zhou, J.-s.; Qi, P.; Hou, W.-h.; You, S.-l.; Gao, X.; Luo, Z.-y. Elemental Mercury Removal from Syngas by Nano-ZnO Sorbent. *J. Fuel. Chem. Technol.* **2013,** *41* (11), 1371-1377.